

# Influence of c-FLIP and A20 on apoptosis regulation

## **Dissertation**

zur Erlangung des akademischen Grades

**doctor rerum naturalium**

**(Dr. rer. nat.)**

genehmigt durch die Fakultät für Naturwissenschaften  
der Otto-von-Guericke-Universität Magdeburg

von M. Sc. Tobias Lübke

geb. am 09.06.1984 in Hannover

Gutachter Prof. Dr. Ingo Schmitz

Prof. Dr. Klaus Schulze-Osthoff

eingereicht am 31.08.2016

verteidigt am 23.01.2017



## Summary

Programmed cell death mechanisms are essential for multicellular organisms. Apoptosis plays an important role during embryonic development, in immune homeostasis and the clearance of altered cells. This type of cell death is tightly regulated by pro- and anti-apoptotic proteins, which is necessary to prevent excessive or insufficient killing of cells. Dysregulated apoptosis leads to various diseases, such as immunodeficiency, autoimmunity or cancer. c-FLIP proteins are the main inhibitors of receptor-mediated apoptosis by blocking caspase-8 activation at the level of the death-inducing signalling complex (DISC). The aim of this thesis was to identify the role of c-FLIP splice variants in mediating resistance against CD95L-induced apoptosis in renal cell carcinomas and to characterise the role of A20 in receptor-mediated caspase-8 activation.

Apoptosis is often impaired in tumours due to increased expression of anti-apoptotic proteins. The role of the anti-apoptotic protein c-FLIP in renal cell carcinoma cell lines was characterised within this thesis. Strikingly, concurrent loss of all c-FLIP isoforms, by introduction of shRNA, induced spontaneous apoptosis in all cell lines. Re-expression of c-FLIP<sub>L</sub> was sufficient to restore viability, demonstrating the importance of c-FLIP for mediating survival functions in renal cell carcinoma. CD95 and its ligand CD95L were highly expressed in all RCC cell lines, compared to TRAIL-R1, TRAIL-R2, TNF-R1 and TRAIL. Further characterisation of clearCa-4 revealed CD95 aggregation upon cell-cell-contact events. Blocking of CD95L resulted in spontaneous caspase-dependent cell death. NF- $\kappa$ B was activated in steady-state-conditions and inducible by CD95L. The findings reveal that renal cell carcinoma cell lines are dependent on c-FLIP expression and CD95 signalling.

The ubiquitin-editing enzyme A20 was previously identified as a binding partner of the TRAIL-DISC and has also been shown to play a role in caspase activation. In this thesis, the function of A20 in CD95L-induced apoptosis and its supposed role in the CD95-DISC was examined. The recently established CRISPR/Cas9 technology was successfully used to generate A20 knockout Jurkat cell lines. These cell lines were used to demonstrate that A20 reduces CD95L-induced apoptosis. While activation of caspase-8 at the level of the DISC was not impaired, active caspase-8 was targeted for proteasomal degradation by a so far unknown mechanism. A direct interaction between A20 and caspase-8 was not identified, proposing an indirect mechanism of A20 on active caspase-8.

# Table of contents

Summary	I
<b>1 Introduction</b>	<b>1</b>
1.1 Cell death . . . . .	1
1.2 Apoptosis . . . . .	3
1.2.1 Caspases . . . . .	4
1.2.2 Signalling pathways of apoptosis . . . . .	6
1.2.2.1 Extrinsic apoptosis . . . . .	6
1.2.2.2 Intrinsic apoptosis . . . . .	8
1.2.2.3 Interplay between extrinsic and intrinsic apoptosis . .	10
1.2.3 Morphological and biochemical features of apoptosis . . . . .	10
1.2.4 The apoptosis inhibitor c-FLIP . . . . .	11
1.2.5 Dysregulated apoptosis . . . . .	14
1.2.6 The role of c-FLIP in cancer . . . . .	14
1.3 Ubiquitin . . . . .	16
1.3.1 Overview . . . . .	16
1.3.2 Ubiquitin linkages . . . . .	17
1.3.3 Ubiquitin-like proteins . . . . .	20
1.3.4 Deubiquitination . . . . .	20
1.3.5 The unusual ubiquitin-converting enzyme A20 . . . . .	22
1.4 Aims of the thesis . . . . .	24
<b>2 Materials</b>	<b>26</b>
2.1 Chemicals . . . . .	26
2.1.1 Molecular biology . . . . .	26
2.1.2 Devices and materials . . . . .	26
2.1.3 Restriction enzymes . . . . .	26
2.1.4 Oligonucleotides . . . . .	27
2.1.4.1 Sequencing of the <i>CFLAR</i> -gene . . . . .	27
2.1.4.2 Generation of c-FLIP <sub>L-MUT</sub> . . . . .	27
2.1.4.3 qRT-PCR of c-FLIP . . . . .	27
2.1.4.4 Generation of A20-targeting CRISPR/Cas9 constructs	27

---

2.2	Cell culture . . . . .	28
2.2.1	Devices and materials . . . . .	28
2.2.2	Mediums and reagents . . . . .	28
2.2.3	Functional antibodies and recombinant proteins . . . . .	29
2.3	Western blot analysis . . . . .	29
2.3.1	Devices and materials . . . . .	29
2.3.2	Primary antibodies . . . . .	30
2.3.3	Secondary antibodies . . . . .	31
2.4	Flow cytometry and microscopy . . . . .	31
2.4.1	Devices and materials . . . . .	31
2.4.2	Antibodies and reagents . . . . .	32
2.5	Frequently used buffers . . . . .	33
2.5.1	Cell lysis . . . . .	33
2.5.2	Flow cytometry . . . . .	33
2.5.3	Western blot . . . . .	34
2.5.4	Miscellaneous . . . . .	34
<b>3</b>	<b>Methods</b>	<b>35</b>
3.1	Molecular biology . . . . .	35
3.1.1	Cloning of DNA fragments . . . . .	35
3.1.2	Transformation of bacteria . . . . .	35
3.1.3	PCR for cloning of DNA fragments . . . . .	36
3.1.4	PCR for verification of plasmid integrity . . . . .	36
3.1.5	Isolation of eukaryotic RNA and cDNA synthesis . . . . .	36
3.1.6	Quantitative real-time PCR (qRT-PCR) . . . . .	37
3.1.7	Purification of genomic DNA . . . . .	37
3.1.8	Gel electrophoresis . . . . .	37
3.1.9	Plasmid purification . . . . .	37
3.1.10	Determination of the DNA/RNA concentration . . . . .	38
3.1.11	Sequencing . . . . .	38
3.2	Cellular and protein biochemical methods . . . . .	38
3.2.1	Cultivation of eukaryotic cells . . . . .	38
3.2.2	Production of lentiviral particles and transduction of target cells	38
3.2.3	Immunoprecipitation of the DISC . . . . .	39

---

---

3.2.4	Immunoprecipitation of ubiquitinated proteins . . . . .	39
3.2.5	Cell lysis for western blot analysis . . . . .	40
3.2.6	Measuring of protein concentration in lysates . . . . .	40
3.2.7	Protein gel electrophoresis . . . . .	40
3.2.8	Western blot transfer . . . . .	40
3.2.9	Probing with antibodies . . . . .	41
3.2.10	Coating of functional antibodies . . . . .	41
3.3	Flow cytometry and microscopy . . . . .	41
3.3.1	Nicoletti staining for analysing DNA fragmentation . . . . .	41
3.3.2	Staining of death receptors and ligands . . . . .	41
3.3.3	Staining of intracellular active caspase-3 . . . . .	42
3.3.4	Staining with AnnexinV and 7AAD . . . . .	42
3.3.5	Confocal fluorescence Microscopy . . . . .	42
3.4	CRISPR/Cas9 target generation . . . . .	42
3.5	Statistics . . . . .	43
<b>4</b>	<b>Results</b>	<b>44</b>
4.1	The role of c-FLIP in renal cell carcinoma . . . . .	44
4.1.1	All RCC cell lines express high levels of CD95 . . . . .	44
4.1.2	RCC cell lines show diverse c-FLIP expression . . . . .	45
4.1.3	Cycloheximide sensitises RCCs to CD95L-induced apoptosis . .	46
4.1.4	Simultaneous knockdown of c-FLIP <sub>L</sub> , c-FLIP <sub>S</sub> and c-FLIP <sub>R</sub> drives RCCs into spontaneous cell death . . . . .	49
4.1.5	Knockdown of c-FLIP <sub>L/S</sub> mediates apoptosis in RCCs . . . . .	52
4.1.6	Re-expression of c-FLIP <sub>L-MUT</sub> rescues cells from spontaneous apoptosis . . . . .	53
4.1.7	NF- $\kappa$ B is constitutively active and independent from FLIP ex- pression in clearCa-4 . . . . .	56
4.1.8	CD95 accumulates upon cell-cell-contact events, but fails to in- duce the DISC . . . . .	57
4.1.9	CD95-signalling is important for survival of clearCa-4 . . . . .	59
4.2	The role of A20 in apoptosis regulation . . . . .	61
4.2.1	Translocation of A20 to the CD95-DISC is not consistent . . . .	61

---

---

4.2.2	Generation of a Jurkat E6-1 A20 knockout cell line with CRISPR/Cas9 . . . . .	61
4.2.3	Loss of A20 leads to increased apoptosis sensitivity . . . . .	63
4.2.4	Levels of active caspase-8 are altered in $\Delta$ A20 cells . . . . .	65
4.2.5	Caspase-8 cleavage products are degraded by the 26S-Proteasome	66
4.2.6	Polyubiquitination of caspase-8 might play a role in apoptosis-regulation . . . . .	67
<b>5</b>	<b>Discussion</b>	<b>69</b>
5.1	The role of c-FLIP in renal cell carcinoma . . . . .	69
5.2	The role of A20 in apoptosis regulation . . . . .	74
5.3	Concluding remarks . . . . .	78
<b>6</b>	<b>Abbreviations</b>	<b>79</b>
	<b>References</b>	<b>85</b>
	<b>Acknowledgements</b>	<b>114</b>
	<b>Curriculum vitea</b>	<b>115</b>
	<b>Declaration of originality</b>	<b>116</b>

# 1 Introduction

## 1.1 Cell death

Regulated, or programmed cell death, firstly described by Lockshin in 1965<sup>1</sup>, is a necessary feature of eukaryotic organisms to keep cell homeostasis. It plays an important role in e.g. embryonic development, immune response and clearance of infected and abnormal cells<sup>2</sup>. Different regulated cell death mechanisms can be discriminated by morphological and biochemical changes<sup>3</sup>. Beside apoptosis, which is the most commonly known form of regulated cell death, there are several other forms. Most importantly and with *in vivo* significance are autophagic cell death, necroptosis and pyroptosis (Fig. 1)<sup>4,5</sup>.

Regulated cell death can be divided into two parts, the initiation and the execution phase. During initiation, a cascade of different proteins, depending on the type of the cell death, is activated. At this stage, the cell death still can be inhibited by other proteins or cellular components. Moreover, the fate of the cell is not determined and it can still survive. The execution phase is defined as the point of no return, since the death of the cell is inevitable due to irreversible structural or biochemical changes<sup>3,6</sup>. The different types of regulated cell death are discriminated by their distinct characteristics of the morphological and biochemical changes (Tab. 1)<sup>3,7-9</sup>.

Autophagy is a complex mechanism for the cell to digest intracellular contents. It is used to recycle nutrients or damaged organelles, but was also found to play an important role to eliminate intracellular pathogens<sup>10</sup>. Autophagy acts as a survival mechanism, e.g. under nutrient deprivation, but it was also reported that it plays a role in programmed cell death<sup>3,5,11</sup>.

Necrosis is an unregulated type of cell death, which is directly induced upon physical, chemical or mechanical stress and results in an uncontrolled lysis of the cell<sup>8,12</sup>. Necroptosis is the programmed form of necrosis<sup>13</sup>. It is induced by death ligands, e.g. tumour-necrosis factor (TNF)  $\alpha$ , initiating the receptor-interacting protein kinase (RIP)-complex. The RIP-complex consists, amongst other proteins, of RIP1, RIP3 and mixed-lineage kinase domain-like (MLKL), leading to the activation of MLKL<sup>14-16</sup>.



MLKL activates downstream effectors, inducing reactive oxygen species (ROS) production and leads finally to the rupture of the plasma membrane, releasing cellular contents<sup>17-19</sup>. During necrotic and necroptotic death, the cell releases damage-associated molecular patterns (DAMP) like the mobility group protein B1 (HMGB1) and spliceosome-associated protein 130 (SAP130)<sup>13,20</sup>, which induce an immunogenic environment to attract immune cells like neutrophils, macrophages and natural killer cells (NK cells)<sup>21-24</sup>.

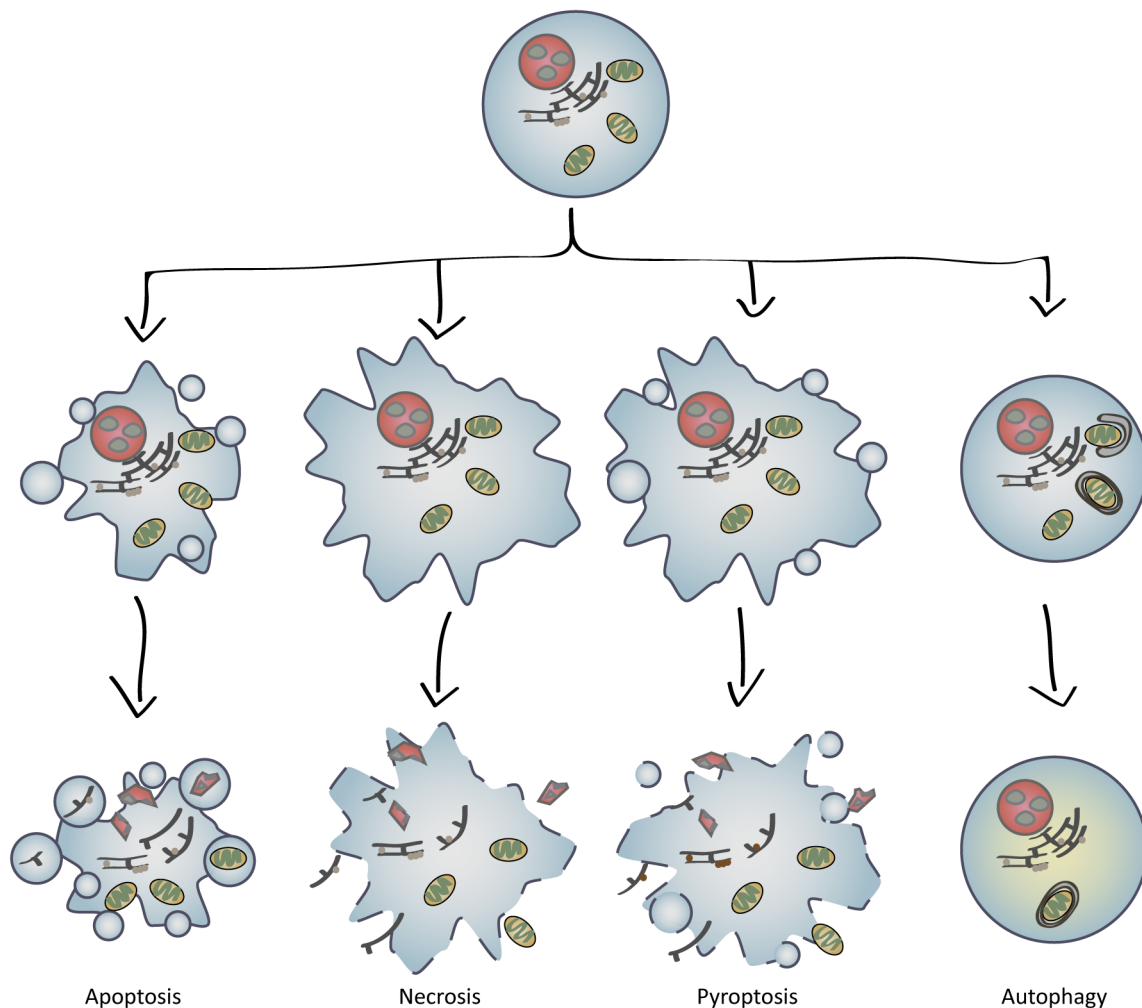


**Figure 1:** Different types of cell death can be detected in multicellular organisms. During apoptosis, the cell shrinks and apoptotic bodies are formed and released, which contain intracellular content, like fragmented mitochondria and DNA. The apoptotic bodies are then recognised by phagocytes to be degraded. This form of cell death is referred to be immunologically silent. Necroptosis and pyroptosis lead to a swelling of the cell and finally a rupture of the cell membrane. The release of intracellular contents triggers an inflammatory environment. Balanced autophagy is a recycling process, where cellular contents are lysed. Upon dysregulation, too many cell contents are degraded. Adapted from Ewald, 2013<sup>25</sup>.

Apoptosis was firstly described in 1972<sup>26</sup> and is the so-far best characterised cell death mechanism. Cells undergoing apoptosis show chromatin condensation, followed by

DNA fragmentation<sup>12</sup>. The morphological features of apoptosis are membrane blebs and the formation of apoptotic bodies<sup>12,27</sup>. The additional release of “find me” and “eat me” signals leads to the uptake of these apoptotic bodies by phagocytes<sup>26</sup>. This tightly regulated cell death mechanism prevents the disruption of the cell and therefore the release of cytoplasmic content<sup>10,28</sup>. Hence, it is referred to as an immunologically silent cell death, although there are studies showing potential immunologically features of apoptotic cells<sup>29-31</sup>. Apoptosis is a cysteinyl-aspartate specific protease (caspase)-dependent form of cell death<sup>32</sup>. If execution of apoptosis fails, for example because of a diminished caspase activation, necroptosis, which is caspase-independent<sup>33</sup> is triggered as a back-up mechanism, to assure cell death<sup>4,14,34</sup>.

**Table 1:** Cell death features<sup>5,9,35</sup>. \*mtDNA is released by necroptotic cell<sup>33</sup> \*\*Pro-inflammatory cytokines and chemokines are released to attract phagocytes. But in total an anti-inflammatory environment is build up by additional cytokines and chemokines<sup>29,36</sup>.

Feature	Autophagy	Necroptosis	Apoptosis	Pyroptosis
Caspase activation	-	-	+	+/-
DNA fragmentation	-	-	+	+
Membrane blebs	-	-	-	+
Pro-inflammatory	-	+*	+	(+)**
Cell lysis	-	+	+	-

Pyroptosis is a caspase-1 or -5-dependent cell death, which shows necrotic and apoptotic features. Infections with pathogens induce the assembly of the inflammasome, consisting of NLR family, pyrin domain containing 3 (NLRP3), adaptor protein apoptosis-associated speck-like protein containing CARD (ASC) and caspase-1<sup>37,38</sup>. Activated caspase-1 generates mature IL-1 $\beta$  and IL-18<sup>39</sup>, leading to an inflammatory environment after cell bursting<sup>40</sup>. It was shown that gasdermin D has an essential role in execution of pyroptosis and release of cytokines<sup>41,42</sup>.

## 1.2 Apoptosis

Apoptosis is an evolutionarily conserved form of programmed cell death which is important for several phases of a multicellular organism’s life<sup>43</sup>. First, it is required for morphogenesis during embryonic development<sup>44-46</sup> and essential to maintain tissue homeostasis<sup>2,45-48</sup>. Secondly, during T- and B-cell development, autoreactive or

---

non-functional cells are removed by apoptosis to prevent autoimmunity<sup>49</sup>. To downregulate an immune response after an infection, T cells are deleted by activation-induced cell death (AICD) via apoptosis<sup>50,51</sup>. Finally, cells undergo apoptosis when they are infected with pathogens as a defence mechanism<sup>52</sup>.

### 1.2.1 Caspases

Apoptosis execution is mainly mediated by cysteine-dependent aspartate specific proteases (caspases). There are twelve known caspases in humans (caspase-1-10, 12 and 14)<sup>53</sup>. Since caspases do not only have apoptotic functions, they can be divided into three groups: Keratinocyte differentiation-related caspase-14<sup>54</sup>, inflammatory (caspase-1, -4, -5 and -12) and apoptotic caspases. The apoptotic caspases can further be divided into two distinct groups, the initiator (caspase-2, -8, -9 and -10) and the effector caspases (caspase-3, -6 and -7), according to their function in apoptosis (Fig. 2). While initiator caspases are required for the activation of effector caspases, activated effector caspases lead to the proteolytic cleavage of various cellular targets, resulting in the death of the cell<sup>55</sup>.

Caspases are ubiquitously expressed as an inactive form, called zymogen<sup>56</sup>. Initiator caspases harbour two N-terminal death effector domains (DED) or one caspase recruitment domain (CARD), which mediate the recruitment to a caspase activation platform<sup>57</sup>. All caspases consist of two Carboxy-terminal (C-terminal) subunits, a large (20 kDa) and a small (10 kDa) subunit<sup>56,58</sup>, which possess catalytic activity. This activity is mediated by two catalytically conserved residues: histidine-237 and cysteine-285 (numbering originated from caspase-1), where cysteine-285 is located within the conserved pentapeptide motif QACXG (with R, Q or G for X)<sup>59,60</sup>.

Initiator caspases are present as monomers, however recruitment to the death inducing signalling complex (DISC) via their DED promotes dimerisation and subsequently autoproteolytic cleavage to a pro-activated form. In a second step the pro-activated form is further cleaved, which generates a heterotetrameric active form, consisting of two small (p10) and two large (p18) subdomains<sup>56,61</sup>. This heterotetramer is then released into the cytosol, where it can activate downstream caspases<sup>58,62</sup>.

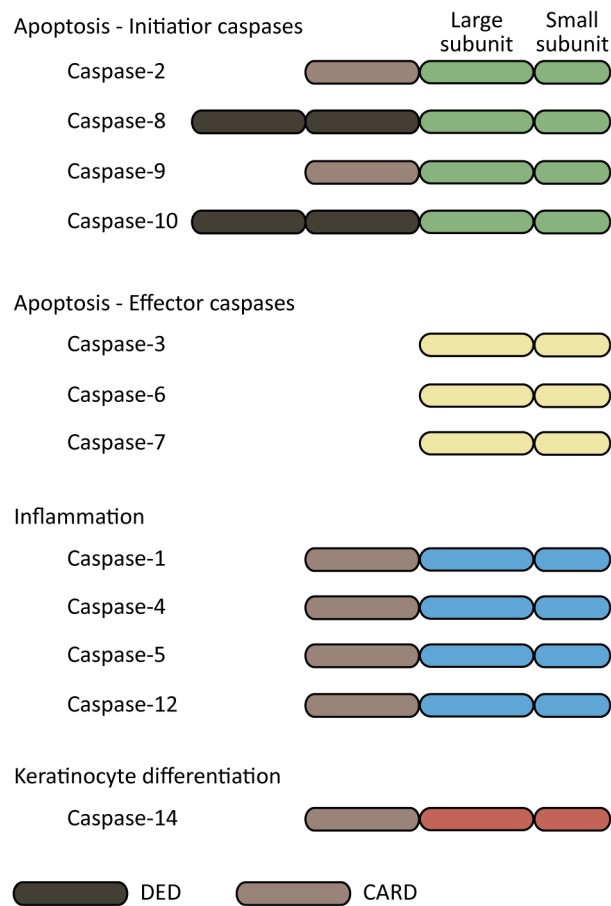


**Figure 2:** Caspases can be divided into different groups according to their function. All caspases harbour a catalytic domain to fulfil their protease function. Initiator caspases are recruited via their C-terminal DED or CARD to death signalling platforms. Effector caspases lack the recruiting domain and execute apoptosis. Caspase activity is mediated by the large and small subunits. Adapted from Fuentes-Prior and Salvesen, 2004 <sup>56</sup>.

Effector caspases lack the DED or CARD and are present in the cell as homodimers. Their Activation is achieved solely by proteolytic cleavage by initiator caspases without any prior activation <sup>56</sup>, also resulting in a heterotetrameric active effector caspase.

Caspases cleave their substrates C-terminal of a tetrapeptide sequence with an aspartate in the last position. The inflammatory caspases 1, 4 and 5 cleave a (W/Y)EXD motif (with X for amino acid any residue). Within the apoptotic caspases, the cleavage site of caspase-2, -3 and -7 is DEXD, while caspase-6, -8, -9 and 10 cleave C-terminal of (I/L/V)EXD, although variations within these sequences are possible. Coming along with different recognition sites, caspases have different substrates specificities <sup>63</sup>. While initiator caspases have only a few set of substrates, e.g. the effector caspases, many morphological and biochemical features of apoptosis are mediated by the proteolytic activity of effector caspases <sup>56,64</sup>.

### 1.2.2 Signalling pathways of apoptosis

Activation of apoptosis can be mediated by two different pathways, the extrinsic and the intrinsic pathway<sup>65,66</sup>. Upon activation, both pathways lead to the subsequent death of the cell, depending on the strength of apoptosis induction and the lack of inhibitory mechanisms (Fig. 3).

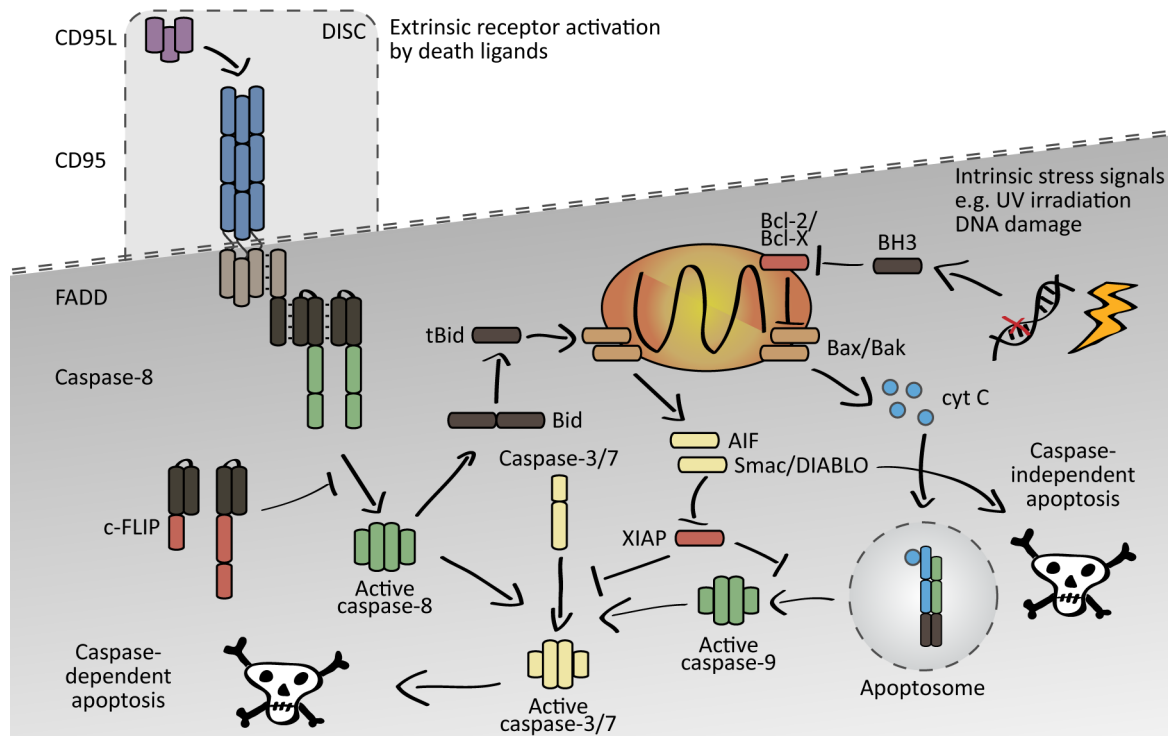


**Figure 3:** Apoptosis can be induced by extrinsic or intrinsic signals. Extrinsic apoptosis is mediated by binding of death ligands (e.g. CD95L) to their respective receptors (e.g. CD95). Upon binding, death receptor aggregation is initiated and the death inducing signalling complex (DISC) is formed. Thereby, caspase-8 gets autocatalytically activated. In type I apoptotic cells, caspase-8 directly activates the effector caspases caspase-3 and -7 to execute apoptosis. In type II apoptotic cells, the apoptosis signal is triggered via the mitochondrium. The mitochondrial pathway is also induced by intrinsic signals, like UV irradiation or extensive DNA damage. Mitochondrial channels release the pro-apoptotic factors cytochrome c, Smac/DIABLO, AIF and Omi/HtrA2. The apoptosome is built and activates caspase-9. Effector caspases are then cleaved and the cell undergoes apoptosis. Adapted from Bouillet and O'Reilly, 2009<sup>67</sup>.

#### 1.2.2.1 Extrinsic apoptosis

Extrinsic, also termed receptor-mediated apoptosis, is triggered by transmembrane death receptors (DR) which belong to the TNF-receptor superfamily<sup>68,69</sup>. Until now, six functional members, containing a death domain, were identified: CD95 (Fas,

Apo-1, TNFRSF6)<sup>70,71</sup>, TRAIL-R1 (DR4, Apo-2)<sup>72</sup>, TRAIL-R2 (DR5, Apo-3)<sup>73</sup>, TNF-R1<sup>74</sup>, DR3 (Apo-3)<sup>75</sup> and DR6<sup>76</sup> (Fig. 4a).

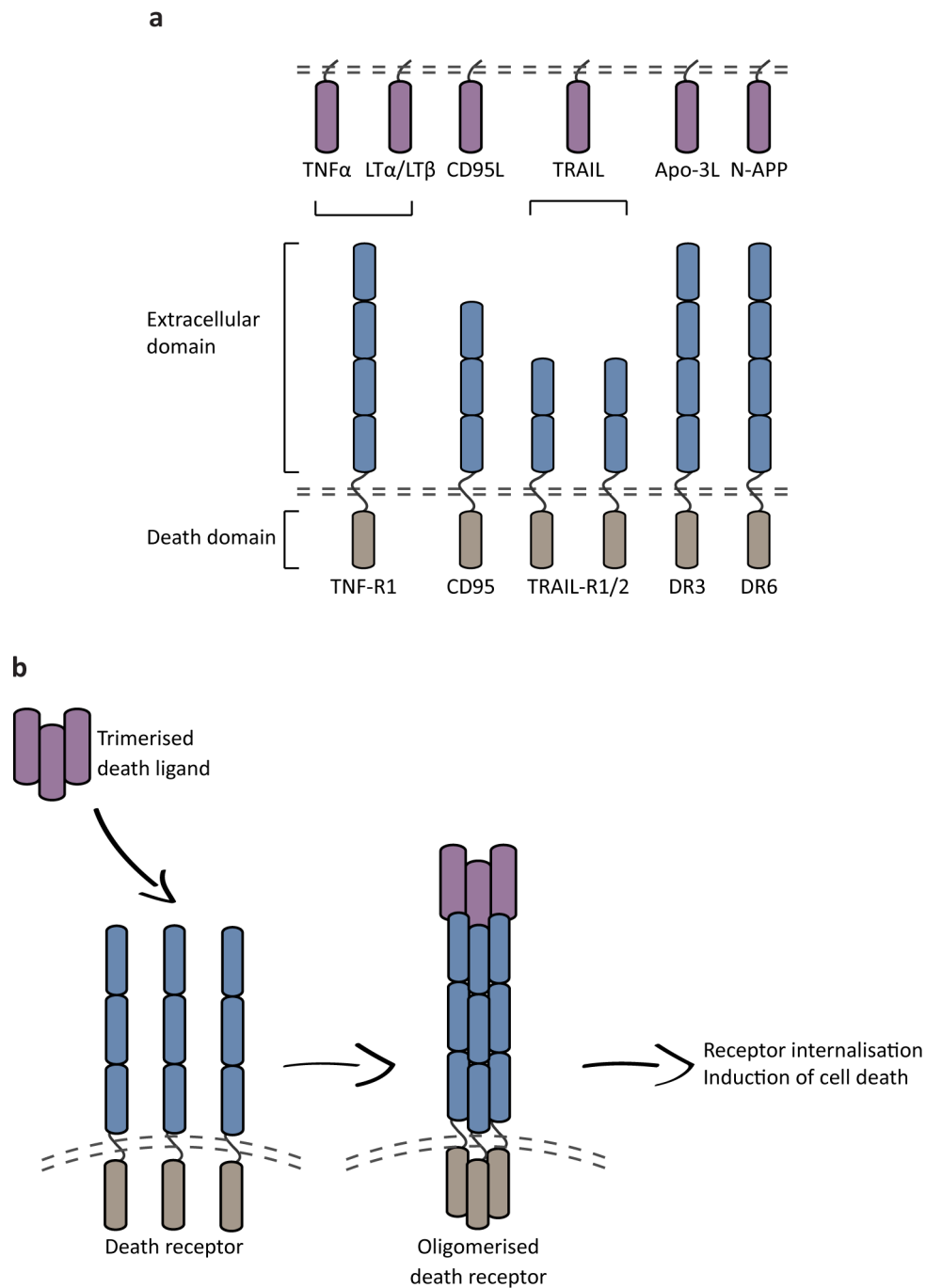


**Figure 4:** **a:** Death receptors belong to the TNF-receptor superfamily and consist of extracellular cysteine rich domains (blue) and an intracellular death domain (grey). Death ligands (purple) are expressed as membrane-bound proteins, but can be cleaved by metalloproteases to a soluble form. Adapted from Igney and Krammer, 2002<sup>76</sup>. **b:** The trimerised death ligand binds to its respective death receptor and initiates its oligomerisation. For signal transduction the receptor has to be internalised.

The death receptors are built up by cysteine-rich domains and can be bound by their respective death ligands.<sup>77</sup> Additionally, an intracellular death domain (DD) is required,

to transduce the death signal<sup>78,79</sup>. Interestingly, receptors lacking the intracellular DD were identified, thus they are unable to transduce the death signal<sup>77</sup>. These receptors are termed decoy receptors (DcR) and compete for binding with the functional death receptors for the death ligands, thereby inhibiting apoptosis<sup>76</sup>.

The so called death ligands bind to the death receptors to stimulate them (Fig. 4a): The death receptor CD95 is bound by CD95L<sup>80</sup>, TRAIL-R1 and TRAIL-R2 by TRAIL<sup>72,81</sup> and TNF-R1 by TNF $\alpha$  and LT $\alpha/\beta$ <sup>82</sup>. The ligand for DR3 is APO-3L<sup>83</sup> and for DR6 it is the N-terminal fragment of the amyloid precursor protein (N-APP), which was discovered in the context of Alzheimer's disease<sup>84,85</sup>.

For death receptor activation, the respective death ligand needs to be a homo-oligomer<sup>86-88</sup>. Upon binding by their respective ligand, the death receptor oligomerises, which leads to the recruitment of adaptor proteins via their DD (Fig. 3). CD95 and TRAIL-R1/R2 recruit the Fas-associated death domain protein (FADD). FADD contains, beside the DD, a DED. Via this DED, pro-caspase-8 and pro-caspase-10 are recruited<sup>89-91</sup>. This protein complex, consisting of death receptor, adaptor proteins and pro-caspases is called DISC. It serves as a caspase activation platform where two caspase-proteins dimerise and undergo autoproteolytic cleavage<sup>92</sup>. Another model suggests that not only dimers, but chains of pro-caspases are recruited to the DISC, leading to caspase activation<sup>91,93</sup>. The activated and cleaved caspase-dimer leaves the DISC and activates downstream substrates, depending on the type of apoptosis<sup>94</sup>. For apoptosis induction it is required that this complex is then internalised by an endosomal pathway (Fig. 4b)<sup>90</sup>.

Beside the DISC, there is another caspase activation platform, the TNF-receptor complex II. When TNF-R1 binds TNF $\alpha$ , the adaptor protein TNFR-associated death domain (TRADD) is recruited. Since TRADD does not harbour a DED, but only a DD, FADD is recruited to the complex, thereby recruiting pro-caspases and initiating their activation similar to the DISC complex<sup>95,96</sup>.

### 1.2.2.2 Intrinsic apoptosis

The intrinsic pathway is activated by several receptor- and caspase-independent stimuli and requires the mitochondria to release pro-apoptotic factors<sup>97,98</sup> (Fig. 3). Among these stimuli are DNA damage, ROS production and other cellular stress factors<sup>97</sup>.

---

Regulation of the intrinsic pathway involves different B cell lymphoma-2 (Bcl-2) family proteins. They all share the Bcl-2 homology (BH) domains. The proteins can be divided into three groups, according to their number of BH domains and their function in apoptosis regulation. The anti-apoptotic Bcl-2 proteins share all four BH domains (BH1-BH4), while the Bcl-2 effector proteins only have three BH domains (BH1-BH3). The BH3-only proteins Bid, Bim, Puma and Bad have, as their name suggests, only the BH3 domain and are pro-apoptotic, since they inhibit the anti-apoptotic Bcl-2 proteins<sup>65,99</sup>.

The proteins within the anti-apoptotic Bcl-2 group, Bcl-2, B cell lymphoma x, large form (Bcl-xL), Myeloid cell leukemia-1 (Mcl-1) and Bcl-2-related gene A1 (A1) stabilise the mitochondrial membrane integrity by binding to the pro-apoptotic Bcl-2 proteins to homo- and heterodimers<sup>99-101</sup>. In contrast to this, the activation of the pro-apoptotic family members Bcl-2-associated x protein (Bax), Bcl-2 antagonist killer 1 (Bak) and Bcl-2-related ovarian killer (Bok) results in the dimerisation of these family members and consequently mitochondrial outer membrane permeabilisation (MOMP), prompting the release of apoptosis inducing factor (AIF), endonuclease G (endoG), cytochrome c (CytC) and second mitochondria-derived activator of caspases (Smac), also known as direct IAP binding protein with low pI (DIABLO)<sup>98,101-103</sup>. While endoG translocates into the nucleus, where it exhibits DNase activity, AIF activates mitochondrial DNase, leading to DNA fragmentation<sup>103,104</sup>. Cytochrome c binds to the apoptotic protease activating factor 1 (APAF-1) and subsequently activates it. In addition with dATP, pro-caspase-9 is recruited via its CARD domain to the activated APAF-1-complex, called the apoptosome<sup>105,106</sup>. This complex facilitates the dimerisation of two pro-caspase-9 molecules which become activated by cleavage. Active caspase-9 subsequently cleaves pro-caspase-3 into its active form, resulting in apoptosis completion. At this stage, apoptosis can still be inhibited by the X-linked inhibitor of apoptosis (XIAP) which can bind to active caspase-9 and active caspase-3, thereby preventing apoptosis<sup>105,107</sup>. XIAP itself is targeted by the protein Smac (which is released by the mitochondria upon stress induction) to inhibit XIAP's anti-apoptotic function<sup>108</sup>.



### 1.2.2.3 Interplay between extrinsic and intrinsic apoptosis

Extrinsic caspase activation is dependent on receptor internalisation<sup>90,109</sup>. In type I apoptotic cells, receptor internalisation and thereby caspase activation at the DISC is sufficient to induce apoptosis, whereas in type II apoptotic cells, the apoptotic signal has to be triggered via the mitochondrial pathway<sup>62,110</sup>. In type II apoptotic cells, where caspase activation at the DISC is not sufficient to induce apoptosis, the signal is amplified via the mitochondrial pathway<sup>66,111</sup>. As a result, the N-terminal region of the BH3-interacting domain death agonist (Bid) is cleaved by active caspase-8, resulting in the truncated form of Bid (tBid), a member of the BH3-only family, which then translocates to the mitochondria (Fig. 3). There it inhibits the anti-apoptotic BH3 family members and promotes the oligomerisation of Bax and Bak, promoting MOMP<sup>99,112</sup>. Consequently, overexpression of Bcl-2 leads to resistance of type II, but not type I, apoptotic cells towards extrinsic apoptosis<sup>113</sup>.

### 1.2.3 Morphological and biochemical features of apoptosis

Apoptosis is characterised by an interplay of many different morphological and biochemical changes, which allows organisms to clear apoptotic cells in an immunologically silent manner. These changes also allow researchers to discriminate apoptosis from other types of programmed cell death<sup>35,114,115</sup>.

The main morphological changes during apoptosis are induced by effector caspase activity, cleaving and reordering cytoskeletal proteins<sup>6,116,117</sup>. Cleavage and thereby activation of rho-associated coiled-coil kinase-1 (ROCK-1), leads to actinomyosin ring contraction and therefore membrane blebs<sup>118,119</sup>. Changes in the actin cytoskeleton are induced by cleavage of  $\beta$ -catenin<sup>120</sup>. Activation of p21-activated kinase 2 (PAK2) prompts the formation of apoptotic bodies<sup>121</sup> by reorganising the microfilament structure<sup>27</sup>. In living cells, phosphatidylserine is held by its flippase on the inner side of the cell membrane. Caspase-mediated inactivation of flippase leads to the exposure of phosphatidylserine to the outside of the cell<sup>122</sup>.

DNA fragmentation is another feature of apoptosis<sup>115,123</sup>. Poly ADP ribose polymerase (PARP)<sup>124</sup>, and the DNA-dependent protein kinase (DNA-PK)<sup>125</sup>, proteins which are involved in DNA repair, are cleaved and thereby inactivated. Caspase-activated DNase (CAD), normally inhibited by the inhibitor of caspase-activated DNase (iCAD), can

---

degrade DNA upon cleavage of iCAD by caspase-3<sup>49,126</sup>. Additionally, DNA fragmentation is induced upon activation of protein kinase C family members<sup>125</sup>. Lamin A and B are targeted by caspases, leading to nuclear condensation and the breakdown of the nucleus<sup>127,128</sup>.

One main feature of apoptosis is that the dying cell and the corresponding apoptotic bodies are taken up by phagocytes to avoid further tissue damage<sup>36</sup> and secondary necrosis<sup>129</sup>. Although apoptosis is termed as an immunologically-silent mode of cell death, recent studies revealed a large impact of pro-inflammatory factors that serve as so-called “find me” signals for phagocytes. Apoptotic cell death leads to the release of cytokines and chemokines like sphingosine 1-phosphate (S1P)<sup>130</sup>, LPC<sup>131</sup>, CX3CL1<sup>132</sup>, IL-6, IL-8, MCP-1 and GM-CSF, but also nucleotides<sup>133</sup> to attract phagocytes for clearing apoptotic cells<sup>29</sup>. This effect is independent of caspase-activity<sup>29</sup>. After migration, phagocytes need so-called “eat me” signals to recognise apoptotic cells for uptake. The exposure of phosphatidylserine serves as a main “eat me” signal which is bound by phagocytic receptors, leading to the clearance of apoptotic cells<sup>134,135</sup>. To compensate the pro-inflammatory effects of the “find me” and “eat me” signals, Lactoferrin is released by the apoptotic cell to block neutrophil and granulocyte attraction<sup>136</sup>. Additionally, anti-inflammatory cytokines, such as IL-10 and TGF $\beta$ , are released from the apoptotic cell<sup>137–139</sup>.

#### 1.2.4 The apoptosis inhibitor c-FLIP

Apoptosis has to be regulated very precisely to avoid unwanted cell death, hence inhibition of this pathway is crucial. While Bcl-2 family proteins inhibit the intrinsic pathway, the major players in inhibition of the extrinsic pathway are cellular FLICE inhibitory proteins (c-FLIP), proteins homologous to caspase-8. The discovery of viral FLIP (v-FLIP) in  $\gamma$ -herpesviruses, which blocks receptor-mediated apoptosis of infected cells, and thereby ensures higher viral replication rates and persistence, led to an emerging field of research in the last 20 years<sup>140</sup>. Mammalian homologues in humans were quickly found by independent work groups, thus also termed differently as CASH, Casper, CLARP, FLAME, I-FLICE, MRIT, or Usurpin<sup>141–147</sup>.

c-FLIP is encoded within the *CFLAR* gene, localised near the coding regions for caspase-8 and caspase-10 on chromosome 2q33-34, leading to the assumption that

c-FLIP and caspase-8 arose from gene duplication (Fig. 5a)<sup>147</sup>. Locus analysis suggested eleven different c-FLIP splicing variants<sup>148</sup>, whereof only three could be detected on protein level up to now: c-FLIP long (c-FLIP<sub>L</sub>), c-FLIP short (c-FLIP<sub>S</sub>) and c-FLIP Raji (c-FLIP<sub>R</sub>)<sup>149,150</sup>, which are constitutively expressed in a broad variety of cell types (Fig. 5b)<sup>145,151</sup>.

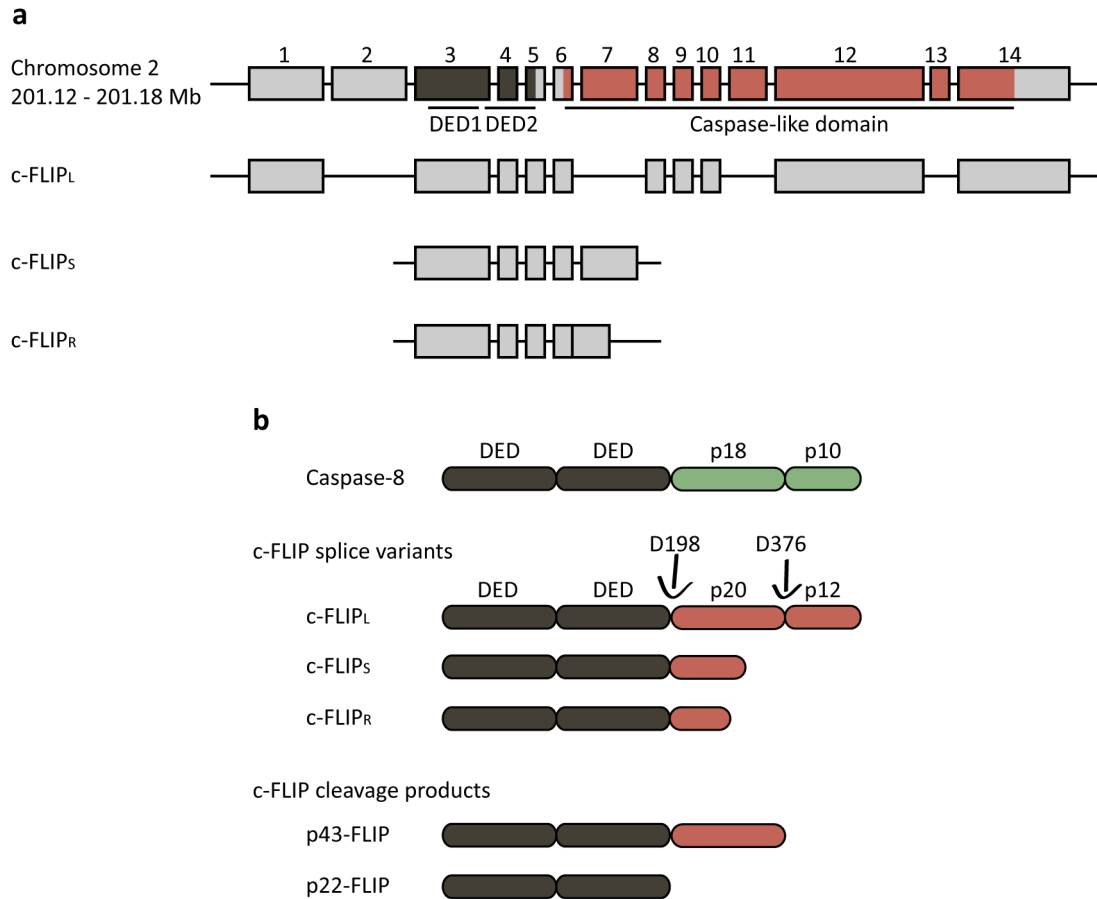


**Figure 5: a:** Genomic locus of c-FLIP. c-FLIP is encoded on chromosome 2q33-34. Three known isoforms, c-FLIP long (c-FLIP<sub>L</sub>), c-FLIP short (c-FLIP<sub>S</sub>) and c-FLIP Raji (c-FLIP<sub>R</sub>), are expressed in humans due to alternative splicing. A SNP in the 3' splicing of intron 6 is responsible for expression of c-FLIP<sub>S</sub> or c-FLIP<sub>R</sub>. Adapted from Ueffing et al., 2009<sup>152</sup>. **b:** Schematic protein structure and their cleavage products of c-FLIP isoforms: All c-FLIP splice variants harbour two death effector domains (DED) (dark grey) in the C-terminus. c-FLIP<sub>L</sub> has a catalytically inactive caspase-like domain (red) which is lacking in c-FLIP<sub>S</sub> and c-FLIP<sub>R</sub>. Cleavage sites (D198, D376) and the resulting c-FLIP cleavage products p43- and p22-FLIP are shown. Adapted from Budd et al., 2006<sup>151</sup>

These three isoforms differ in their molecular weight and their biological function. c-FLIP<sub>L</sub> has a molecular weight of 55 kDa, while c-FLIP<sub>S</sub> and c-FLIP<sub>R</sub> only have a molecular weight of 26 kDa and 24 kDa, respectively<sup>151</sup>. While c-FLIP<sub>L</sub> is generated through alternative splicing, the expression of c-FLIP<sub>S</sub> or c-FLIP<sub>R</sub> is determined by a single nucleotide polymorphism (SNP) in the 3' splicing site of intron 6<sup>152</sup>.

All c-FLIP proteins harbour two N-terminal DEDs, facilitating the interaction with other DED-containing proteins, like FADD, caspase-8 and -10<sup>56</sup>, however, a new study showed binding only to caspase-8<sup>153</sup>. Additionally, c-FLIP<sub>L</sub> has a catalytically inactive caspase-like domain, while this domain is lacking in c-FLIP<sub>S</sub> and c-FLIP<sub>R</sub>. This inactivity is achieved by substitutions of the amino acid residues histidine-237 and cysteine-285 in the catalytic active site<sup>56,141</sup>. Due to the interaction of DEDs, c-FLIP is competent to block CD95-, TRAIL-receptor- and TNF-receptor-mediated apoptosis at the level of the DISC or the TNF-receptor complex II, by inhibiting caspase activation<sup>150,154–156</sup>. Furthermore, c-FLIP was shown to block necroptosis and autophagy<sup>157,158</sup>. Depending on the c-FLIP splice variant, different outcomes in the apoptotic signal transduction are possible (Fig. 6). Dimerisation of caspase-8 and c-FLIP<sub>L</sub> leads to partial cleavage of both, c-FLIP<sub>L</sub> and caspase-8<sup>150</sup>. Since c-FLIP<sub>L</sub> lacks catalytic activity, only the initial cleavage products c-FLIP p43 and caspase-8 p43/41 can be formed, but caspase-8 cannot be fully processed to active caspase-8 heterotetramer with p18 and p10, resulting in limited caspase-8 activity<sup>150,155</sup>.

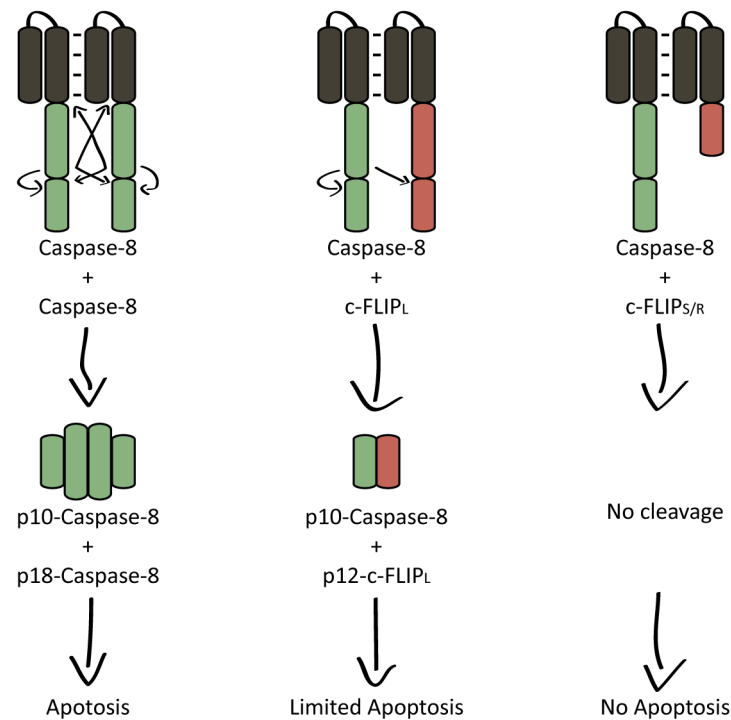


**Figure 6:** After triggering and aggregation of death receptors, caspase-8 is recruited to the DISC via its DED. Homodimerisation of caspase-8 leads to autoproteolytic cleavage, resulting in an enzymatically active heterotetramer, containing two p18 and two p10 fragments. Interaction of caspase-8 with c-FLIP<sub>L</sub> leads to incomplete cleavage of caspase-8 and partial cleavage of c-FLIP. This results in a heterodimer with limited activity. When caspase-8 dimerises with c-FLIP<sub>S</sub> or c-FLIP<sub>R</sub>, caspase-8 cannot be cleaved, hence caspase-8 activation is blocked. Adapted from Budd et al., 2006<sup>151</sup>.

It was shown that c-FLIP<sub>L</sub> not only has an anti-, but also a pro-apoptotic function, depending on c-FLIP<sub>L</sub> expression levels and the strength of receptor stimulation (Fig. 6) <sup>155,159,160</sup>. However, dimerisation of c-FLIP<sub>S</sub> or c-FLIP<sub>R</sub> with caspase-8 and -10 leads to complete inhibition of caspase activation, due to the lacking caspase-like-domain within the two short isoforms <sup>148,155,161</sup>. It was shown that c-FLIP<sub>L</sub> and c-FLIP<sub>S</sub> suppress apoptosis in activated T cells <sup>162-164</sup>. The p43-FLIP cleavage product of c-FLIP<sub>L</sub> not only has an anti-apoptotic function, but additionally leads to the caspase-8-mediated activation of the nuclear factor 'κ-light-chain-enhancer' of activated B-cells (NF-κB) pathway by interacting with RIP1 and TNF-receptor associated factor (TRAF) 2 <sup>165,166</sup>. It can also trigger Erk- and NF-κB-mediated IL-2 expression in activated T cells <sup>167-169</sup>, while the C-terminal fragment of c-FLIP<sub>L</sub> inhibits caspase-8 binding to the DD of RIP1, thereby inhibiting caspase-8 activation <sup>170</sup>.

### 1.2.5 Dysregulated apoptosis

Apoptosis is a tightly regulated system which has to be kept in balance. Since many pro- and anti-apoptotic proteins are involved in this regulated pathway of cell death, any change in protein expression or activity can change the cell's behaviour to death stimuli, making it a potentially dangerous cell for the whole organism <sup>2,76,171</sup>. Increased apoptosis activation and execution leads to higher cell removal rates, leading to diseases like the acquired immune deficiency syndrome (AIDS) <sup>172</sup> and neurodegenerative disorders <sup>48,173</sup>. Downregulation of apoptosis can cause autoimmune lymphoproliferative syndrome (ALPS) and it is also impaired in tumour development <sup>174-176</sup>.

### 1.2.6 The role of c-FLIP in cancer

Defects in apoptosis induction or execution lead to the accumulation of cells. If other cell death mechanisms, like necroptosis fail to remove mutated cells, tumours can arise <sup>177</sup>. Several mutations in anti- and pro-apoptotic proteins are described, leading to a gain- or loss-of-function, respectively, promoting tumour growth.

Elevated expression levels of Bcl-2 are linked to tumour progression by blocking the intrinsic pathway <sup>178-180</sup>. The CD95-mediated extrinsic pathway has a considerable impact on proliferation in normal tissue through NF-κB activation <sup>181-183</sup>. Tumour cells also benefit from CD95 expression, leading to progression and invasiveness <sup>184-191</sup>. Interestingly, high CD95 expression can be found in various cancer types, associated with

an aggressive phenotype and a poor clinical prognosis<sup>191–195</sup>. Interestingly, reduced CD95 activation, due to loss-of-function, also can lead to tumour progression<sup>196–198</sup>.

To maintain tissue homeostasis, c-FLIP blocks excessive apoptosis<sup>158</sup>. Hence, dysregulated c-FLIP expression is present in many types of cancer, like breast cancer<sup>199</sup>, prostate cancer<sup>200</sup>, urothelial cell carcinoma<sup>201</sup>, adenocarcinoma<sup>202</sup>, hodgkin's lymphoma<sup>203</sup>, malignant melanoma<sup>204</sup> and hepatocellular carcinoma<sup>205</sup>. Since c-FLIP has anti-apoptotic and NF- $\kappa$ B activating abilities, tumours, which upregulate c-FLIP, can profit from both effects. Drug-induced downregulation of c-FLIP with simultaneously stimulation of CD95 showed tumour regression in a variety of cancer cells, e.g. follicular lymphoma<sup>152,185,186,206–210</sup>, giving evidence that c-FLIP is protecting tumour cells from receptor-mediated apoptosis.

Renal Cell Carcinoma (RCC) represent about 2-3 % percent of all tumours, but over 90 % of all types in the kidney. RCC comes mostly without any symptoms until the late stages of the disease. Clear cell carcinoma (clearCa), a dominant RCC subtype is resistant to chemotherapeutic approaches, making it a cancer type with poor prognosis after diagnosis<sup>211</sup>.

The best known risk factors for RCC are smoking, obesity and hypertension<sup>212</sup>. Mutations in the von Hippel-Landau protein (pVHL), a tumour suppressor gene<sup>213,214</sup>, are also associated with tumour progression. Loss of pVHL leads to cyst formation in RCCs<sup>212,215,216</sup>. Resistance to chemotherapy,  $\gamma$ -irradiation and CD95-induced apoptosis of several surgically removed RCC tumours was shown<sup>217,218</sup>.

Several studies demonstrated that elevated CD95 expression in RCCs leads to a poorer prognosis of the patient's survival<sup>219–222</sup>. It can be considered that late stages of tumour progression come with increased NF- $\kappa$ B activation and decreased apoptosis, mediated by the CD95 pathway. Since it was already shown that c-FLIP is important for resistance of CD95-mediated apoptosis in other tumours, this makes c-FLIP an attractive target for tumour-treatment<sup>223</sup>.

---

## 1.3 Ubiquitin

### 1.3.1 Overview

Ubiquitination is a reversible post-translational modification, which regulates cellular processes in eukaryotic cells <sup>224</sup>. The ubiquitination of target proteins is involved in gene transcription <sup>225</sup>, protein degradation <sup>226</sup>, cell cycle control <sup>227</sup>, DNA-repair <sup>228</sup> and many intracellular signalling pathways <sup>229,230</sup>. Ubiquitin (Ub) is a protein with a molecular weight of 8 kDa <sup>231</sup>, which is encoded by four different genes, UBA52, UBB, UBC and RPS27A, located on the human chromosomes 19 <sup>232</sup>, 17 <sup>233</sup>, 12 <sup>234</sup> and 2 <sup>235</sup>, respectively. Despite the assumption that these genes have a redundant function, it could be shown that knockout of single ubiquitin-encoding genes lead to defects in embryonic development or even lethality in mice <sup>224</sup>. All four genes express an ubiquitin-precursor, which needs to be activated <sup>236-238</sup>. They are either expressed as poly-proteins or in fusion with ribosomal proteins <sup>239</sup>.

Ubiquitin is covalently bound via its C-terminal glycine residue to a lysine residue on target proteins <sup>240,241</sup>. This bonding is mediated by an ubiquitin-conjugation system, consisting of three proteins, an ubiquitin-activating enzyme (E1), an ubiquitin-conjugating enzyme (E2) and an ubiquitin ligase (E3) <sup>242</sup>. This enzymatic cascade consists of two E1, at least 38 E2 and more than 600 putative E3 proteins, encoded in the human genome <sup>243,244</sup>. In a first step, E1 activates ubiquitin under the release of PPi from ATP <sup>245,246</sup> (Fig. 7). The activated ubiquitin is then transferred to E2, which builds a complex with E3. Finally, the E2-Ub-E3 complex mediates the last step, the ubiquitination of the substrate <sup>247</sup>. This transfer can occur either directly, or indirectly, depending on the type of E3. The E3 can be subdivided into three protein families, harbouring different catalytic activities, the homologous to the E6-AP carboxyl terminus (HECT), the Really Interesting New Gene (RING), and the RING between RING (RBR) E3s <sup>241,248</sup>. While E3 ligases with a RING domain mediate a direct Ub transfer to the target protein, E3 ligases with a HECT domain bind Ub itself in a first step to subsequently transfer it to the target protein <sup>241</sup>. The RBR family proteins contain a triad of the RING1, in-between RING (IBR) and RING2 domains which combine the mechanisms of both, the HECT and the RING domain in order to ubiquitinate its target <sup>248,249</sup>.

The catalysed reaction mostly leads to an isopeptide bond between the C-terminus of the Ub and a lysine residue of the substrate <sup>241,245</sup>. However, N-terminal ubiquitination, not requiring a substrate lysine residue, is also possible <sup>250</sup>.

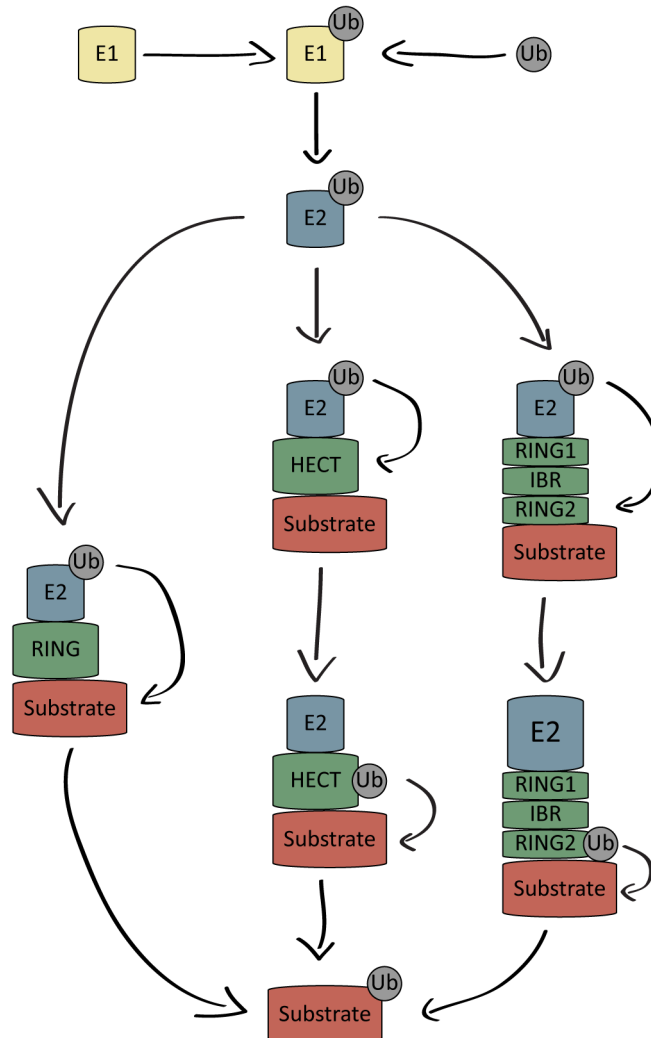


**Figure 7:** Ubiquitin (grey) is activated by the ubiquitin-activating enzyme E1 (yellow). The ubiquitin is then transferred to the ubiquitin-conjugating enzyme E2 (blue). The ubiquitin ligase E3 (green) builds a complex with E2 and ubiquitin and mediates the covalent binding of ubiquitin to a lysine residue of a substrate (red). This transfer can be executed by three different E3 protein groups, RING, HECT and RBR. RING-E3s mediate the direct transfer of ubiquitin from E2 to a substrate, while HECT-E3s bind ubiquitin themselves during the transfer. RBR-E3s contain a RING1 domain which is essential for the transfer of ubiquitin to the RING2 domain and then subsequently ubiquitin is transferred to the substrate. Adapted from Di Fiore et al., 2003 <sup>229</sup>

### 1.3.2 Ubiquitin linkages

Different patterns of ubiquitination lead to diverse structural and functional outcomes. Ubiquitin can either be attached to substrates as monoubiquitin, or as polyubiquitin chains (Fig. 8) <sup>247</sup>. In case of monoubiquitination, only one ubiquitin is transferred to



one specific lysine residue on the substrate. Also multi-monoubiquitination of a protein is possible, where different lysine residues become monoubiquitinated <sup>251</sup>. Monoubiquitination of proteins is linked with their localisation, activity or behaviour to interact with other proteins <sup>243,251</sup>. For example, after stimulation, receptors, such as the EGF-receptor, <sup>252</sup> undergo endocytosis for an efficient signal transduction, before being lysosomal degraded. The monoubiquitination of these receptors promote their fate in endocytosis and lysosomal degradation <sup>253,254</sup>.

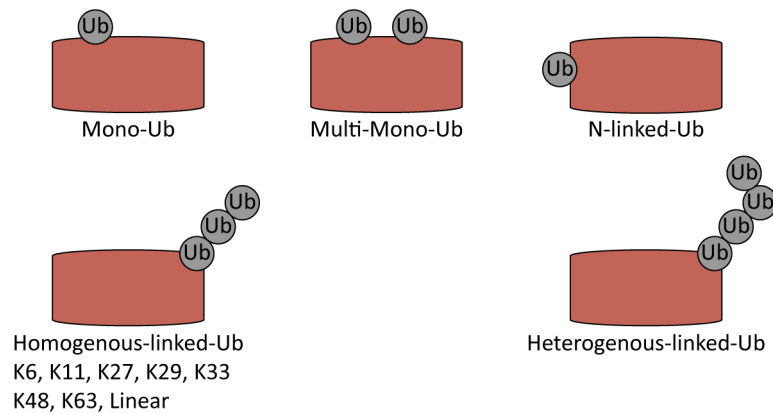


**Figure 8:** Different ubiquitin-linkage types affect the regulation of ubiquitinated proteins (red). Ubiquitination leads to an altered binding behaviour, translocation or stability of the modified protein. Adapted from Suryadinata et al., 2014 <sup>255</sup>.

It was shown that MHC class I and II molecules undergo endocytosis after they were polyubiquitinated <sup>256,257</sup>. Polyubiquitination chains arise, when an ubiquitin is bound via its C-terminal glycine to another ubiquitin. The transfer of a new ubiquitin to the N-terminus of an already bound ubiquitin, results in a linear ubiquitin chain, termed M1-linkage <sup>250</sup>.

Additionally, more complex linkage-types can be built by the ubiquitination machinery. Ubiquitin itself harbours seven lysine residues (K6, K11, K27, K29, K33, K48, and K63), which act as acceptors for another ubiquitin <sup>255</sup>. This leads to different linkage compositions with versatile functions (Fig. 8, Tab. 2) <sup>247,258</sup>. Although some studies about K6-, K11-, K27-, K29- and K33-linked polyubiquitination exist <sup>227,259-262</sup>, their role in cell signalling is not well understood, despite the observed connection to proteasomal degradation <sup>263,264</sup>. The best characterised linkage types are K48- and K63-linked polyubiquitination. A protein which is decorated with at least four K48-linked ubiquitin molecules can be sensed by receptors of the 26S proteasomal degradation machinery <sup>265,266</sup>. In contrast to this, K63-linkage serves as inducer of protein complexes

and protein-stabiliser by blocking proteasomal degradation of K63-linked proteins<sup>259</sup> and is well studied in the context of activation of the NF- $\kappa$ B pathway and the DNA repair machinery<sup>243,267</sup>.

**Table 2:** Ubiquitin linkage types and their role in the cell.

Linkage type	Function
Mono-Ub	Endocytosis, DNA repair, nuclear export <sup>230</sup>
Multi-Ub	Endocytosis <sup>230</sup>
M1-Ub	Activation of the NF- $\kappa$ B pathway <sup>268</sup>
K48-Poly-Ub	Proteasomal degradation <sup>230</sup>
K6,11,27,29,33	Proteasomal degradation <sup>264</sup>
K63-Poly-Ub	Endocytosis, activation of kinases <sup>230</sup>
Heterogeneous Poly-Ub	Proteasomal degradation <sup>269</sup> Activation of IKK complex <sup>270</sup>

The complex ubiquitination patterns are the result of the interplay between E2, E3, ubiquitin and a specific substrate. How a specific lysine residue is targeted and ubiquitinated with a specific chain type and pattern is still not completely understood, but it is known that the interaction of a specific E2 with a specific E3 defines the substrate and the type of ubiquitin-linkage which can be added<sup>243,255,271–273</sup>.

Even more complexity is generated with a mixture of different linkages within one polyubiquitin chain (e.g. K11- and K63-linkages), leading to a heterogeneous<sup>258</sup> polyubiquitination<sup>269,274</sup>, which is specifically recognised by ubiquitin-interacting proteins (Tab. 2)<sup>275</sup>. This demonstrates how diverse and sophisticated ubiquitination can be. It should be mentioned here, that most of these studies were performed *in vitro* and may not reflect the *in vivo* situation. Still, the broad variety of possible ubiquitination patterns shows how difficult it is to understand the whole ubiquitination machinery.

The interaction between an ubiquitinated protein and its binding partner is mediated by ubiquitin binding domains (UBD)<sup>276</sup>. Different UBDS have been identified, mediating the binding to different ubiquitin-linkage types. Since K48-polyubiquitinated proteins are targeted by receptors of the 26S proteasome, these receptors harbour UBDS which are more specific for K48-polyubiquitination than for other linkage

---

types<sup>226,276,277</sup>. In contrast, proteins containing a K63-specific UBD prevent the proteasomal degradation of K63-linked polyubiquitinated proteins<sup>226,278</sup>.

### 1.3.3 Ubiquitin-like proteins

Ubiquitin-like proteins (UBL) represent a group of proteins which have a similar role in cell signalling like ubiquitin itself. The attachment of UBL to substrates is mediated by an ubiquitin-like conjugation system. Like ubiquitin, the UBL-modified substrates also change their translocation status, or the ability to be bound by other proteins<sup>279</sup>. Ubiquitin is only expressed in eukaryotes, but ubiquitin-like proteins, e.g. the prokaryotic ubiquitin-like protein (Pup) from *Mycobacterium tuberculosis*<sup>280</sup>, were identified in prokaryotes<sup>281</sup>.

Autophagy is an example for the important role of UBL in eukaryotes, where the UBL autophagy-related gene 12 (ATG12) is linked with help of the E1 ATG7 and the E2 ATG10 to a lysine residue of ATG5<sup>10</sup>. In complex with ATG16, ATG5-ATG12 then acts as E3 ligase and recruits one of the UBL ATG8 family members, like LC3<sup>10</sup>, to the autophagosomal membrane, where it is conjugated with phosphatidylethanolamine (PtdEth)<sup>282</sup>. This conjugation step is crucial for the formation of the autophagosomal membrane to degrade intracellular cargo<sup>279,283</sup>.

### 1.3.4 Deubiquitination

Since ubiquitination is a reversible post-translational modification, ubiquitin or UBLs can be removed from modified proteins again. This process is mediated by deubiquitinating enzymes (DUB), a family of ubiquitin-specific proteases<sup>224,239</sup>. In total, DUBs have three roles in the ubiquitination system (Fig. 9)<sup>284,285</sup>. First of all, as mentioned above, ubiquitin needs to be processed after the expression of ubiquitin precursors<sup>242</sup>. These precursors are cleaved at distinct positions, releasing free ubiquitin which can be used by the ubiquitin-conjugation system<sup>237,238</sup>. Second, DUBs have an opposing role to E3 ligases, by cleaving ubiquitin from previously ubiquitinated proteins<sup>286</sup>. This changes the activation status of proteins by removing K63-linked polyubiquitination, or prevents their proteasomal degradation by removing e.g. K48-linked polyubiquitination. The third function of DUBs is the recycling of polyubiquitin chains, which

were cleaved off from proteins and can be reused by the ubiquitin-conjugation system<sup>287</sup>. For recognition of ubiquitinated proteins, DUBs can also contain an UBD, which defines the linkage type that can be targeted<sup>288</sup>.

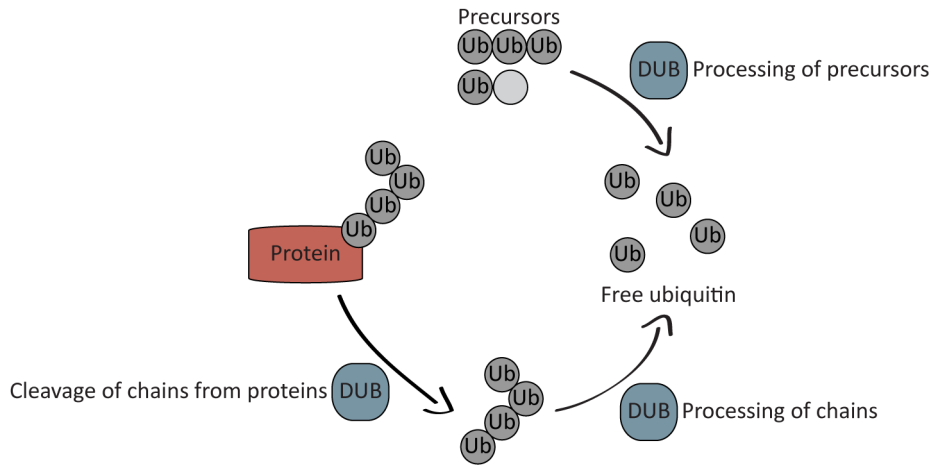


**Figure 9:** DUBs have different roles in the ubiquitin pathway. Ubiquitin is expressed as a precursor which is activated by DUBs. Ubiquitin can be cleaved from proteins to alter their ubiquitination status. The recycling from ubiquitin chains leads to free ubiquitin molecules which can be used by the ubiquitination pathway. Adapted from Komander et al., 2009<sup>285</sup>.

DUBs are important to downregulate signalling cascades, which are activated by ubiquitination or vice versa<sup>284,289</sup>. Defects in the expression or activity of DUBs have been linked to several diseases like inflammation and cancer<sup>290,291</sup>.

There are almost 100 different known DUBs<sup>292</sup> encoded on the human genome, which are divided into five families, according to the structural homology of their catalytic domains: ubiquitin-specific proteases (USP), ovarian tumour proteases (OTU), Machado-Josephin domain proteases (MJD), ubiquitin C-terminal hydrolases (UCH) and the JAB1/MPN/Mov34 metalloenzyme (MPN+/JAMM)<sup>285</sup>. However, the substrate- and linkage-specificity within the DUB-families is very diverse. Within the USP- and OTU-family were DUBs identified which either cleave K48- or K63-linked chains<sup>285</sup>, showing that the catalytic domain alone is not sufficient to obtain linkage-specificity, but that other structural motifs, like the UBD, play a critical role in mediating linkage- and substrate-specific protease activity<sup>285</sup>.

The interplay of ubiquitination-patterns on proteins is very important to initiate, maintain or terminate the activation of signalling pathways. TNF $\alpha$ -induced NF- $\kappa$ B activation leads to complex formation at the TNF-receptor, including TRAF2, RIP1 and

cellular inhibitors of apoptosis (cIAPs)<sup>293,294</sup>. The E3 ligase activity of cIAP1 and cIAP2 leads to K63-linked polyubiquitination of RIP1<sup>295,296</sup>, while cIAP1 additionally adds K11-linked polyubiquitin chains to RIP1<sup>297</sup>. The linear ubiquitin chain assembly complex (LUBAC)<sup>298</sup> and the transforming growth factor  $\beta$ -activated kinase 1 (TAK1) complex are recruited via the K63-linked chains to the TNF-receptor complex<sup>299</sup>. LUBAC adds M1-linked polyubiquitin to RIP1<sup>300</sup>, thereby promoting the recruitment of the inhibitor of nuclear factor  $\kappa$ -B kinase (IKK) complex<sup>297</sup>. The IKK subunit NEMO (IKK $\gamma$ ) is then also M1-linked polyubiquitinated by LUBAC<sup>301</sup>. This leads to a conformational change of the IKK complex, which then can be phosphorylated by the TAK1-complex at IKK $\beta$ , initiating its kinase activity<sup>302</sup>. The activated IKK complex then phosphorylates I $\kappa$ B $\alpha$ , which is subsequently decorated with K48-linked polyubiquitin chains<sup>303</sup>. This leads to the proteasomal degradation of I $\kappa$ B $\alpha$ , facilitating the translocation of NF- $\kappa$ B subunits into the nucleus and finally the transcription of proinflammatory target genes<sup>303,304</sup>.

As described above, NF- $\kappa$ B activation is dependent on the interplay of many proteins, harbouring UBDs or ligase activity and on different ubiquitin-patterns (M1-, K11- and K63-linked polyubiquitin) for a correct and efficient signal transduction.

### 1.3.5 The unusual ubiquitin-converting enzyme A20

The downregulation of NF- $\kappa$ B signalling is, amongst other proteins like cylindromatosis (CYLD)<sup>305</sup>, mainly mediated by the TNF $\alpha$ -induced protein 3 (TNFAIP3), also known as A20<sup>284</sup>. Its expression is induced upon TNF $\alpha$  stimulation of the NF- $\kappa$ B pathway, leading to a negative feedback loop<sup>306,307</sup>. A20 is encoded by the gene *TNFAIP3*, which is located on chromosome 6q23<sup>308</sup>. Its expression results in a 80 kDa protein, with unusual properties, because it combines E3 ligase and deubiquitinating activities, making it an ubiquitin-editing enzyme (Fig. 10)<sup>309</sup>. The DUB activity is mediated by the N-terminal OTU-domain, in which the residue C103 is critical for catalytic activity (Fig. 10)<sup>310</sup>. Within the C-terminal zinc finger (ZnF) region, which consists of seven ZnF repeats, ZnF4 mediates E3 ligase activity<sup>276,311</sup>. Additionally, ZnF4 and ZnF7 harbour ubiquitin-binding domains, important for interactions between A20 and ubiquitinated proteins<sup>312,313</sup>, initiating its NF- $\kappa$ B inhibitory function<sup>314</sup>. The modification of K63-linked to K48-linked polyubiquitination of RIP1 by A20 was shown to be important for the downregulation of TNF $\alpha$ -induced NF- $\kappa$ B activation<sup>311,315,316</sup>.

The interaction with RIP1 is mediated by the ZnF4 motif, binding to K63-linked polyubiquitin<sup>312</sup>. A20 inhibition of NEMO can be achieved by two different ways: M1-linked polyubiquitinated NEMO is bound by A20's ZnF7, without affecting NEMO's ubiquitination status<sup>314</sup>, or the A20-binding inhibitor of NF- $\kappa$ B (ABIN-1) mediates the binding of A20 to NEMO to target it for proteasomal degradation by editing the ubiquitin-linkage type<sup>317</sup>. In general, A20 relies on interactions with other ubiquitin-binding proteins, like ABIN-1<sup>318</sup> and TAX1 binding protein 1 (TAX1BP1)<sup>319</sup>, and other E3 ligases like Itch<sup>320</sup> and ring finger protein 11 (RNF11)<sup>321</sup>, showing that A20 cannot mediate its complete inhibitory function alone.

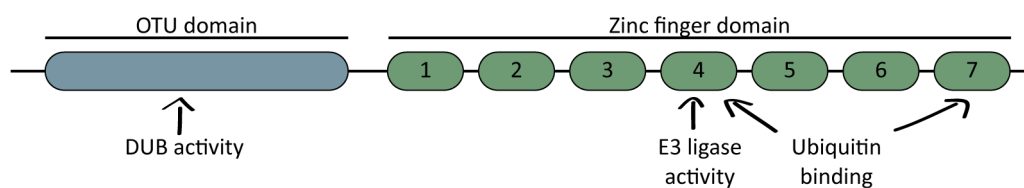


**Figure 10:** A20 consists of two domains, the C-terminal OTU (blue) and the N-terminal Znf-domain with 7 zinc finger repeats (green). The OTU domain harbours deubiquitination activity, while ubiquitination activity is mediated by zinc finger 4. Additionally, zinc finger 4 and 7 bind ubiquitin for substrate recognition. Adapted from Vereecke et al., 2009<sup>309</sup>.

Furthermore, A20 can block the interaction of E2 and E3 proteins, thereby inhibiting their potential to ubiquitinate target proteins<sup>322</sup> within the NF- $\kappa$ B cascade. Besides its function in the TNF $\alpha$ -induced NF- $\kappa$ B pathway, A20 is also counteracting in other NF- $\kappa$ B activating pathways, like TLR-, NOD and TCR-signalling<sup>323-325</sup>.

Additionally to the downregulation of NF- $\kappa$ B, A20 was shown to have a protective influence on TNF $\alpha$ -, TRAIL- and TCR-induced apoptosis<sup>326-329</sup>, as well as on caspase-independent necroptosis<sup>330</sup>. In contrast to this, A20 enhances necrotic cell death, induced by oxidative stress<sup>331</sup>. But functions of A20 vary in different cell types<sup>332,333</sup>.

Due to its role in downregulation of NF- $\kappa$ B, A20 inhibits chronic inflammation<sup>334</sup>. Constitutive NF- $\kappa$ B activation through loss of function of A20 is linked to autoimmune disorders like Crohn's disease, rheumatoid arthritis<sup>335</sup> and several tumour types<sup>308,336</sup>. Diminished expression levels of A20 are linked to mutations in the N-terminal noncoding region of the *TNFAIP3* gene<sup>310</sup>. On the other hand, elevated A20 expression levels can also lead to tumour formation and resistance to TRAIL-treatment by inhibiting

the apoptotic pathway<sup>327,337,338</sup>. In endothelial cells, upregulation of A20 was shown to inhibit CD95-induced apoptosis<sup>339</sup>.

Restoring the natural A20 expression and function, makes A20 a potential drug target in dysregulated NF- $\kappa$ B activation and apoptosis<sup>332,334</sup>.

#### **1.4 Aims of the thesis**

Apoptosis is important for multicellular organisms to maintain cell homeostasis. The correct regulation of apoptosis is critical for an organism, because any dysregulation can lead to severe diseases. Many proteins, controlling the extrinsic and intrinsic apoptotic pathway, can be affected by mutations, which lead to a loss- or gain-of-function. Increased apoptosis inhibition often leads to tumour formation. c-FLIP, an inhibitor of extrinsic apoptosis is a main target in research to restore apoptosis induction in tumours, by downregulating its expression or suppressing its ability to inhibit pro-apoptotic proteins<sup>207,340</sup>. Another apoptosis inhibitor which attained focus of research in the last years is the NF- $\kappa$ B inhibitory protein A20. It was shown that A20 interacts with different proteins in the extrinsic apoptotic pathway, modulating the outcome of apoptosis induction<sup>339,341,342</sup>.

RCC is often diagnosed in a very late stage, because the tumour is symptomless in the early stages. Late staged RCCs usually come with a multiple drug resistance, leading to a poor prognosis of patients diagnosed with RCC<sup>212,343,344</sup>. Therefore, new therapeutic approaches for the treatment of RCCs need to be developed. c-FLIP was found to play a major role in apoptosis-resistance in different tumour types and knockdown of c-FLIP sensitises them to apoptosis induction via TRAIL or CD95L<sup>207,340</sup>. There are no available studies about the role of c-FLIP in mediating CD95L-induced apoptosis resistance in RCCs. Four immortalised clear RCC cell lines from patients were generated, which were further studied in this thesis for the characterisation of the role of c-FLIP<sub>L</sub> and c-FLIP<sub>S</sub> in apoptosis-resistance<sup>345,346</sup>. The RCC cell lines used in this thesis were mostly resistant against TRAIL-induced apoptosis, even in combination with irradiation, due to deficient caspase-9 activation<sup>218</sup>. Deficient CD95 activation was also shown, but the mechanism how this resistance is mediated is not clear<sup>347</sup>. The role of c-FLIP isoforms on mediation of resistance towards CD95L-induced apoptosis and NF- $\kappa$ B activation was investigated.

The NF- $\kappa$ B inhibitory protein A20 was found to be interacting with the CD95L-induced DISC in mass spectrometry and western blot analysis <sup>25</sup>. It is known that A20 modulates and inhibits ligand-induced apoptosis, but the role in CD95L-mediated apoptosis has not yet been revealed. The DISC-interacting proteins FADD <sup>348</sup> and caspase-8 <sup>349</sup> are known to be ubiquitinated for pro-survival signalling. After TRAIL-stimulation, caspase-8 is targeted by A20 in an anti-apoptotic manner <sup>349</sup>. The expression status of pro- and anti-apoptotic cells in Jurkat E6-1 wildtype and A20-deficient cell lines, and the response to CD95L-induced apoptosis were studied.



## 2 Materials

### 2.1 Chemicals

If not stated otherwise, chemicals were purchased from Carl Roth (Karlsruhe, Germany) or Sigma Aldrich (Munich, Germany).

#### 2.1.1 Molecular biology

#### 2.1.2 Devices and materials

For cloning purposes, DNA was amplified with the high-fidelity Phusion Flash II DNA Polymerase (Thermo Scientific, Rockford, USA). For checking insert integrity, colony-PCRs were done with 2x KAPA2G fast ReadyMix PCR Kit (Kapa Biosystems, Boston, USA). The DNA amplification was performed with peqSTAR 96 universal thermocyclers from PEQLAB (Erlangen, Germany). Digestion of DNA was done with restriction enzymes from New England Biolabs (Ipswich, USA). DNA was ligated with T4 DNA ligase from New England Biolabs. For plasmid amplification, *Escherichia coli* (*E. coli*) TOP10 from Life technologies (Grand Island, USA) were transformed with DNA in a thermomixer comfort (Eppendorf, Hamburg, Germany). Centrifugation was done in an Eppendorf microcentrifuge 5417R (Eppendorf). Bacteria were cultured in a Heraeus<sup>®</sup> Incubator Function Line B6 (Thermo Scientific) or in a Multitron Standard shaker (Infors AG, Bottmingen, Switzerland). Gel electrophoresis was done in a Perfect Blue<sup>™</sup> Gel System mini M (PEQLAB). Documentation of gels was performed with a UV documentation system by INTAS science imaging (Göttingen, Germany).

#### 2.1.3 Restriction enzymes

Enzyme	Restriction site
NotI-HF <sup>®</sup>	5' - GC∇GGCC GC - 3' 3' - CG CCGG∧CG - 5'
XhoI	5' - C∇TCGA G - 3' 3' - G AGCT∧C - 5'
BsmBI	5' - CGTCTC(N)1∇ - 3' 3' - GCAGAG(N)5∧ - 5'
KpnI-HF <sup>®</sup>	5' - G GTAC∇C - 3' 3' - C∧CATG G - 5'
BamHI-HF <sup>®</sup>	5' - G∇GATC C - 3' 3' - C CTAG∧G - 5'

## 2.1.4 Oligonucleotides

### 2.1.4.1 Sequencing of the *CFLAR*-gene

Primer	Sequence (5'- ... -3')
c-FLIP_seq	CCTAAAGGCAGCTGTTGTC

### 2.1.4.2 Generation of c-FLIP<sub>L</sub>-MUT

Primer	Sequence (5'- ... -3')	Tm
c-FLIP_BamHI fwd	CGAGGATCCACCGGAGCTTACCATGTCTGCTGAAGTCATCC	53 °C
c-FLIP_BamHI fwd2	CGAGGATCCACCGGAGCTTAC	64 °C
c-FLIP <sub>L</sub> _KpnI rev	GCTGGTACCTTATGTGTAGGAGAGGATAAG	64 °C
c-FLIP_MUT fwd	CCCTCACTTGGTCAGCGACTATAG	64 °C
c-FLIP_MUT rev	CTATAGTCGCTGACCAAGTGAGGG	64 °C

### 2.1.4.3 qRT-PCR of c-FLIP

Primer	Sequence (5'- ... -3')	Tm
c-FLIP_WT fwd	AACCCTCACCTTGTTTCG	55 °C
c-FLIP_MUT fwd	AACCCTCACTTGGTCAGC	55 °C
c-FLIP rev	AACTCAACCACAAGGTCCA	55 °C
β-Actin fwd	TGTTACCAACTGGGACGACA	58 °C
β-Actin rev	TCTCAGCTGTGGTGGTGAAG	58 °C

### 2.1.4.4 Generation of A20-targeting CRISPR/Cas9 constructs

Primer	Sequence (5'- ... -3')	Tm	Misc
A20_gRNA#1 fwd	<u>CACCGAGAGGAGTCGTATTAAGTC</u>		5'-P
A20_gRNA#1 rev	AAACGACTTTAATACGACTCCTCTC		5'-P
A20_gRNA#2 fwd	<u>CACCGTCCAGTGTGTATCGGTGCA</u>		5'-P
A20_gRNA#2 rev	AAACTGCACCGATACACACTGGAAC		5'-P
A20_gRNA#3 fwd	<u>CACCGAACCATGCACCGATACACAC</u>		5'-P
A20_gRNA#3 rev	AAACGTGTGTATCGGTGCATGGTTC		5'-P
A20_cloning fwd	AGTCCTCGAGCTCCCTGACAAACATTACTG	53 °C	
A20_cloning rev	AGTCGCGCCGCTTTGAGTTTGGGCTTGTC	53 °C	
U6_seq	TCACACGACCTGGATGGAGT		
A20_seq	AAGAGCAGGAGTGCTTGGTG		

## 2.2 Cell culture

### 2.2.1 Devices and materials

Cells were cultured in cell culture flasks, 10 cm dishes or 6-well, 12-well and 96-well plates from Sarstedt (Nümbrecht, Germany). Sterile 5 mL, 10 mL and 25 mL pipettes were used from Sarstedt, 10  $\mu$ L, 200  $\mu$ L and 1 mL sterile pipette tips were from Starlab (Hamburg, Germany). Greiner bio-one (Frickenhausen, Germany) provided 15 mL and 50 mL reaction tubes, 1.5 and 2 mL reaction tubes were bought from Sarstedt. Syringes were from Becton Dickinson (Heidelberg, Germany) and 0.45  $\mu$ m sterile filters from Merck Millipore (Billerica, USA). Counting of cells was performed with a Neubauer improved counting chamber from BRAND scientific (Wertheim, Germany). Culturing of cells was done in a HERAcell™ 240i incubator (Thermo Scientific). Cells were handled in SterilGARD® III by The Baker Company (Sanford, USA). Centrifugation was performed in a 5810R centrifuge from Eppendorf (Hamburg, Germany) or a Megafuge® 1.0 from Heraeus® (Osterode, Germany).

### 2.2.2 Mediums and reagents

Medium/Reagent	Order No	Company
Bortezomib	sc-217785	Santa Cruz Biotechnology
DMEM (high glucose)	11965	Gibco® - Life technologies
Fetal calf serum (FCS) (Lot# A 10108-2367)	A15-101	PAA Laboratories (Paschen, Austria)
Ionomycin	I-0634	Sigma Aldrich
LPS from <i>E. coli</i>	L4516	Sigma Aldrich
Necrostatin-1 (Nec-1)	AP-309	Enzo Life Sciences (Lauen, Austria)
Penicillin/Streptomycin	15070	Gibco® - Life technologies
Q-VD-OPh (QVD)	03OPH109	MP Biomedicals (Aurora, OH, USA)
Protein A from <i>S. aureus</i>	P6031	Sigma Aldrich
Phorbol 12-myristate 13-acetate (PMA)	P8139	Sigma Aldrich
Puromycin	P8833	Sigma Aldrich
RPMI 1640	12440	Gibco® - Life technologies
Trypsin/ EDTA (0.05 %)	25300	Gibco® - Life technologies

### 2.2.3 Functional antibodies and recombinant proteins

Specificity	Clone name	Company
FLAG <sup>®</sup> -anti-K48-TUBE		Lifesensors (Malvern, USA)
FLAG <sup>®</sup> -anti-K63-TUBE		Lifesensors
CD95L	scErbB2	Recombinant protein, self-purified
CD95L	5G51	Dr. K. Schulze-Osthoff (Tübingen, Germany)
CD95	2R2	Dr. K. Schulze-Osthoff
TRAIL	2E5	Sigma Aldrich

## 2.3 Western blot analysis

### 2.3.1 Devices and materials

Lysates were sonicated using a Bioruptor<sup>®</sup> (NextGen, Diagenode, USA). Protein separation was done with a Mini-PROTEAN<sup>®</sup> Tetra Vertical Electrophoresis Chamber and transfer of proteins to PVDF membranes (GE Healthcare, Buckinghamshire, UK) was performed in a mini Trans-Blot<sup>®</sup> Electrophoretic Transfer Cell (Biorad, München, Germany). Antibodies were incubated with the Stuart roller mixer SRT9 from Bibby Scientific (Staffordshire, UK) and Duomax 1030 (Heidolph Instruments, Schwabach, Germany). Chemiluminescence detection reagents were provided from GE Healthcare or Li-Cor (Lincoln, USA). Chemiluminescence was detected by the camera system Fusion FX7 (PEQLAB) or with photosensitive Amersham Hyperfilm<sup>™</sup> ECL<sup>™</sup> (GE Healthcare). Development of photosensitive films was done with the Curix 60 system from AGFA Healthcare (Greenville, USA).

### 2.3.2 Primary antibodies

Specificity	Clone name	Isotype	Company
A20	A-12	Mouse IgG2a	Santa Cruz Biotechnology (Dallas, USA)
$\beta$ -Actin	Ac-74	Mouse IgG2a	Sigma Aldrich (St. Louis, USA)
Bcl-x	Polyclonal	Rabbit IgG	BD Biosciences (San Jose, USA)
Cleaved caspase-3	Asp175	Rabbit IgG	Cell Signaling Technology (CST) (Danvers, USA)
Caspase-8	12F5	Mouse IgG2b	Dr. K. Schulze-Osthoff
Caspase-8	C-20	Goat IgG	Santa Cruz Biotechnology
Cleaved caspase-8	18C8	Rabbit IgG	CST
CD95	C-20	Rabbit IgG	Santa Cruz Biotechnology
c-FLIP	Dave-2	Rat IgG2a	Adipogen (Liestal, Switzerland)
c-FLIP	NF6	Mouse IgG1	Enzo Life Sciences (Lörrach, Germany)
FADD	1F7	Mouse IgG1	Merck Millipore
FADD	1C4	Mouse IgG1	Dr. P. H. Krammer (Heidelberg, Germany)
FLAG	M2	Mouse IgG1	Sigma Aldrich
I $\kappa$ B $\alpha$	C-21	Rabbit IgG	Santa Cruz
PARP	4C10-5	Mouse IgG1	BD Biosciences
P-I $\kappa$ B $\alpha$	14D4	Rabbit IgG	CST
P-p65	93H1	Rabbit IgG	CST
Tubulin	DM-1A	Mouse IgG1	Sigma Aldrich
XIAP	48	Mouse IgG1	BD Biosciences

### 2.3.3 Secondary antibodies

All secondary antibodies are coupled with horseradish peroxidase (HRP) to visualise proteins via chemiluminescence.

Reactivity	Host species	Order number	Company
Mouse IgG	Goat	sc-2055	Santa Cruz Biotechnology
Mouse IgG1	Goat	1070-05	Southern Biotechnology (Birmingham, USA)
Mouse IgG2a	Goat	1080-05	Southern Biotechnology
Mouse IgG2b	Goat	1090-05	Southern Biotechnology
Goat IgG	Rabbit	6160-05	Southern Biotechnology
Rabbit IgG	Goat	4030-05	Southern Biotechnology
Rabbit IgG light chain	Mouse	211-032-171	Jackson ImmunoResearch (Bar Harbor, USA)
Rat IgG	Goat	3050-05	Southern Biotechnology

## 2.4 Flow cytometry and microscopy

### 2.4.1 Devices and materials

Stainings for flow cytometric analysis were performed in polypropylene tubes from Sarstedt. Samples, stained with specific, fluorescently labelled, antibodies were analysed by BD FACSCalibur™, BD FACSCanto™ or BD FACS LSRFortessa™ (BD Biosciences). Acquired data was analysed by FlowJo software (Tree Star, Ashland, USA). Cover glasses and slides for microscopic analysis were purchased from Thermo Scientific.

Confocal fluorescence microscopy pictures were taken with an Eclipse Ti (Nikon, Düsseldorf, Germany), supplied with an UltraViewVox Spinning Disc from Perkin Elmer (Waltham, USA) and analysed with Volocity 3D Image (PerkinElmer).

Cells were analysed with a Nikon Eclipse TE300 microscope (Nikon instruments, Melville, USA). Bright field images were taken with a Nikon DS 2MBWC camera and NIS-Elements software (Nikon instruments, Melville, USA).

### 2.4.2 Antibodies and reagents

Specificity/Reagent	Clone name/ Order Number	Fluorochrome	Company
CD95	2R2		Dr. K. Schulze-Osthoff
CD95L	5G51		Dr. K. Schulze-Osthoff
TRAIL	2E5		Enzo Life Sciences
TRAIL-R1	HS101		Enzo Life Sciences
TRAIL-R2	DJR2-4	PE	eBiosciences
TNF-R1	H398		Dr. H. Wajant (Würzburg, Germany)
Active-Caspase-3	C92-605	PE	BD Biosciences
Mouse IgG	A-11005	AF-594	Invitrogen (Carlsbad, USA)
Mouse IgG	115-116-146	PE	Jackson ImmunoResearch
7-amino-actinomycin D (7AAD)	559925	647	BD Biosciences
AnnexinV	550475	APC	BD Biosciences
Fluorescence mounting medium	S3023		Dako (Hamburg, Germany)

## 2.5 Frequently used buffers

If not stated otherwise, buffers were prepared in dH<sub>2</sub>O.

### 2.5.1 Cell lysis

Buffer	Ingredients
DISC lysis buffer	30 mM Tris-HCl pH 7,4, 150 mM NaCl, 10 % v/v Glycerin, 1 % v/v Triton™ X-100, 2 mM EDTA, 10 mM NaF
TPNE lysis buffer	Ad 300 mM NaCl, 1 % v/v Triton™ X-100, 1 mM EDTA in PBS, pH 7.4
TUBE lysis buffer	100 mM Tris-HCl, pH 8.0, 0.15 M NaCl, 5 mM EDTA, 1 % v/v NP-40, 0.5 % v/v Triton™ X-100
TUBE reaction buffer	100 mM Tris-HCl, pH 8.0, 0.15 M NaCl, 5 mM EDTA, 0.1 % v/v NP-40, 0.05 % v/v Triton™ X-100
TUBE wash buffer	100 mM Tris-HCl, pH 8.0, 0.15 M NaCl, 5 mM EDTA, 0.05 % v/v NP-40
100x protease inhibitor cocktail	100 µg/mL Aprotinin, 100 µg/mL, 100 µg/mL Leupeptin, 100 µg/mL Pepstatin A, 100 µg/mL Chymostatin

### 2.5.2 Flow cytometry

Buffer	Ingredients
10x AnnexinV buffer	0.1 mM HEPES/NaOH, 1.4 M NaCl, 25 mM CaCl <sub>2</sub> , pH 7.4
FACS buffer	2 % w/v BSA, 0.01 % w/v Sodium azide in PBS
Nicoletti buffer	0.1 % (v/v) Triton™ X-100, 0.1 % Trisodium citrate, 50 µg/mL Propidium iodide
PBS	155 mM NaCl, 3 mM NA <sub>2</sub> HPO <sub>4</sub> , 1.1 mM K <sub>2</sub> HPO <sub>4</sub> , pH 7.4



### 2.5.3 Western blot

Buffer	Ingredients
5x Reducing sample buffer (RSB)	50 mM Tris, pH 6.8, 10 % w/v SDS, 25 % v/v $\beta$ -Mercaptoethanol, 50 % v/v Glycerin, 0.25 mg/ml Bromphenolblue
Blocking buffer	5 % w/v Non-fat dry milk, 0.2 % v/v Tween <sup>®</sup> -20 in PBS
Running buffer	25 mM Tris, pH 8.0, 192 mM Glycerin, 1 % v/v SDS
TBS	137 mM NaCl, 2.68 mM KCl, 24.76 mM Tris, pH 7.4
Transfer buffer	25 mM Tris, pH 8.0, 192 mM Glycerin, 20 % v/v Methanol
Washing buffer	0.05 % v/v Tween <sup>®</sup> -20 in TBS

### 2.5.4 Miscellaneous

Buffer	Ingredients
HBS	0.28 M NaCl, 0.05 M HEPES, 1.5 mM Na <sub>2</sub> HPO <sub>4</sub> , pH 7.0
LB medium	1 % w/v Tryptone, 0.5 % w/v Yeast extract, 85.6 mM NaCl, 1 mM NaOH
TAE buffer	40 mM Tris Base, 20 mM Acetic acid, 1 mM EDTA, pH 8.5

## 3 Methods

### 3.1 Molecular biology

#### 3.1.1 Cloning of DNA fragments

For cloning, the target vector and the insert were cleaved with restriction enzymes. Up to 5 µg of DNA were incubated with 5 U of restriction enzyme(s) with the appropriate reaction buffer, adjusted with dH<sub>2</sub>O, in a total volume of 30 µL. The reaction was incubated according to the manufacturer's protocol for at least one hour. When advised, reactions were inactivated by heating the samples for 20 min. After DNA purification with QIAquick<sup>®</sup> PCR purification Kit or QIAquick<sup>®</sup> Gel Extraction Kit (QIAGEN, Hilden, Germany), 50 ng of the linearised and dephosphorylated vector and 50 or 150 ng of the insert were ligated with T4 ligase in ligase buffer and dH<sub>2</sub>O in a total reaction volume of 20 µL. The ligation was incubated at 16 °C overnight in a thermocycler.

#### 3.1.2 Transformation of bacteria

Chemically competent *E. coli* TOP10 cells were transformed with the ligated plasmids. 50 µL of *E. coli* TOP10 cells were thawed on ice, mixed with 10 µL of the ligated plasmids and incubated on ice for 10 min. After a heat shock at 42 °C for 30 seconds, the cells were incubated on ice for 2 min. 500 µL LB-medium was added and the bacteria were incubated in a thermomixer at 37 °C with 700 rpm for one hour. The bacteria were plated on LB agar plates with 100 µg/mL ampicillin and incubated at 37 °C overnight.

### 3.1.3 PCR for cloning of DNA fragments

For cloning purposes, a PCR was performed in a total volume of 50  $\mu\text{L}$  with 0.25  $\mu\text{M}$  of the forward and reverse primer, 25  $\mu\text{L}$  2x Phusion Flash PCR Master Mix (Thermo Scientific) and up to 50 ng of template DNA, adjusted with  $\text{dH}_2\text{O}$ .

Step	Temperature	Time	Cycles
Initial denaturation	98 °C	10 sec	
Denaturation	98 °C	1 sec	x32
Annealing	X °C*	5 sec	
Extension	72 °C	15 sec/kb	
Final extension	72 °C	2 min	
Storage	8 °C	forever	

\* Optimal primer annealing temperature is variable and can be found in chapter 2.1.4.

### 3.1.4 PCR for verification of plasmid integrity

To test transformation efficiency of *E. coli* TOP10 cells with plasmids, a colony-PCR was performed. One colony was added to 10  $\mu\text{L}$  total reaction volume, containing appropriate primers.

Step	Temperature	Time	Cycles
Initial denaturation	95 °C	5 min	
Denaturation	95 °C	10 sec	x32
Annealing	X °C*	15 sec	
Extension	72 °C	5 sec/kb	
Final extension	72 °C	2 min	
Storage	8 °C	forever	

\* Optimal primer annealing temperature is variable and can be found in chapter 2.1.4.

### 3.1.5 Isolation of eukaryotic RNA and cDNA synthesis

Total RNA from  $5 \times 10^5$  eukaryotic cells was purified with RNeasy<sup>®</sup> Plus mini Kit (QIAGEN) according to the manufacturer's protocol. 100 ng of the purified RNA was used to generate cDNA with RevertAid<sup>™</sup> RT Kit (Thermo Scientific, Rockford, USA), using Oligo(dt)18 and random hexamer primers. The synthesis was done according to the manufacturer's protocol in a thermocycler.

### 3.1.6 Quantitative real-time PCR (qRT-PCR)

To detect double stranded DNA, the fluorescent dye SYBR Green was used. The previously synthesised cDNA was mixed with primers and 2x SYBR<sup>®</sup> Green I Master (Roche, Mannheim, Germany). Relative quantification of the gene expression was done by using  $\beta$ -Actin as reference gene. The qPCR was run in triplicates in a LightCycler<sup>®</sup> 96 System (Roche, Mannheim, Germany).

Step	Temperature	Time	Cycles
Initial denaturation	95 °C	10 min	
Denaturation	95 °C	10 sec	x45
Annealing	X °C*	10 sec	
Extension	72 °C	10 sec	
Acquisition	Measure fluorescence		
Melting curve	95 °C	10 sec	
	65 °C	60 sec	
	97 °C	Slow incline	
Acquisition	Measure fluorescence (5x/°C)		

\* Optimal primer annealing temperature is variable and can be found in chapter 2.1.4.

### 3.1.7 Purification of genomic DNA

Whole genomic eukaryotic DNA was purified using DNeasy<sup>®</sup> Blood & Tissue Kit (QIAGEN) from  $1 \times 10^6$  cells.

### 3.1.8 Gel electrophoresis

PCR reactions were loaded on a 1 % (w/v) agarose gel (PEQLAB), supplemented with 0.5  $\mu$ g/mL ethidium bromide, to separate DNA fragments by their length in an electric field with 80 V with 1x TAE buffer. To verify the fragment length, the GeneRuler<sup>™</sup> 1 kB DNA ladder (Thermo Scientific, Rockford, USA) was used.

### 3.1.9 Plasmid purification

For sequencing, 5 mL LB medium was inoculated with one transformed *E. coli* TOP10 colony and incubated at 37 °C with 180 rpm overnight. The plasmid DNA was purified with Zippy<sup>™</sup> Plasmid miniprep Kit (Zymo research, Irvine, USA) according to the manufacturer's protocol. For virus production, 200 mL LB medium were inoculated with 5 mL of a preculture and incubated at 37 °C with 180 rpm overnight. The

---

plasmid DNA was purified with QIAfilter™ Plasmid Maxi kit (QIAGEN) according to the manufacturer's protocol.

### 3.1.10 Determination of the DNA/RNA concentration

The concentration of DNA and RNA was determined with a NanoDrop™ 1000 spectrophotometer (PEQLAB) by measuring the absorbance of the DNA at 260 and 280 nm.

### 3.1.11 Sequencing

For sequencing analysis, plasmid or genomic DNA was sent to Eurofins MWG Operon (Ebersberg, Germany). Sequences were analysed with Geneious™ software (Auckland, New Zealand).

## 3.2 Cellular and protein biochemical methods

### 3.2.1 Cultivation of eukaryotic cells

Adherent renal cell carcinoma (RCC) clear cell lines clearCa-2, -3, -4 and -6 were generated from tumour dissections<sup>345,346</sup> and provided by the Institute of Pathology (University Hospital of Düsseldorf, Germany). RCC and HEK293T cell lines were cultured in DMEM medium, supplemented with 10 % FCS and 1 % Penicillin/Streptomycin. Jurkat E6-1 cells were cultured in RPMI medium with the above given supplements. The culturing conditions were 37 °C with 5 % CO<sub>2</sub> and 95 % humidity. For selecting lentiviral transduced Jurkat E6-1 cells, 1 µg/mL puromycin was added to the culture medium.

### 3.2.2 Production of lentiviral particles and transduction of target cells

The production of lentiviral particles was done in HEK293T cells. The generation of shRNA constructs was previously described<sup>164</sup>. Briefly, cells were transfected with either the lentiviral vector pLKO.1, containing a defined shRNA target sequence, or the gRNA containing Clustered Regularly Interspaced Short Palindromic Repeats/CRISPR-associated endonuclease 9 (CRISPR/Cas9) knockout vector, together with the envelope vector pMD2.G (Addgene, #12259) and the gag-pol expression plasmid pCMV\_dR8.2dvpr (Addgene, #8455). In total, 6 µg of each plasmid were mixed with 500 µL 1x HBS and 30 µL 2.5 M CaCl<sub>2</sub>. For virus production, 2\*10<sup>6</sup> HEK293T cells

---

were transfected. The lentivirus-containing supernatant was collected 24 and 48 h after transfection, filtered through 0.45  $\mu\text{m}$  PVDF filters and stored at 4 °C.

For knockdown of c-FLIP isoforms,  $1 \times 10^5$  RCC cells were transduced with 100  $\mu\text{L}$  of the lentivirus-containing supernatant with 1 mL medium and 5  $\mu\text{g}/\text{mL}$  polybrene. After virus addition, the cells were centrifuged for 90 min with 930 x g at 30 °C. The cells were harvested two or three days after transduction for further analysis.

For CRISPR/Cas9 knockout,  $1 \times 10^6$  Jurkat E6-1 cells were transduced with 500  $\mu\text{L}$  of the lentivirus-containing supernatant with 1 mL medium and 5  $\mu\text{g}/\text{mL}$  polybrene. Transduced clones were selected by adding 0.5  $\mu\text{g}/\text{mL}$  puromycin to the culture medium. Single clone selection was done with the LSR II SORP (BD Biosciences) in a 96-well plate.

### 3.2.3 Immunoprecipitation of the DISC

For immunoprecipitation of the DISC,  $5 \times 10^6$  -  $1 \times 10^7$  cells were stimulated with 5  $\mu\text{g}$  FLAG-tagged sc-Erb2-CD95L or 2  $\mu\text{g}/\text{mL}$  anti-CD95 (2R2) and 10 ng/mL Protein A for one hour. Cells were lysed in 750  $\mu\text{L}$  DISC buffer for 20-30 minutes on ice and centrifuged with 21.000 x g at 4 °C for 15 minutes. 20  $\mu\text{L}$  of the lysates were mixed with 5  $\mu\text{L}$  5x RSB buffer and stored as lysate control. The remaining lysate was transferred to anti-FLAG<sup>®</sup> M2 Affinity Gel and incubated on a rotating wheel for at least 2 hours at 4 °C. Afterwards, the beads were washed three times with 500  $\mu\text{L}$  DISC lysis buffer to remove unbound proteins. After removal of the supernatant, the beads were resuspended in 25  $\mu\text{L}$  1x RSB buffer and boiled for 5 min at 95 °C. The samples were analysed by western blotting.

### 3.2.4 Immunoprecipitation of ubiquitinated proteins

For immunoprecipitation of ubiquitinated proteins,  $5 \times 10^6$  -  $1 \times 10^7$  cells were stimulated with 2  $\mu\text{g}/\text{mL}$  anti-CD95 antibody and 10 ng/mL Protein A for one hour. Cells were resuspended in 100  $\mu\text{L}$  TUBE lysis buffer and incubated for 10 minutes at 95 °C. The samples were sonicated 15 times for 10 seconds each with high intensity. The samples were diluted with 900  $\mu\text{L}$  TUBE reaction buffer and centrifuged for 15 minutes with 21.000 x g at 4 °C. 20  $\mu\text{L}$  of the supernatant were mixed with 5  $\mu\text{L}$  5x RSB buffer and stored as lysate control. The lysates were divided into two reaction

---

tubes and 4 µg FLAG<sup>®</sup> -anti-K48-TUBEs or FLAG<sup>®</sup> -anti-K63-TUBEs were added. The samples were incubated for 2 hours on a rotating wheel at 4 °C. For precipitation of ubiquitinated proteins, 2.5 µg M2 anti-FLAG<sup>™</sup> antibody were bound to 10 µL Dynabeads<sup>™</sup> Protein G and added to the TUBE-IPs and incubated overnight at 4 °C on a rotating wheel. Afterwards, the beads were washed three times with 500 µL TUBE wash buffer to remove unbound proteins. The supernatant was removed and the beads were resuspended in 25 µL 1x RSB buffer and boiled for 5 min at 95 °C. The samples were analysed by western blotting.

### **3.2.5 Cell lysis for western blot analysis**

Up to  $1 \times 10^6$  cells were harvested, once washed with 1 mL PBS and lysed in 40 µL TPNE or DISC lysis buffer, supplemented with protease inhibitors for 20-30 min on ice. After centrifugation for 15 min with 21.000 x g at 4 °C, the supernatant was used for western blot analysis.

### **3.2.6 Measuring of protein concentration in lysates**

When samples were probed in western blot analysis, the protein concentration of TPNE and DISC protein lysates was measured with the Pierce BCA Protein Assay Kit (Thermo Scientific) according to the manufacturer's protocol. After incubating the samples for 30 min at 37 °C in the dark, the absorption was measured at 562 nm with the TECAN Infinite<sup>®</sup> M200 device (Tecan Group, Männedorf, Switzerland).

### **3.2.7 Protein gel electrophoresis**

According to the results of the BCA assay, the required volume for 20-40 µg protein content was mixed with 5x RSB. The samples were boiled for 5 min at 95 °C, before they were loaded on a 12 % polyacrylamide gel. The proteins were separated by their molecular weight with 1x SDS running buffer and 80 V.

### **3.2.8 Western blot transfer**

After separation in electrophoresis, proteins were transferred to a methanol-activated polyvinylidene fluoride (PVDF) membrane using 1x transfer buffer for 90 minutes with 100 V.

---

### 3.2.9 Probing with antibodies

After protein transfer, the membrane was incubated in blocking buffer for 1 hour. Afterwards the membrane was incubated in primary antibody solution overnight at 4 °C (see 2.3.2). After washing the membrane three times with TBS-T for 10 min each, it was incubated in HRP-coupled secondary antibody solution for 1 hour at room temperature (see 2.3.3). Finally the blots were washed again three times with TBS-T. The detection was done using different substrates, depending on the signal strength of the given antibodies. For reprobing, the membrane was treated with ReBlot Plus Antibody Stripping Solution (Merck, Darmstadt, Germany) for 30 min, followed by a blocking step with blocking buffer for 1 hour.

### 3.2.10 Coating of functional antibodies

Coating of functional antibodies was previously described Lu and Krauss, 2010<sup>350</sup>. Briefly, 7 µg/cm<sup>2</sup> Protein A was bound to a 24-well polystyrene plate overnight at 4 °C. The next day, the plate was washed with PBS and the plate blocked with 1.5 % BSA overnight at 4 °C. After washing with PBS, 7 µg/cm<sup>2</sup> of functional antibodies were added with 200 µL PBS to the well and incubated overnight at 4 °C (see 2.4.2). The wells were washed with PBS and 50.000 RCC cells plated in the prepared wells.

## 3.3 Flow cytometry and microscopy

### 3.3.1 Nicoletti staining for analysing DNA fragmentation

To measure cell death by DNA fragmentation, cells were incubated in 250 µL Nicoletti buffer for 1-2 hours at 4 °C in the dark. Fluorescence was measured in the PE-channel and the sub-G1 DNA peak rated as dead cells.

### 3.3.2 Staining of death receptors and ligands

For surface marker expression analysis, 5\*10<sup>5</sup> cells were stained with specific primary antibodies for 20 min at 4 °C in FACS buffer (see 2.4.2). After washing, samples with unconjugated primary antibody were stained with a PE-conjugated antibody for 20 min at 4 °C. Fluorescence was measured in the PE-channel.



---

### 3.3.3 Staining of intracellular active caspase-3

Cells were stained for intracellular active caspase-3 with the PE Active Caspase-3 Apoptosis Kit (BD Pharmingen) according to the manufacturer's protocol. The staining was performed with 3  $\mu$ L anti-active-caspase-3-antibody per sample. Fluorescence was measured in the PE-channel.

### 3.3.4 Staining with AnnexinV and 7AAD

For distinguish between early and late apoptosis, cells were stained with 3  $\mu$ L AnnexinV and 0.2  $\mu$ g 7AAD in 100  $\mu$ L AnnexinV binding buffer for 15 min at room temperature. For measurement, 100  $\mu$ L AnnexinV binding buffer was added. Fluorescence of AnnexinV was measured in the FITC-channel, 7AAD was measured in PerCP-Cy5.5-channel.

### 3.3.5 Confocal fluorescence Microscopy

Up to 50.000 cells were seeded on microscopy glass coverslips and incubated overnight. The next day, cells were washed 3 times with PBS and fixed with 3 % paraformaldehyde for 30 minutes at 37 °C. After washing three times with PBS, the cells were stained with 50  $\mu$ L staining solution with specific antibodies, recognizing surface death receptors, overnight at 4 °C in the dark (see 2.4.2). Following another washing step with PBS, cells were incubated in secondary antibody solution for 1 hour at room temperature in the dark. Following another washing step, the nuclei were stained with DAPI for 10 minutes (see 2.4.2). After a final washing step, the glass slips were mounted on microscopy glass slides for analysis.

## 3.4 CRISPR/Cas9 target generation

To target the A20 gene for knockout studies, the online software CRISPR Design (<http://crispr.mit.edu/>) was used <sup>351</sup>. The software generated and validated gRNA sequences against the gene, encoding for A20. Validated gRNA sequences were used to generate CRISPR/Cas9 knockout plasmids (see 2.1.4, target sequences are underlined). Annealing of gRNA-oligonucleotides was performed as followed. 100  $\mu$ M of the 5'- and 3'-oligo were mixed and incubated at 95 °C for 10 minutes in a thermocycler. Afterwards, the device was switched off to cool down the oligonucleotides slowly. A

5'-overhang, complementary to the 3'-overhang of the BsmBI-digested plasmid was inserted by overlapping nucleotides. This feature was used to anneal the gRNA with the plasmid pUC-DHC008 (provided by Dr. Dirk Heckl and Prof. Emmanuelle Charpentier, Hannover Medical School). The generated construct expresses the validated gRNA and the endonuclease Cas9 for targeting and modification of genomic sequences

### **3.5 Statistics**

Statistical analysis was performed with the software GraphPad Prism (GraphPad Software, La Jolla, USA). Significances were calculated with one- or two-tailed non-parametric Mann-Whitney U test.

## 4 Results

### 4.1 The role of c-FLIP in renal cell carcinoma

Late stages of chemoresistant clear cell RCC are characterised by elevated expression levels of CD95. However, this type of cancer fails to be treated with chemotherapy and anticancer drugs, due to resistance against death ligands<sup>218,347,352</sup>. Gerharz et al. generated immortalised clearCa cell lines from RCC patient sample material<sup>345,346</sup>. The characterisation of these cell lines is incomplete in terms of CD95L-induced apoptosis and the role of c-FLIP splice variants<sup>353</sup>. Expression of death receptors was shown in western blot analysis, lacking the information if these receptors are exposed on the cell surface<sup>218</sup>. Furthermore, CD95 expression was not shown for all generated cell lines<sup>347</sup>. Resistance to CD95-induced apoptosis was reported, but the mechanism which mediates this resistance is unclear<sup>217</sup>. To analyse the influence of c-FLIP in CD95L-mediated apoptosis in renal cell carcinoma, four cell lines, clearCa-2, -3, -4 and -6, were chosen<sup>345,346</sup>.

#### 4.1.1 All RCC cell lines express high levels of CD95

The cell lines clearCa-2, -3, -4 and -6 were stained with specific antibodies to detect surface-bound death receptors TRAIL-R1, TRAIL-R2, TNF-R1 and CD95 by flow cytometry (Fig. 11). All four cell lines expressed the four death receptors, but to different extents. Highest TNF-R1 expression was found on clearCa-2, while clearCa-3 and clearCa-6 displayed higher levels of TRAIL-R2. TRAIL-R1 was only expressed in low levels by all four cell lines. CD95 was highly expressed on the surface of all cell lines. Compared to the other cell lines, clearCa-4 showed lower levels of TNF-R1, TRAIL-R1 and TRAIL-R2, but equivalent surface expression of CD95 (Fig. 11). To investigate the role of c-FLIP in CD95L-mediated apoptosis, expression of the CD95-receptor is important to induce apoptosis by stimulation with CD95L. Since all four cell lines showed high surface expression of CD95, all of them were selected for further experiments.

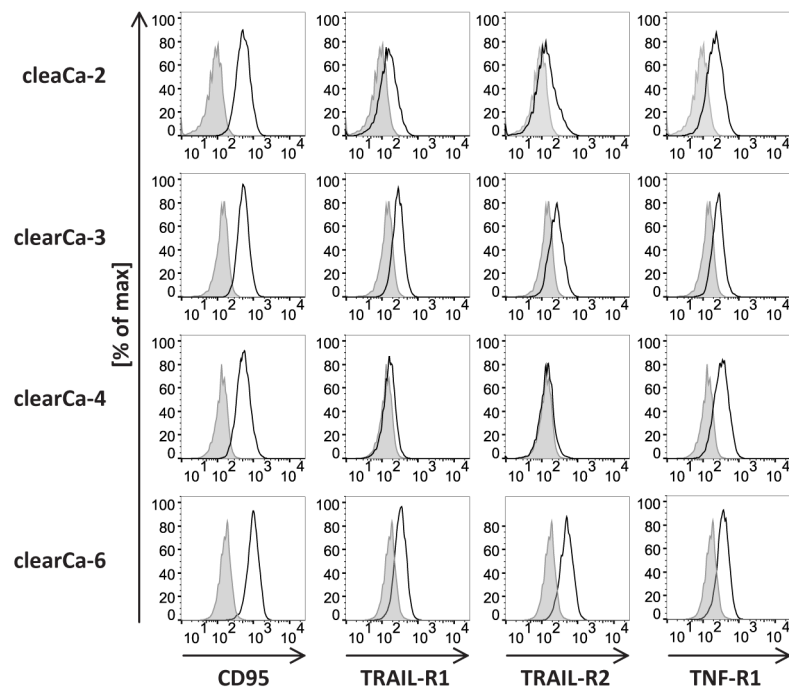


**Figure 11:** Surface expression of death receptors CD95, TRAIL-R1, TRAIL-R2 or TNF-R1 (black line) on RCC cell lines clearCa-2, -3, -4 and -6 was detected by flow cytometry with specific antibodies. Unstained samples are shown in grey.

#### 4.1.2 RCC cell lines show diverse c-FLIP expression

Expression levels of the c-FLIP splice variants c-FLIP<sub>L</sub>, c-FLIP<sub>S</sub> and c-FLIP<sub>R</sub> were examined via western blot analysis under steady-state conditions (Fig. 12). All four cell lines expressed c-FLIP<sub>L</sub>, with higher expression levels detectable in clearCa-2 and clearCa-6. Expression of c-FLIP<sub>S</sub> or c-FLIP<sub>R</sub> was detectable in clearCa-4 and clearCa-6, but was absent in clearCa-2 and only hardly present in clearCa-3. Noticeable is that the p43-FLIP cleavage product, which is generated by cleavage of c-FLIP<sub>L</sub> by caspase-8, was identified. However, the p43-FLIP cleavage product was not detectable throughout all experiments (Fig. 12).

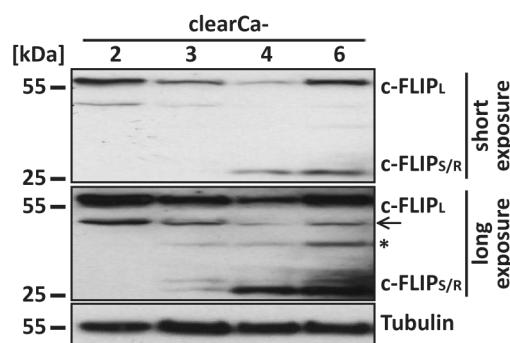


**Figure 12:** c-FLIP protein expression levels of RCC cell lines clearCa-2, -3, -4 and -6 were analysed via western blot with tubulin as loading control.

The expression of c-FLIP<sub>S</sub> and c-FLIP<sub>R</sub> is determined by a SNP in the 3' splice site of intron of 6 in the *CFLAR* gene<sup>152</sup>. When the nucleotide 3' to the sequence TACA is a G, the splice site is functional and leads to expression of c-FLIP<sub>S</sub>, while an A disrupts the splice site, thereby leading to expression of c-FLIP<sub>R</sub>. To analyse the expression of both isoforms, the coding region of c-FLIP was sequenced (Tab. 3).

**Table 3:** Genomic analysis of the *CFLAR* gene in RCC cell lines

Cell line	3' splice site of intron 6	Short c-FLIP splice variant
clearCa-2	TAC <b>AA</b> AT / TAC <b>AA</b> AT	c-FLIP <sub>R</sub>
clearCa-3	TAC <b>AG</b> AT / TAC <b>AA</b> AT	c-FLIP <sub>S</sub> and c-FLIP <sub>R</sub>
clearCa-4	TAC <b>AG</b> AT / TAC <b>AG</b> AT	c-FLIP <sub>S</sub>
clearCa-6	TAC <b>AG</b> AT / TAC <b>AA</b> AT	c-FLIP <sub>S</sub> and c-FLIP <sub>R</sub>

The sequencing result revealed a diverse c-FLIP expression profile in the RCC cell lines. clearCa-2 only expressed the splice variant c-FLIP<sub>R</sub> as short c-FLIP isoform, since the 3' splice site of intron 6 is not functional on both alleles. In clearCa-3 and clearCa-6 one allele harbours a functional splice site, one allele does not, and thus they express both short isoforms, c-FLIP<sub>S</sub> and c-FLIP<sub>R</sub>. The 3' splice site in clearCa-4 is functional on both alleles, hence, clearCa-4 only expresses the short isoform c-FLIP<sub>S</sub> (Tab. 3).

#### 4.1.3 Cycloheximide sensitises RCCs to CD95L-induced apoptosis

c-FLIP blocks receptor-mediated apoptosis. Hence, downregulation of c-FLIP was performed to analyse c-FLIP-dependent apoptosis induction. c-FLIP is a short-lived protein<sup>354</sup>. To inhibit translation of new proteins, and thereby inducing loss of c-FLIP, cells were incubated with cycloheximide (CHX) (Fig. 13a). Cultivation of cells with CHX resulted in almost complete loss of c-FLIP<sub>L</sub>, c-FLIP<sub>S</sub> and c-FLIP<sub>R</sub> expression in all four cell lines after 8 hours of incubation, while XIAP and Bcl-x levels, anti-apoptotic proteins of the intrinsic apoptosis pathway, remained almost stable. Similarly, expression and activation of caspase-8 was not affected by treatment with CHX (Fig. 13a).

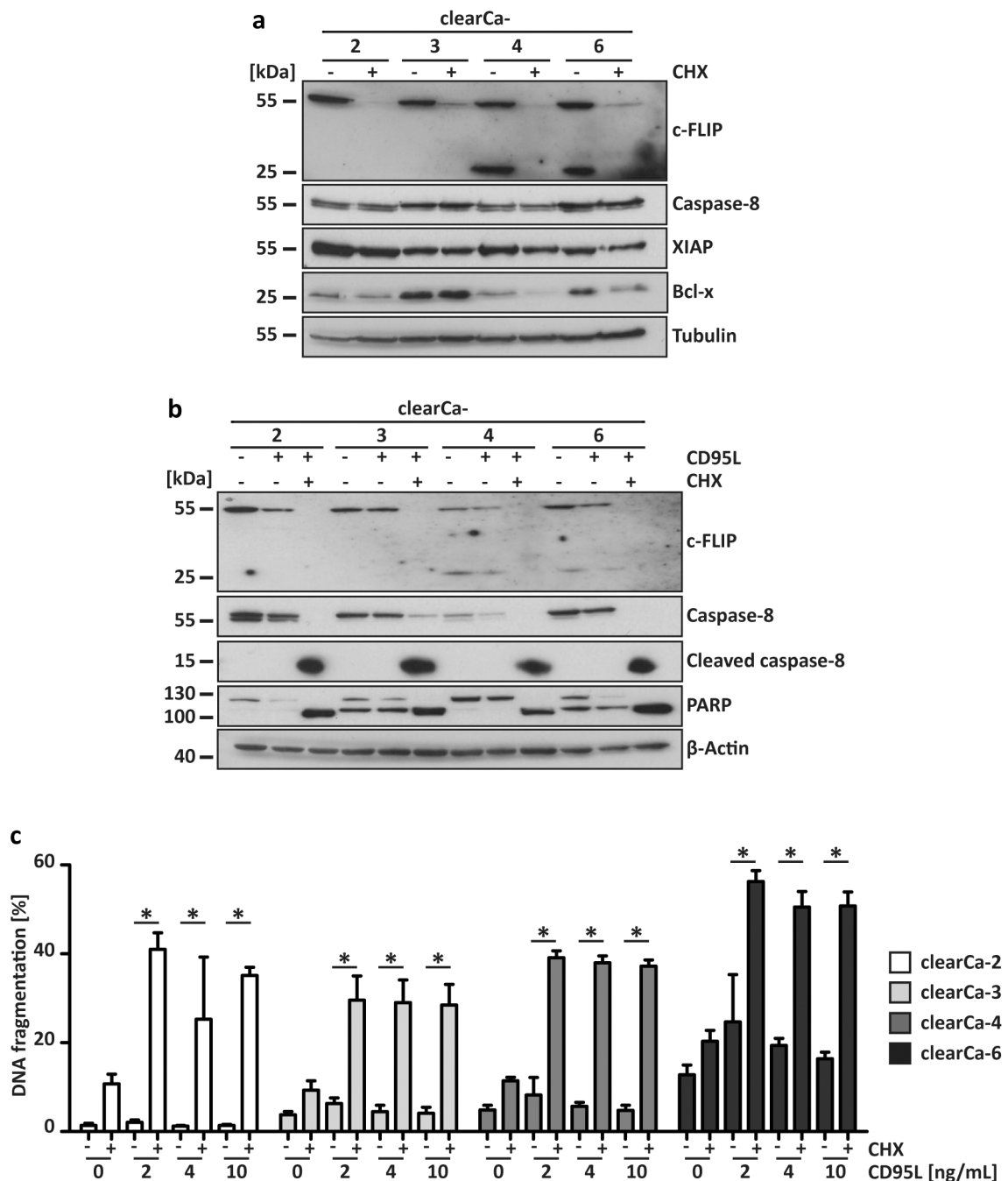


**Figure 13: a:** Analysis of the influence of cycloheximide on anti-apoptotic protein levels in western blot. Cells were treated with 10  $\mu$ g/mL CHX for 8 hours. Tubulin was used as loading control **b:** Western blot analysis of CD95L-induced apoptosis after stimulation with 10 ng/mL CD95L in the presence or absence of 10  $\mu$ g/mL CHX for 8 hours.  $\beta$ -Actin was used as loading control. **c:** Analysis of DNA fragmentation after stimulation of RCC cell lines with 0, 2, 4 or 10 ng/mL CD95L in the presence or absence of 10  $\mu$ g/mL CHX for 16 hours. Bars display the mean of at least three experiments, error bars represent SD. Statistical significances were calculated by one-tailed Mann-Whitney U test; \*  $p \leq 0.05$ .

To investigate if RCC cell lines can be killed by CD95L-induced apoptosis, cells were incubated with CD95L in the presence or absence of CHX and samples were examined by western blot analysis (Fig. 13b). Stimulation with CD95L alone was not sufficient to induce apoptosis, since no cleaved caspase-8 was identified. Furthermore, PARP-

cleavage was not increased in CD95L-stimulated samples compared to unstimulated samples. However, addition of CHX to CD95L-treated cells led to the activation of caspase-8 and subsequently elevated cleavage of PARP, showing CD95L-induced apoptosis after downregulation of c-FLIP (Fig. 13b) in all cell lines.

Cell death was addressed by measuring the DNA fragmentation in flow cytometry upon stimulation with different CD95L concentrations in the presence or absence of CHX (Fig. 13c). All cell lines were resistant against CD95L-induced apoptosis without addition of CHX. Furthermore, apoptosis induction was independent of CD95L-concentration when CHX was present, since even low CD95L-concentrations efficiently induced apoptosis in all cell lines. clearCa-6 showed higher basal cell death levels and an increased sensitivity towards CD95L-induced apoptosis than the other cell lines.

Caspase activation is a hallmark of extrinsic apoptosis. To examine caspase-8 and caspase-3 activation, clearCa-4 was stimulated with 10 ng/mL CD95L for up to 8 hours in the presence or absence of CHX (Fig. 14). Caspase-8- and caspase-3-cleavage were not detectable in cells which were stimulated with CD95L only. However, simultaneous stimulation with CHX sensitised clearCa-4 towards CD95L-mediated apoptosis. Caspase-8- and caspase-3 activation was identified after 6 and 8 hours of stimulation, since the cleavage products p43/41 and p18 of caspase-8 and p19/17 of caspase-3 were detected. c-FLIP proteins were completely degraded at these time points (Fig. 14). Taken together, c-FLIP, but not other anti-apoptotic-proteins, mediates resistance towards CD95L-induced apoptosis in all RCC cell lines (compare Fig. 13a,b).

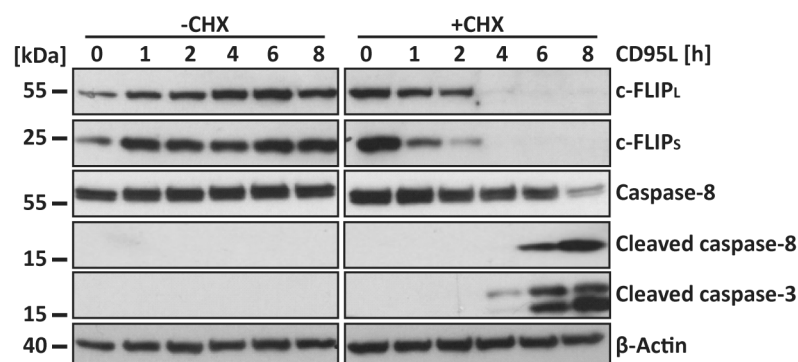


**Figure 14:** clearCa-4 was treated with 10 ng/mL CD95L in the presence or absence of 10 µg/mL CHX for up to 8 hours. Caspase activation was followed by western blot analysis. β-Actin was used as loading control.

---

#### 4.1.4 Simultaneous knockdown of c-FLIP<sub>L</sub>, c-FLIP<sub>S</sub> and c-FLIP<sub>R</sub> drives RCCs into spontaneous cell death

As shown in figure 13, loss of c-FLIP leads to sensitisation of RCCs towards CD95L-induced apoptosis. To further analyse the role of c-FLIP splice variants in CD95L-induced apoptosis, side effects of drugs on other proteins had to be excluded. An efficient approach to decrease protein levels is the use of lentiviral constructs, harbouring a shRNA sequence to specifically target mRNA and thereby blocking their translation to new proteins. Lentiviral constructs, targeting all three isoforms c-FLIP<sub>L</sub>, c-FLIP<sub>S</sub> and c-FLIP<sub>R</sub> (in the following termed c-FLIP<sub>L/S</sub>), and single knockdown constructs for either c-FLIP<sub>L</sub> or c-FLIP<sub>S</sub> were used. There is no functional shRNA targeting c-FLIP<sub>R</sub> only. To further investigate the influence of the two splice variants c-FLIP<sub>L</sub> and c-FLIP<sub>S</sub> in RCCs, it is important that they can be targeted by the single knockdown constructs.

For further analysis, the cell line clearCa-4 was used, since it expresses c-FLIP<sub>L</sub> and c-FLIP<sub>S</sub>, but not c-FLIP<sub>R</sub>, and thereby can be targeted by all lentiviral shRNA constructs (compare Tab. 3). The lentiviral knockdown of c-FLIP isoforms in cell lines is an established method<sup>164,201</sup>. Though, the cultivation of cells treated with the shRNA construct targeting c-FLIP<sub>L/S</sub> was not possible, because cells targeted with this construct died within a few days. While untreated, control-treated and single knockdown cells for c-FLIP<sub>L</sub> or c-FLIP<sub>S</sub> were morphologically unchanged, severe morphological changes were visible after treatment with the c-FLIP<sub>L/S</sub> knockdown construct, showing membrane blebs and apoptotic body formation on day 3 after lentiviral transduction (Fig. 15a). Western blot analysis was performed on day 3 after lentiviral transduction with all knockdown constructs (Fig. 15b). Knockdown efficiency of c-FLIP was moderate to high with all constructs. Interestingly, cells with c-FLIP<sub>L</sub> knockdown expressed more c-FLIP<sub>S</sub> than wild type cells. While single knockdown of c-FLIP<sub>L</sub> or c-FLIP<sub>S</sub> showed no effect on caspase activation, concurrent loss of c-FLIP<sub>L</sub> and c-FLIP<sub>S</sub> led to excessive caspase-8 and caspase-3 activation in clearCa-4 (Fig. 15b).



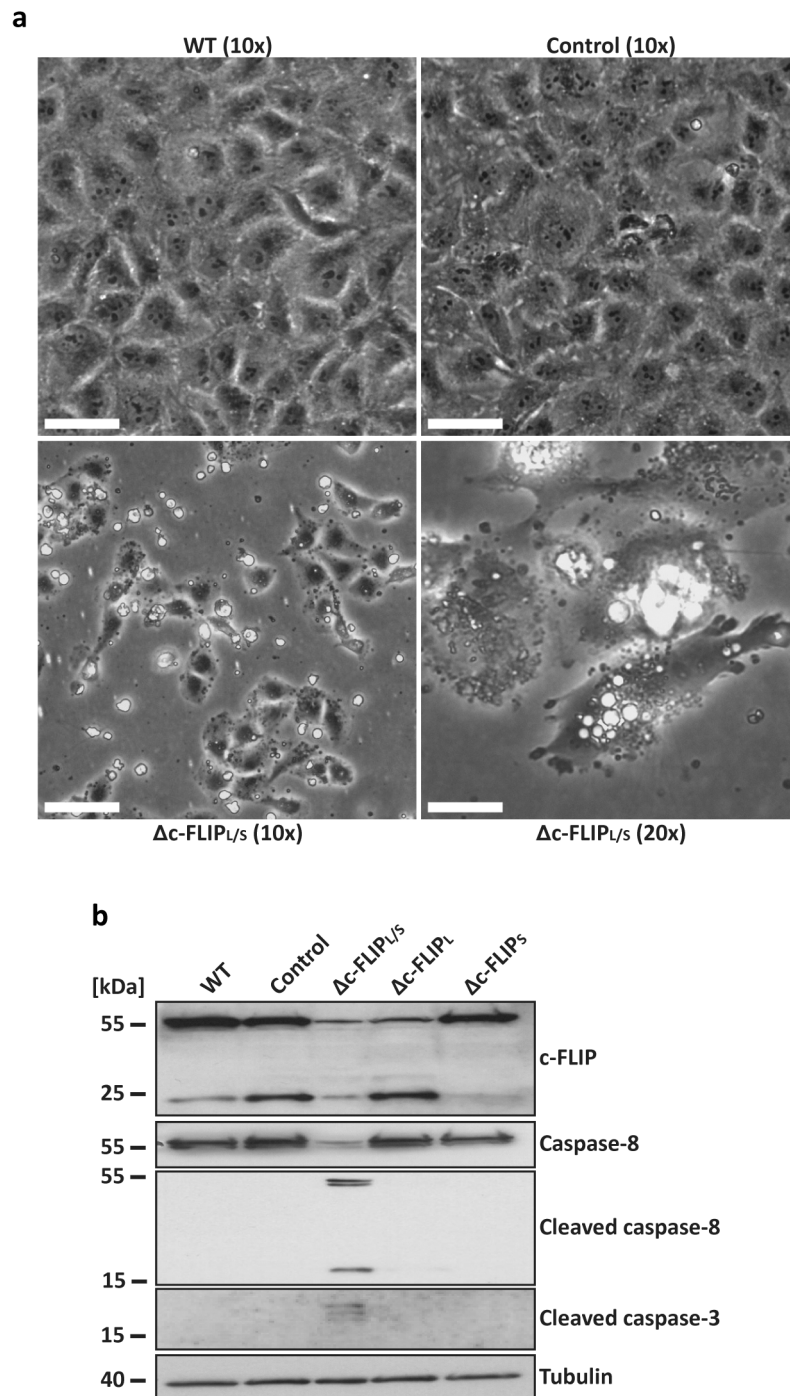


**Figure 15: a-b:** Cells were treated with lentiviral constructs to knockdown c-FLIP isoforms. **a:** Microscopic pictures were taken on day 3 after lentiviral transduction. White bar represents 100  $\mu$ m (10x magnification) or 50  $\mu$ m (20x magnification). **b:** Efficiency of c-FLIP knockdown and caspase activation was verified by western blot analysis.

To analyse if activation of caspase-3 drives cells into death, cells were stained with AnnexinV and 7AAD (Fig. 16a). High rates of viable cells (AnnexinV<sup>-</sup>/7AAD<sup>-</sup>) were identified in unstimulated, control and single knockdown cells, whereas knockdown of c-FLIP<sub>L/S</sub> led to high frequencies of early (AnnexinV<sup>+</sup>/7AAD<sup>-</sup>) and late (AnnexinV<sup>+</sup>/7AAD<sup>+</sup>) apoptotic cells. Knockdown of c-FLIP<sub>L</sub> or c-FLIP<sub>S</sub> did not

increase frequencies of AnnexinV<sup>+</sup>/7AAD<sup>-</sup> and AnnexinV<sup>+</sup>/7AAD<sup>+</sup> cells (Fig. 16a). To corroborate this result, total DNA fragmentation was analysed by staining DNA with propidium iodide (Fig. 16b). DNA fragmentation was almost absent in unstimulated and control cells. Also, single knockdowns of c-FLIP<sub>L</sub> and c-FLIP<sub>S</sub> did not result in elevated levels of DNA fragmentation. However, high frequencies of DNA fragmentation were present after knockdown of c-FLIP<sub>L/S</sub>, displaying cell death. Summarised, clearCa-4 cells died spontaneously after concurrent knockdown of c-FLIP<sub>L</sub> and c-FLIP<sub>S</sub>, without any further stimulation.

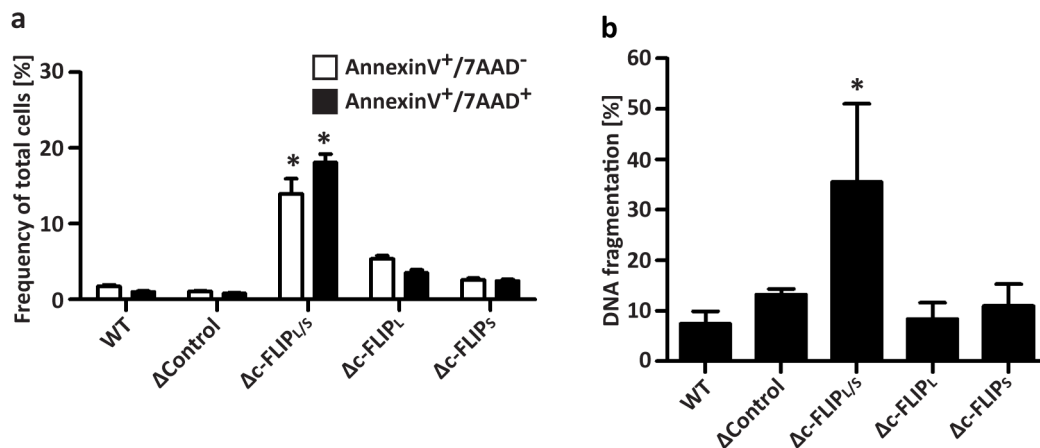


**Figure 16: a-b:** Cells were treated with lentiviral constructs to knockdown c-FLIP isoforms. Cell death was assessed by staining with AnnexinV/7AAD or analysis of DNA fragmentation. Bars display the mean of at least three experiments, error bars represent SD. Statistical significances were calculated by one-tailed Mann-Whitney U test in respect to Control sample; \*  $p \leq 0.05$ .

To examine whether the spontaneous death after loss of c-FLIP<sub>L</sub> and c-FLIP<sub>S</sub> is a clearCa-4-dependent mechanism or true for other RCC cell lines, knockdown of c-FLIP<sub>L/S</sub> was also performed in clearCa-2, -3 and -6. Cell death was examined by flow cytometric analysis of DNA fragmentation (Fig. 17). clearCa-6 generally showed elevated DNA fragmentation even in control treated cells (compare Fig. 13c). DNA fragmentation in the cell lines clearCa-2 and clearCa-3 was detectable only after c-FLIP<sub>L/S</sub> knockdown. These results indicate that c-FLIP expression is required for survival of all RCC cell lines.

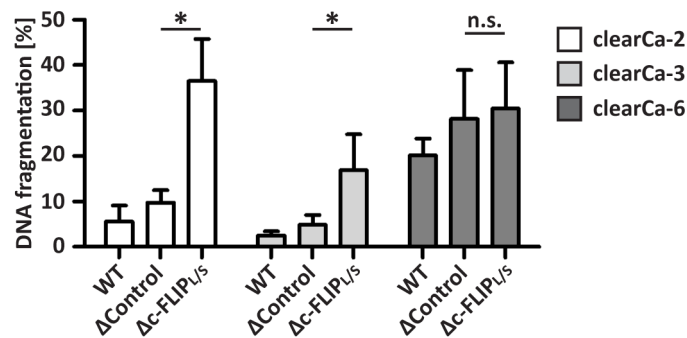


**Figure 17:** Analysis of DNA fragmentation after knockdown of c-FLIP<sub>L/S</sub> on D3 after lentiviral transduction in clearCa-2, -3 and -6. Bars display the mean of at four experiments, error bars represent SD. Statistical significances were calculated by one-tailed Mann-Whitney U test; n.s.=not significant, \*  $p \leq 0.05$ .

#### 4.1.5 Knockdown of c-FLIP<sub>L/S</sub> mediates apoptosis in RCCs

Knockdown of c-FLIP resulted in cell death in all RCC cell lines as described above. The mode of cell death was investigated by culturing clearCa-4 with either the pan-caspase inhibitor Q-VD-OPh (QVD), or the necroptosis inhibitor necrostatin-1 (Nec-1) during lentiviral transduction. Protein lysates were probed in western blot for caspase activation (Fig. 18a). Control cells displayed normal c-FLIP<sub>L</sub> and c-FLIP<sub>S</sub> expression and no caspase activation. Addition of the inhibitors alone had no effect on c-FLIP and caspase-8 expression levels in untransduced cells. Loss of c-FLIP<sub>L/S</sub> led to caspase-8 activation and PARP-cleavage. The pan-caspase inhibitor QVD blocks the protease activity of active caspases, but does not block their initial cleavage potential<sup>355</sup>. The addition of QVD had no effect on caspase-8-cleavage after loss of c-FLIP<sub>L/S</sub> (Fig. 18a), but caspase-activity was blocked, shown by the absence of active caspase-3 (Fig. 18b). Since Nec-1 blocks RIPK1-mediated necroptosis, but not caspase-dependent apoptosis, caspase-activity was not impaired by Nec-1 addition. Hence, Nec-1 did not inhibit caspase-3 activation and PARP-cleavage after loss of c-FLIP<sub>L/S</sub> (Fig. 18).

Additionally to PARP-cleavage, DNA fragmentation was analysed by flow cytometry (Fig. 18c). While the addition of both inhibitors alone had no effect, loss of c-FLIP<sub>L/S</sub> led to increased DNA fragmentation, which was blocked by QVD, but not Nec-1. The impact of single knockdowns of c-FLIP<sub>L</sub> and c-FLIP<sub>S</sub> on DNA fragmentation was analysed, but no cell death was detected. The spontaneous apoptotic cell death, which was blocked by addition of QVD, indicates the importance of all c-FLIP splice variants in RCC on cell survival by impeding the apoptotic pathway.

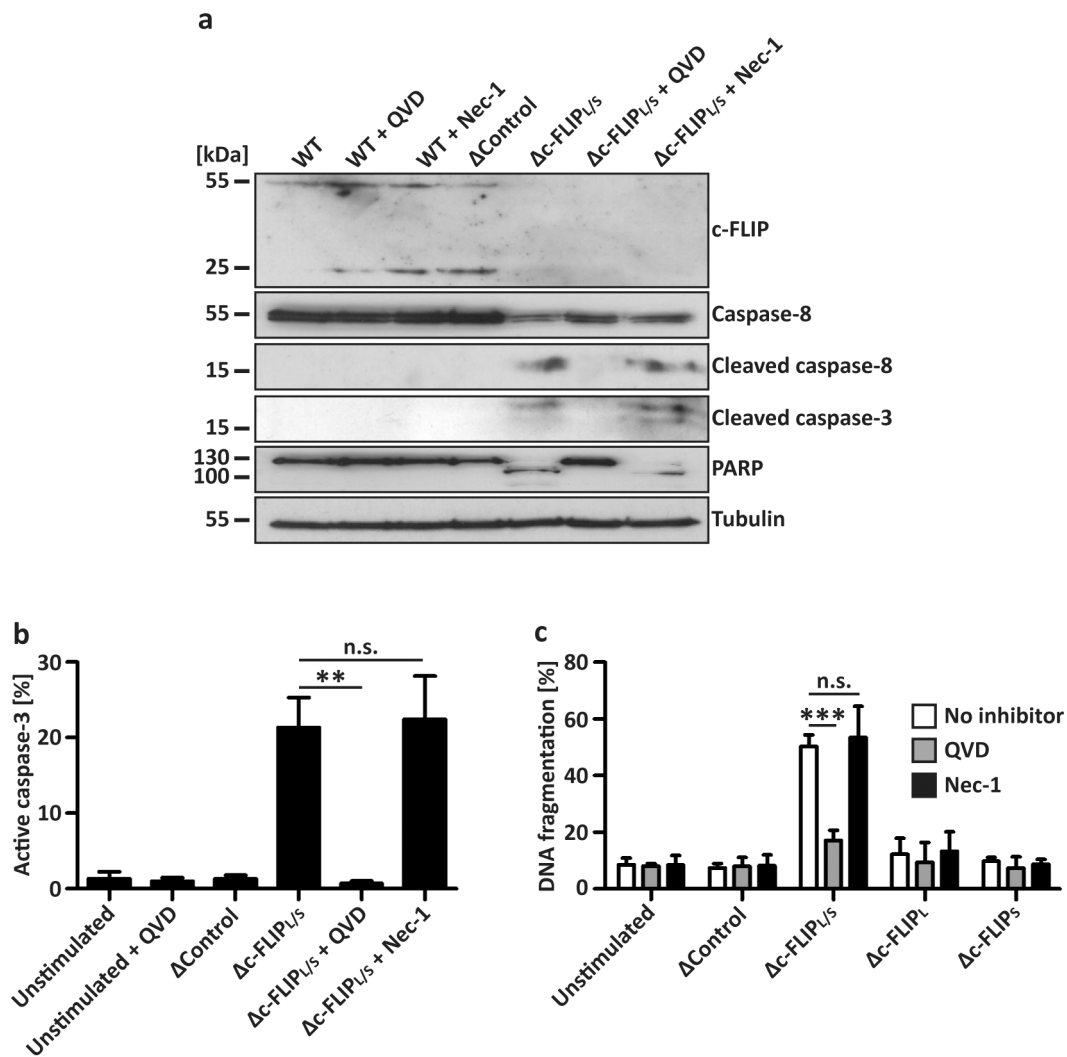


**Figure 18: a-c:** clearCa-4 was treated with a control or c-FLIP<sub>L/S</sub>-targeting construct in the presence or absence of 10  $\mu$ M QVD or 50  $\mu$ M Nec-1. Cells were analysed by western blot (a), caspase-3 activation (b) or DNA fragmentation (c). Tubulin was used as loading control (a). Bars display the mean of at least 4 experiments, error bars represent SD (b-c). Statistical significances were calculated by one-tailed Mann-Whitney U test; n.s.=not significant, \*\*  $p \leq 0.01$ , \*\*\*  $p \leq 0.001$ .

#### 4.1.6 Re-expression of c-FLIP<sub>L-MUT</sub> rescues cells from spontaneous apoptosis

To rule out any consequences on cell viability by side effects of the lentiviral transduction or off-target effects by the introduced shRNA, which could lead to spontaneous apoptotic cell death, a lentiviral construct was generated to re-express a mutated form of c-FLIP<sub>L</sub> during knockdown of c-FLIP<sub>L/S</sub> (in the following termed c-FLIP<sub>L/S</sub>+c-FLIP<sub>L-MUT</sub>). The puromycin-cassette of the c-FLIP<sub>L/S</sub>-targeting plasmid was exchanged with the coding sequence of c-FLIP<sub>L</sub>, harbouring mutations in the shRNA target sequence to avoid the degradation by the simultaneously introduced

shRNA. The inserted mutations were silent, providing expression of functional c-FLIP<sub>L</sub> (c-FLIP<sub>L-MUT</sub>). clearCa-4 cells were transduced with either the knockdown construct targeting c-FLIP<sub>L/S</sub> or the re-expression construct c-FLIP<sub>L/S</sub>+c-FLIP<sub>L-MUT</sub> and cultured for three days.

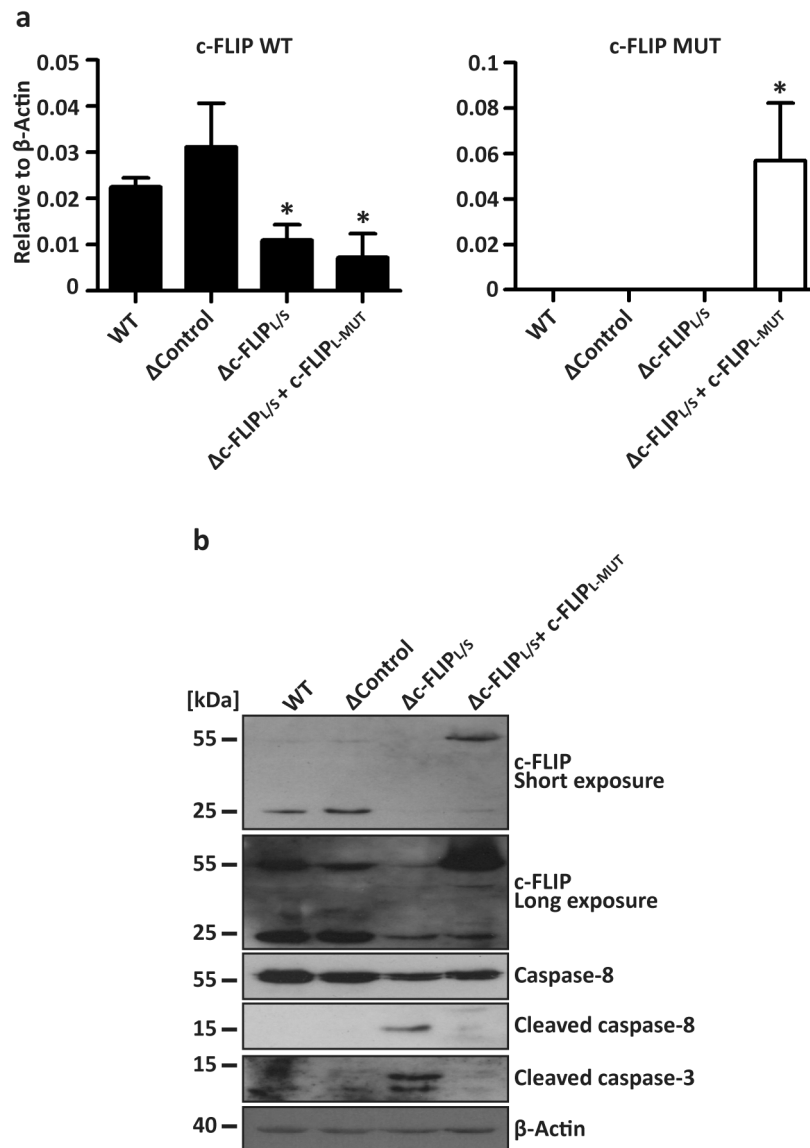


**Figure 19: a-b:** Cells were treated with a control, c-FLIP<sub>L/S</sub>-targeting or a c-FLIP<sub>L/S</sub>-targeting construct with simultaneous expression of c-FLIP<sub>L-MUT</sub>. The cells were analysed 3 days after lentiviral transduction. **a:** Analysis of total c-FLIP mRNA with specific primers for wild type or mutated c-FLIP mRNA. Bars display the mean of 3 experiments, error bars represent SD. **b:** Western blot analysis of c-FLIP expression levels and caspase activation.  $\beta$ -Actin was used as loading control. Statistical significances were calculated by one-tailed Mann-Whitney U test in respect to WT sample; \*  $p \leq 0.05$ .

Knockdown of c-FLIP<sub>L/S</sub>, as well as re-expression of c-FLIP<sub>L-MUT</sub> was confirmed by quantitative real-time PCR. Specific primers, amplifying either wild type or mutant total c-FLIP mRNA, were used (Fig. 19a). Expression of wild type c-FLIP-mRNA was

significantly decreased in c-FLIP<sub>L/S</sub> knockdown cells, but not in the control knockdown. Detection of c-FLIP<sub>L-MUT</sub> mRNA was only detected after lentiviral transduction with the c-FLIP<sub>L/S</sub>+c-FLIP<sub>L-MUT</sub> construct, while wild type c-FLIP mRNA was significantly decreased. Protein levels of c-FLIP were verified by western blot analysis (Fig. 19b). Expression of c-FLIP<sub>L</sub> and c-FLIP<sub>S</sub> was considerably decreased in cells after knockdown of c-FLIP<sub>L/S</sub>. The c-FLIP<sub>L/S</sub>+c-FLIP<sub>L-MUT</sub> plasmid was capable of expressing c-FLIP<sub>L-MUT</sub> without being targeted by the introduced c-FLIP<sub>L/S</sub>-targeting shRNA. c-FLIP<sub>S</sub> expression was not detectable, since it is targeted by the shRNA and not re-expressed. Activation of caspase-8 was inhibited upon re-expression of c-FLIP<sub>L-MUT</sub>, demonstrating the protective effect of functional c-FLIP<sub>L-MUT</sub> in clearCa-4 (Fig. 19).

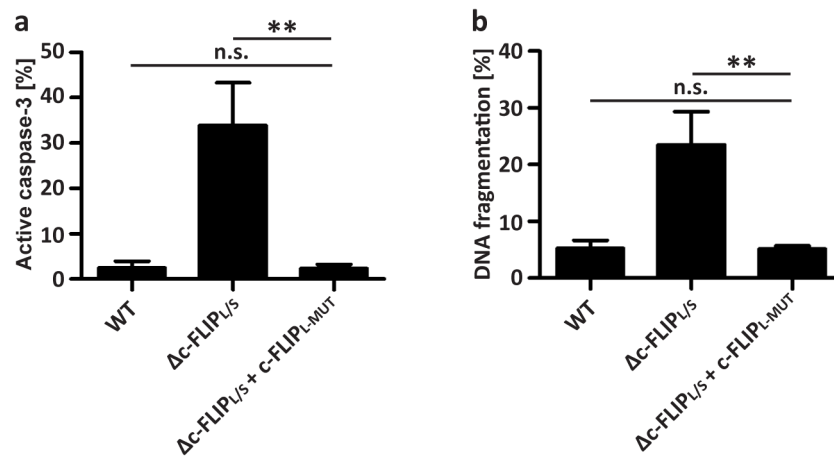


**Figure 20: a-b:** Cells were treated with a control, c-FLIP<sub>L/S</sub>-targeting or a c-FLIP<sub>L/S</sub>-targeting construct with simultaneous expression of c-FLIP<sub>L-MUT</sub>. Analysis of intracellular active caspase-3 (a) or DNA fragmentation (b). Bars display the mean of 3 experiments, error bars represent SD. Statistical significances were calculated by one-tailed Mann-Whitney U test; n.s. = not significant, \*\*  $p \leq 0.01$ .

The protective effect of c-FLIP<sub>L-MUT</sub> in cells lacking wild type c-FLIP<sub>L/S</sub> was examined by flow cytometric analysis of intracellular active caspase-3 and DNA fragmentation (Fig. 20). Activation of caspase-3 was only detectable after knockdown of c-FLIP<sub>L/S</sub>, but not upon re-expression of c-FLIP<sub>L-MUT</sub> (Fig. 20a). Also, DNA fragmentation was absent in c-FLIP<sub>L-MUT</sub> re-expressing cells (Fig. 20b). Thus, re-expression of c-FLIP<sub>L-MUT</sub> was sufficient to rescue spontaneous cell death of clearCa-4 after c-FLIP<sub>L/S</sub> knockdown. In summary, c-FLIP<sub>L</sub>, c-FLIP<sub>S</sub> and c-FLIP<sub>R</sub> mediate resistance to apoptosis by blocking caspase activation. Expression of one splice variant is sufficient for survival of RCC, while concurrent loss of c-FLIP<sub>L</sub>, c-FLIP<sub>S</sub> and c-FLIP<sub>R</sub> drives cells into spontaneous death (compare Fig. 15 and Fig. 16).

#### 4.1.7 NF- $\kappa$ B is constitutively active and independent from FLIP expression in clearCa-4

As demonstrated before, the c-FLIP<sub>L</sub> cleavage product p43-FLIP was detectable under steady-state conditions in RCC cell lines (compare Fig. 12). Although this cleavage product was not detectable throughout all experiment, p43-FLIP might play a role in NF- $\kappa$ B activation in renal carcinoma cells. To assess whether the NF- $\kappa$ B pathway can be activated in clearCa-4, cells were stimulated for up to four hours with LPS, TNF $\alpha$  or PMA/Ionomycin (P/I). NF- $\kappa$ B activation was monitored by phosphorylation of the NF- $\kappa$ B inhibitor I $\kappa$ B $\alpha$  in western blot analysis (Fig. 21a). Unstimulated cells showed only weak phosphorylation of I $\kappa$ B $\alpha$ . Stimulation with LPS and TNF $\alpha$  did not lead to an increased phosphorylation status of I $\kappa$ B $\alpha$ . However, strong I $\kappa$ B $\alpha$ -phosphorylation was detected after stimulation with P/I within 60 minutes, with a stable phosphorylation status for up to four hours.

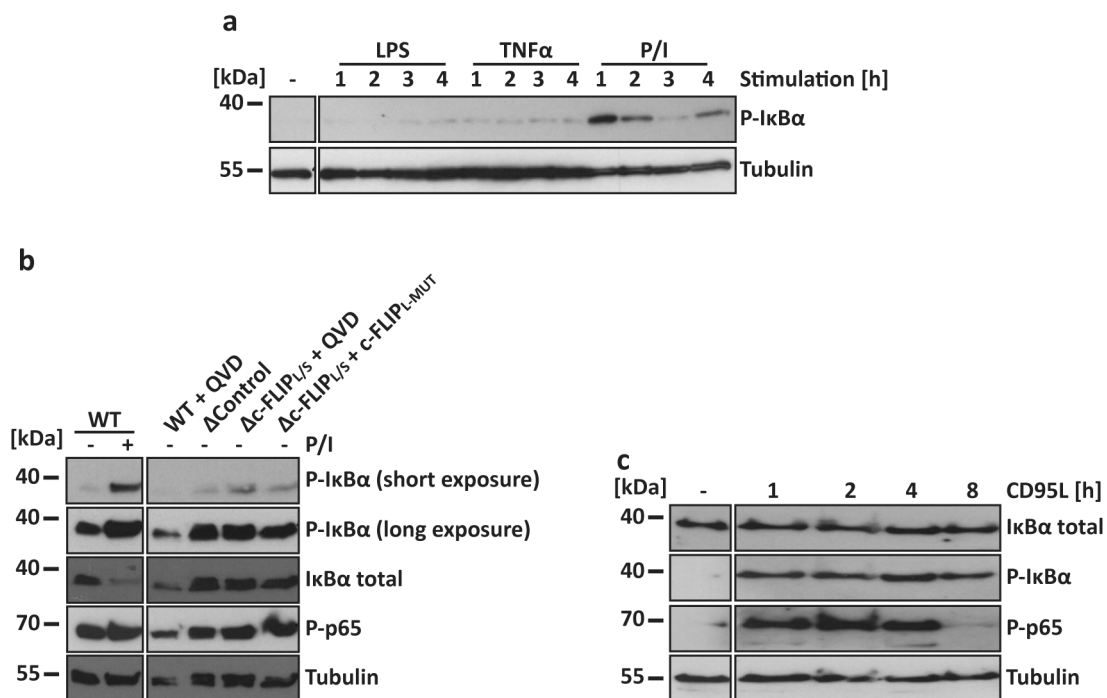


**Figure 21:** **a:** Cells were treated with either 100 ng/mL LPS, 10 ng/mL TNF $\alpha$  or 10 ng/mL PMA and 1 M Ionomycin (P/I) for up to four hours or were left untreated. **b:** Cells were treated with 10 ng/mL PMA and 1  $\mu$ M Ionomycin (P/I) for one hour or were left untreated. **c:** Cells were stimulated with 100 ng/mL CD95L for up to 8 hours. **a-c:** NF- $\kappa$ B activation was assessed by detection of P-I $\kappa$ B $\alpha$  and P-p65 in western blot analysis. Tubulin was used as loading control.

To analyse the influence of c-FLIP on NF- $\kappa$ B activation, c-FLIP<sub>L/S</sub> was knocked down in clearCa-4. QVD was used to block spontaneous apoptosis. Additionally,

---

the c-FLIP<sub>L-MUT</sub> re-expression construct was used to control any impacts of c-FLIP<sub>L</sub> on NF- $\kappa$ B activation. Protein lysates were analysed via western blot (Fig. 21b). Phosphorylation of I $\kappa$ B $\alpha$  was, as shown before, strongly induced upon P/I stimulation. Subsequently, due to its degradation after phosphorylation, lower total protein levels of I $\kappa$ B $\alpha$  were detectable. Knockdown of c-FLIP splice variants, as well as over-expression of c-FLIP<sub>L-MUT</sub>, did not influence the phosphorylation status of I $\kappa$ B $\alpha$  in steady-state conditions, assuming a c-FLIP<sub>L</sub>-independent mechanism. Interestingly, phosphorylation of p65 at position Ser536 was detectable, independent of P/I stimulation and c-FLIP expression (Fig. 21b). Furthermore, the impact of CD95L on NF- $\kappa$ B activation was studied. Cells were stimulated with CD95L for up to eight hours and phosphorylation of I $\kappa$ B $\alpha$  and p65 was studied (Fig. 21c). Again, P-p65 was detectable in unstimulated samples to a low extent. Stimulation with CD95L led to an increase of phosphorylated I $\kappa$ B $\alpha$  and p65.

#### **4.1.8 CD95 accumulates upon cell-cell-contact events, but fails to induce the DISC**

The CD95/CD95L-signaling pathway is most likely playing a major role in spontaneous apoptosis induction in RCC cell lines, since c-FLIP<sub>L/S</sub> knockdown leads to caspase-dependent spontaneous death of RCCs and apoptosis was induced by CD95L after blocking new c-FLIP protein translation with CHX.

Experiments in this thesis revealed that CD95 is highly expressed on the cell surface of all RCCs (compare Fig. 11). To confirm ligand expression, CD95L and TRAIL were stained in clearCa-4 for flow cytometric analysis (Fig. 22a). There was only poor TRAIL surface expression, whereas CD95L was highly expressed. Staining of CD95L in clearCa-2, clearCa-3 and clearCa-6 also showed high expression of CD95L in these cell lines (Fig. 22b). Additionally, the CD95 and TNF-R1 expression patterns on the cell surface were analysed by fluorescence microscopy. TNF-R1 is, besides CD95, the only death receptor which was expressed on the surface of clearCa-4 (compare Fig. 11). The expression of TNF-R1 was evenly distributed on the cell surface of all RCC cells (Fig. 22c). It was noticeable, that cells, which had no contact to other cells, presented equal distribution of CD95 expression on the cell surface. However, upon cell-cell-contact events, CD95 accumulated on the contact surface between the touching cells (Fig. 21c). This indicates, that CD95L and its receptor CD95 prompt



a paracrine activation. CD95 can, beside apoptosis, also induce NF $\kappa$ B activation in a c-FLIP-independent manner<sup>356,357</sup>.

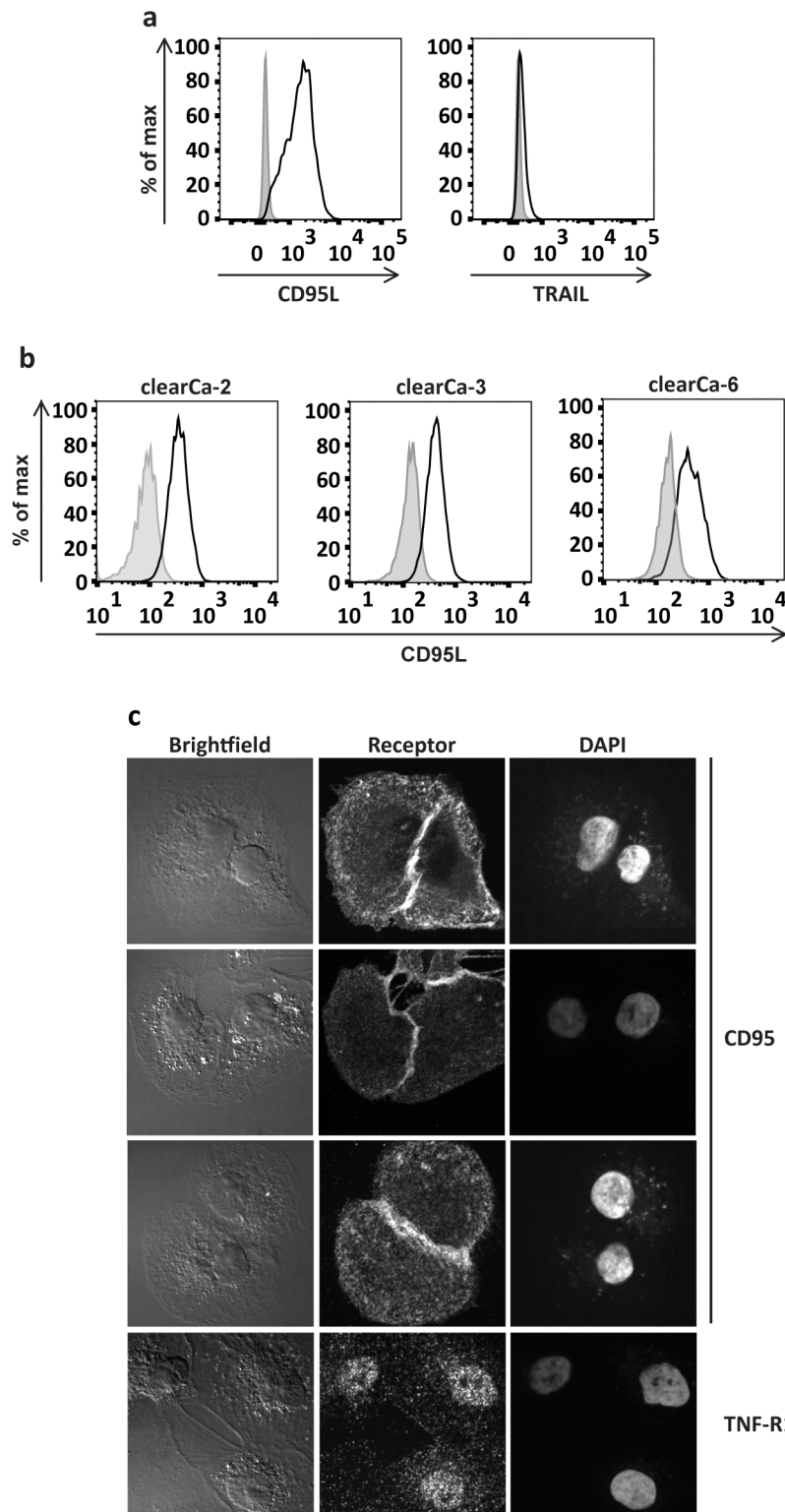


**Figure 22: a-b:** clearCa-4 (a) or clearCa-2, -3 and -6 (b) cells were stained with antibodies against CD95L or TRAIL (black line) and analysed in flow cytometry. Unstained samples are shown in grey. **c:** CD95 or TNF-R1 was stained on clearCa-4 and analysed by fluorescence microscopy.

To assess whether the accumulation of CD95 upon cell-cell-contact triggers the CD95-DISC, immunoprecipitation of the DISC was performed with unstimulated and CD95L-stimulated clearCa-4 cells (Fig. 23a). The immunoprecipitation was performed by FLAG-tagged CD95L to co-immunoprecipitate proteins, which bind to CD95L. Low aggregation of CD95 was detected already in unstimulated samples. However, this aggregation failed to induce the DISC, demonstrated by the absence of c-FLIP and caspase-8. Stimulation of clearCa-4 with anti-CD95 led to high CD95 aggregation and the DISC components caspase-8 and c-FLIP were detected.

To examine whether caspase-8 and c-FLIP are interacting without requirement of the DISC in steady-state conditions, an immunoprecipitation of caspase-8 was performed (Fig. 23b). Unstimulated cells did not show any binding of c-FLIP to caspase-8, however, stimulation of CD95L was sufficient to precipitate the DISC components CD95 and c-FLIP.

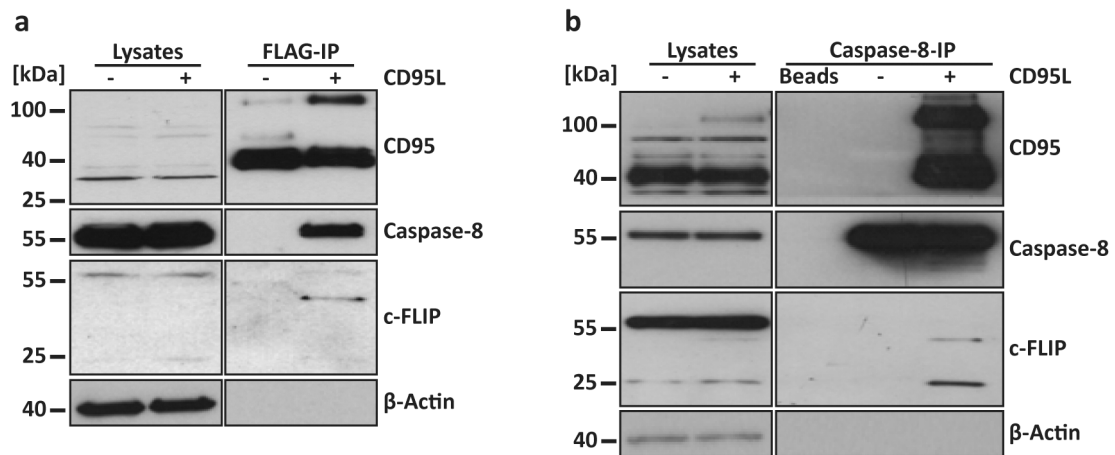


**Figure 23: a-b:** clearCa-4 cells were treated with FLAG-tagged CD95L for 30 minutes or were left untreated. Cells were lysed and immunoprecipitation with anti-FLAG (a) or anti-caspase-8 (b) antibody was performed, proteins were detected by western blotting. β-Actin was used as loading control.

#### 4.1.9 CD95-signalling is important for survival of clearCa-4

To identify a possible mechanism of CD95 accumulation in steady-state conditions, functional antibodies against the death ligands CD95L and TRAIL were used to block possible interactions of the ligands with their respective receptors CD95 or TRAIL-R1 and TRAIL-R2 and thereby preventing the activation of these pathways.

Cells, seeded on plates, pre coated with anti-TRAIL antibody, showed normal attachment and no phenotypic changes in microscopy. However, blocking of CD95L with specific antibodies led to detachment of the cells, without any additional stimulation. Cell survival was assessed by flow cytometric analysis of intracellular active caspase-3 and DNA fragmentation (Fig. 24). Blocking of CD95L, but not TRAIL, led to high levels of intracellular active caspase-3 (Fig. 24a). This activation was blocked by addition of QVD, indicating an apoptotic mechanism of cell death. Moreover, DNA fragmentation appeared in cells where CD95L was blocked. Similar to activation of caspase-3, DNA fragmentation was absent when QVD was added (Fig. 24b). Caspase-3 activation and DNA fragmentation were completely absent in TRAIL-blocked cells. This finding implicates an essential function of the CD95 pathway for survival of clearCa-4, since blocking this pathway leads to spontaneous apoptotic cell death.

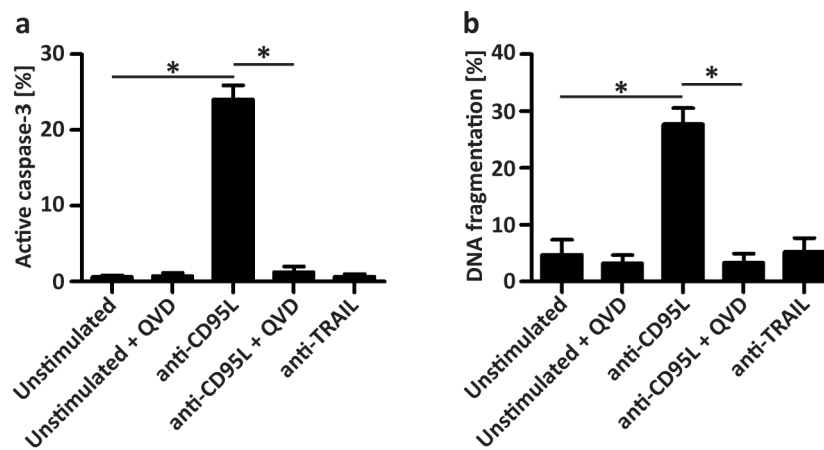


**Figure 24: a-b:** clearCa-4 cells were plated in wells, precoated with functional antibodies against CD95L or TRAIL. Cells were analysed in terms of intracellular active caspase-3 (a) and DNA fragmentation (b) 16 hours later. Bars display the mean of 3 experiments, error bars represent SD. Statistical significances were calculated by one-tailed Mann-Whitney U test; \*  $p \leq 0.05$ .

## 4.2 The role of A20 in apoptosis regulation

A20 was reported to interact with different pro-apoptotic and anti-apoptotic proteins, such as TRAF2<sup>358</sup>, RIP1<sup>328</sup> and caspase-8<sup>339</sup>. Previous binding studies indicated that A20 may translocate to the DISC upon CD95L-stimulation<sup>25</sup>. However, the mechanism for how A20 becomes recruited to the CD95-DISC and modulates apoptosis is still unclear.

### 4.2.1 Translocation of A20 to the CD95-DISC is not consistent

To assess if A20 translocates specifically to the DISC upon stimulation with CD95L, immunoprecipitation of the DISC was performed. However, a convincing DISC-dependent A20 binding was not detectable (Fig. 25a,b). Binding of A20 in precipitation samples showed variations and was, occasionally, also detectable in unstimulated cells, independent of CD95L stimulation.

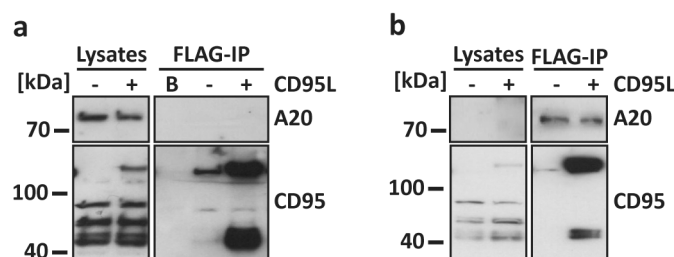


**Figure 25: a-b:** Jurkat E6-1 cells were treated with FLAG-tagged CD95L for 30 minutes or were left untreated. Cells were lysed and immunoprecipitation with anti-FLAG antibody was performed. Proteins were detected by western blotting.

### 4.2.2 Generation of a Jurkat E6-1 A20 knockout cell line with CRISPR/Cas9

The impact of A20 on CD95L-induced apoptosis in general and caspase-8 activation in particular, remains unclear. To analyse the role of A20 and its function in apoptosis regulation, the newly established CRISPR/Cas9-technology was used to generate a Jurkat E6-1  $\Delta$ A20 cell line. Guide RNAs (gRNA) bind specific DNA sequences in the genome to target them for a Cas9-induced double strand break. The cell repairs the double strand break via non-homologous end-joining, which induces mutations of the DNA in the area of the repaired double strand break. This allows modifications of the genome to create specific knockouts in pro- and eukaryotic cells<sup>359,360</sup>.

Three different gRNAs were generated to target the *TNFAIP3* gene by the endonuclease Cas9 (gRNAs are listed in 2.1.4). All three targets were used to target the *TNFAIP3* gene by a lentiviral approach. Bulk cultures were analysed by western blot to determine the knockout efficiency of A20 in Jurkat E6-1 cell lines. Expression of A20 was only decreased in cells treated with gRNA#3, but not with gRNA#1 or gRNA#2 (Fig. 26a).

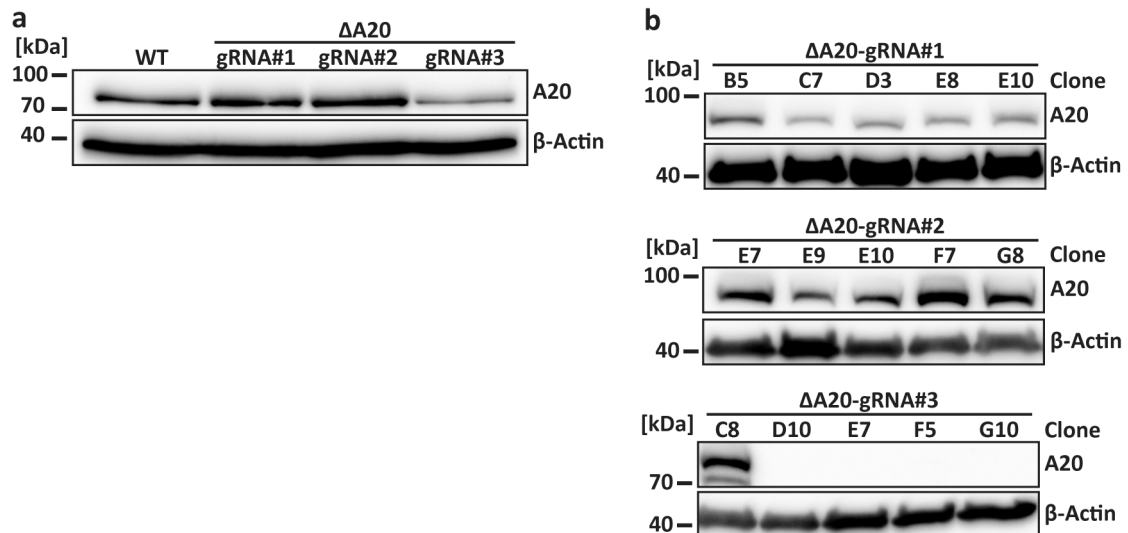


**Figure 26:** **a:** Jurkat E6-1 cells were treated with three different gRNA constructs for knockout of A20 by CRISPR/Cas9-technology. Expression of A20 was analysed by western blotting. **b:** Five single clones of every construct were analysed by western blotting.  $\beta$ -Actin was used as loading control.

For further analysis, single cell clones were isolated and analysed by western blot in matters of A20 expression. All single clones, treated with gRNA#1 or gRNA#2 still showed A20 expression similar to wild type cells, thereby assuming that these two gRNAs were not potent to target the *TNFAIP3* gene (Fig. 26b). However, single clone analysis of Jurkat E6-1 cells, treated with gRNA#3, confirmed the effective knockout of A20. In total, 17 single clones were analysed, from which 8 showed complete loss of A20 expression ( $\Delta$ A20-B10, -D10, -E7, -E8, -F5, -F7, -G4 and -G10; data not shown).

For analysis of differences in apoptosis-resistance, it is important that all proteins of the apoptotic pathway are equally expressed in the wild type and A20-knockout situation. The expression levels of proteins of the extrinsic apoptosis pathway were analysed in steady-state conditions (Fig. 27a). Loss of A20 was previously confirmed in the knockout-clones, generated with gRNA#3 (Fig. 26b). Expression of c-FLIP and caspase-8 displayed similar levels in all four analysed  $\Delta$ A20 cells ( $\Delta$ A20-D10, -F5,

-E7 and -G10) as wild type Jurkat cells (WT cells). FADD expression was reduced in clone G10. Additionally, surface expression of CD95 was analysed via flow cytometry (Fig. 27b). CD95 staining showed equal expression levels in WT and three  $\Delta$ A20 clones D10, E7 and F5, whereas clone G10 displayed an increased CD95 surface expression. In total, three out of four  $\Delta$ A20 clones (D10, E7 and F5) showed similar protein expression levels of the extrinsic apoptosis pathway as WT cells.

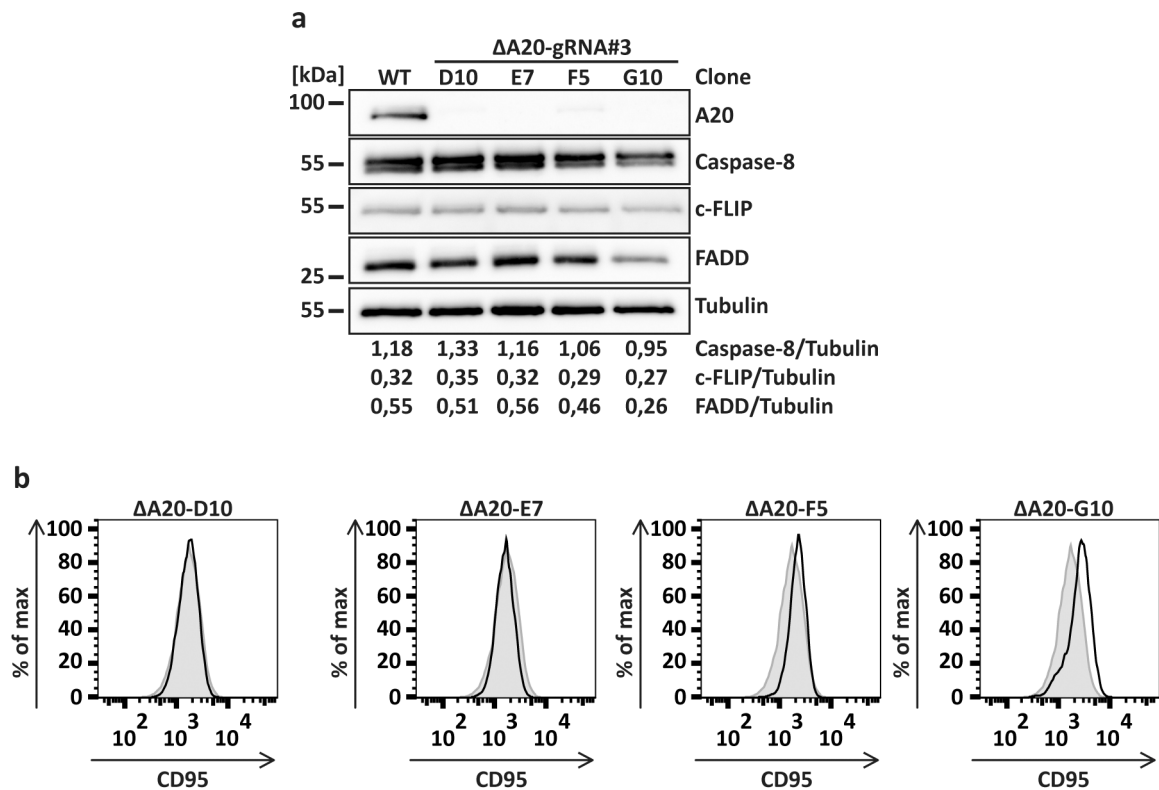


**Figure 27:** **a:** Single clones of A20, generated with gRNA#3, were analysed by western blotting in terms of DISC proteins. Tubulin was used as loading control. Expression levels of DISC proteins were calculated in relation to tubulin. **b:** Cells were stained with anti-CD95 (black line) and analysed in flow cytometry. Wild type samples are shown in grey.

#### 4.2.3 Loss of A20 leads to increased apoptosis sensitivity

All four  $\Delta$ A20-clones, which were previously analysed, were tested in matters of apoptosis-sensitivity ( $\Delta$ A20-D10, -E7, -F5, -G10). Cells were treated with different amounts of CD95L and DNA fragmentation was analysed after 16 hours (Fig. 28). Cells treated with a low dose of CD95L showed increased DNA fragmentation in three of four tested  $\Delta$ A20 clones compared to WT cells, hence increased sensitivity to CD95L-induced apoptosis. This effect was absent, when cells were treated with higher doses of

CD95L, since WT and  $\Delta$ A20 cells displayed similar levels of DNA fragmentation after 16 hours of stimulation.

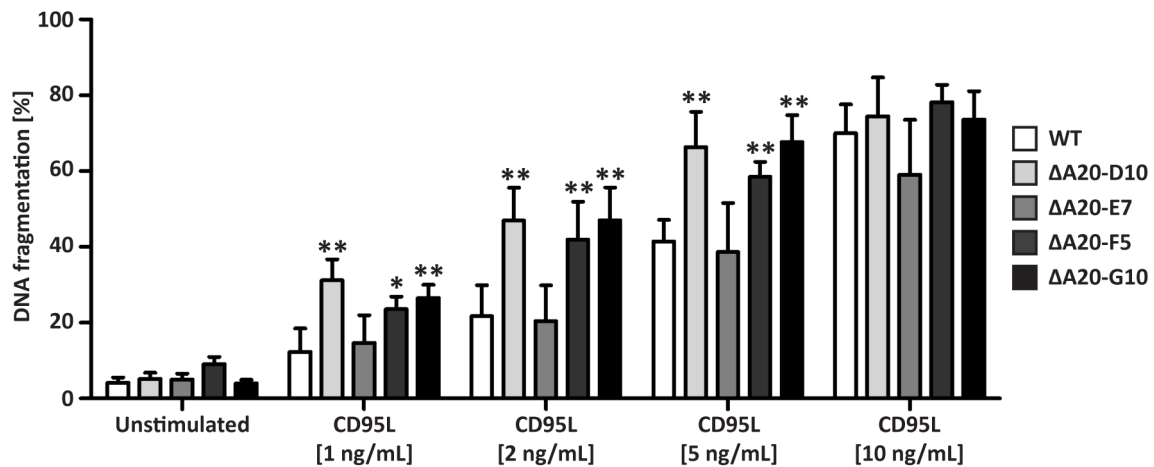


**Figure 28:** WT and  $\Delta$ A20 cell lines (D10, E7, F5, G10) were treated with different amounts of CD95L for 16 hours. DNA fragmentation was analysed by flow cytometry. Bars display the mean of at least 3 experiments, error bars represent SD. Statistical significances were calculated by one-tailed Mann-Whitney U test in respect to equally stimulated WT sample; \*  $p \leq 0.05$ , \*\*  $p \leq 0.01$ .

To examine differences at earlier time points, WT and  $\Delta$ A20-D10 cells (in the following termed  $\Delta$ A20 cells) were treated with a low or a high dose of CD95L for up to 8 hours. Cell death was assessed by DNA fragmentation (Fig. 29). Upon stimulation with a low dose CD95L, differences in DNA fragmentation between WT and  $\Delta$ A20 cells were detected after 4 hours (Fig. 29a). While elevated levels of DNA fragmentation could not be detected in WT cells before 6 hours stimulation,  $\Delta$ A20 cells showed higher DNA fragmentation already after 4 hours. The most prominent difference was detectable after 8 hours stimulation. Upon high CD95L-stimulation, DNA fragmentation in WT and  $\Delta$ A20 cells occurred earlier (Fig. 29b). Still, differences in cell death status were pronounced.  $\Delta$ A20 cells displayed increased DNA fragmentation already after 2 hours compared to unstimulated samples, whereas WT cells did not die before 4 hours of stimulation.  $\Delta$ A20 cells were more sensitive to CD95L-induced cell death at early time points, irrespective of the strength of the signal. At later time points, high induction of apoptosis did not depend on A20 expression, while low induction still showed differences between WT and  $\Delta$ A20 cells (compare Fig. 28).

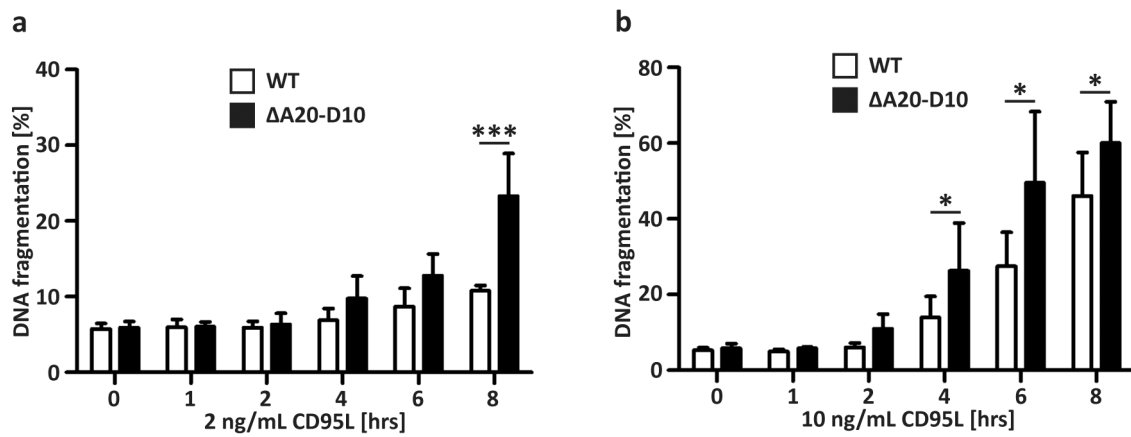


**Figure 29:** WT and  $\Delta A20$  cell lines (D10, E7, F5, G10) were treated with 2 or 10 ng/mL CD95L for up to 8 hours. DNA fragmentation was analysed by flow cytometry. Bars display the mean of at least 3 experiments, error bars represent SD. Statistical significances were calculated by one-tailed Mann-Whitney U test; \*  $p \leq 0.05$ , \*\*\*  $p \leq 0.001$ .

#### 4.2.4 Levels of active caspase-8 are altered in $\Delta A20$ cells

To identify the reason for the higher sensitivity to CD95L-apoptosis, WT and  $\Delta A20$  cells were treated with a high dose of CD95L for up to eight hours and caspase activation was analysed by western blot (Fig. 30). Stimulation with a high dose of CD95L led to an earlier detection of active caspase-8. The cleavage products p43/41 and p18 were pronounced in  $\Delta A20$  cells after two and four hours, respectively. In WT cells, levels of p43/41 were reduced compared to  $\Delta A20$  cells and p18 was not detectable before eight hours of CD95L-stimulation.

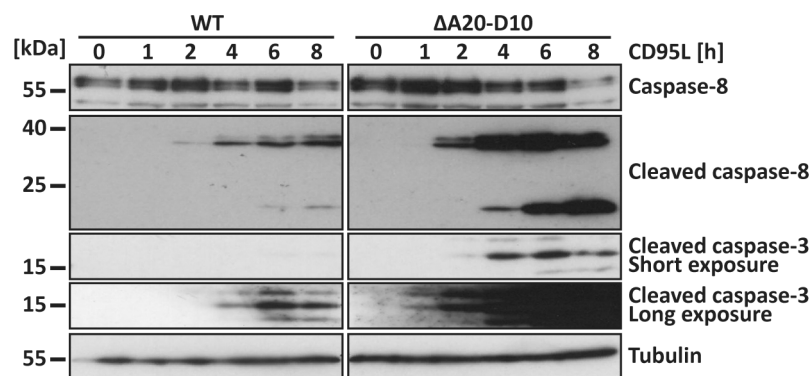


**Figure 30:** WT and  $\Delta A20-D10$  cells were treated with 10 ng/mL CD95L for up to 8 hours. Caspase activation was followed by western blot analysis. Tubulin was used as loading control.

Subsequently, caspase-3 activation appeared earlier in  $\Delta A20$  cells (Fig. Fig. 30). Interestingly, levels of caspase-8 (p55/53) were not differing in WT and  $\Delta A20$  cells. Furthermore, cleavage of c-FLIP<sub>L</sub> to p43-FLIP was only slightly changed after loss of A20.



---

This data supports the elevated DNA fragmentation in  $\Delta$ A20 cells after apoptosis induction by CD95L and suggests an anti-apoptotic function of A20 in CD95L-mediated apoptosis (compare Fig. 28 and Fig. 29).

#### 4.2.5 Caspase-8 cleavage products are degraded by the 26S-Proteasome

As shown above, CD95L-induced cell death is A20-dependent (Fig. 28). Also, levels of the caspase-8 cleavage fragments p43/41 and p18 are connected with A20 expression (Fig. 30), but the mechanism for how A20 might regulate activation of caspase-8 is not clear. It is possible that the initial cleavage of caspase-8 is blocked due to A20 activity, or that the caspase-8 cleavage fragments p43/p41 and p18 are a target of A20. As shown above, levels of p55/53 were not altered in  $\Delta$ A20 cells compared to WT cells (Fig. 30). It is known that A20 edits the ubiquitination pattern of target proteins, by cleaving K63-linked polyubiquitin chains, followed by addition of K48-linked polyubiquitin chains. This leads to the proteasomal targeting of the altered protein <sup>265</sup>.

To investigate the role of the 26S proteasome in the activation and degradation of caspase-8, cells were treated with a high dose of CD95L and bortezomib for one hour (Fig. 31). Bortezomib blocks the 26S proteasome and thereby the degradation of K48-linked proteins <sup>361</sup>. Activation of caspase-8 to p43/p41 was similar in WT and  $\Delta$ A20 cells. However, while the p18 fragment of active caspase-8 was detectable in  $\Delta$ A20 cells, the it was absent in WT cells, treated with CD95L only. Addition of bortezomib led to restoration of the p18-fragment in WT cells (Fig. 31a). Also, levels of c-FLIP<sub>L</sub> and p43-FLIP were not altered in  $\Delta$ A20 compared to WT cells (Fig. 31b). These results show the importance of the 26S proteasome in degradation of active caspase-8.

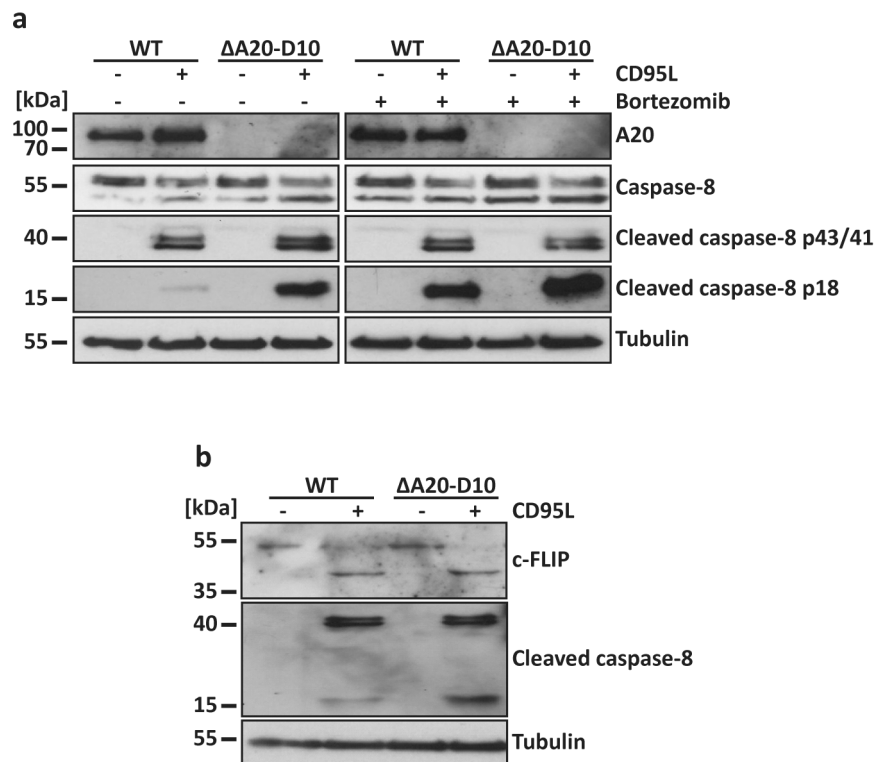


**Figure 31: a-b:** WT and  $\Delta$ A20-D10 cells were treated with CD95L for one hour in the presence or absence of 50 nM bortezomib. Caspase activation was followed by western blot analysis. Tubulin was used as loading control.

#### 4.2.6 Polyubiquitination of caspase-8 might play a role in apoptosis-regulation

After induction of the TRAIL-DISC, RBX1 (CUL3) polyubiquitinates caspase-8 in the p10-region, leading to its activation<sup>349</sup>. Additionally caspase-8 gets targeted by TRAF2 and K48-linked polyubiquitinated in the p18 region. The ubiquitin-editing enzyme A20 translocates to the TRAIL-induced DISC via RIP<sup>362</sup>. Since the TRAIL- and CD95L-induced DISC show similar composition, i.e. binding of FADD, caspase-8 and c-FLIP, the question is, whether A20 modulates active caspase-8 after CD95L-stimulation or not.

To test the hypothesis that the cleavage products p43/41 or p18 of caspase-8 are targeted by A20 and their ubiquitination from K63- to K48-linked polyubiquitination is edited, different approaches were used. Though a broad variety of methods were previously described to address ubiquitination, the ubiquitination status of caspase-8 was not completely resolved. Also, a direct interaction between A20 and caspase-8 or its cleavage products in steady state and CD95L-stimulated WT cells could not be found. Additionally, it remains unclear, if A20 actively translocates to the DISC

upon CD95L-stimulation, since immunoprecipitations of the DISC were not consistent regarding A20 translocation (compare Fig. 25).

For detection of different ubiquitin patterns, tandem ubiquitin binding entities (TUBE), which bind specifically K48- or K63-polyubiquitinated proteins, were used (Fig. 32). WT and  $\Delta$ A20 cells were stimulated with CD95L to promote DISC-dependent caspase-8 activation and K48- and K63-polyubiquitinated proteins were precipitated using K-linkage specific TUBEs. Total amounts of active caspase-8 were increased in the lysates of  $\Delta$ A20 cells compared to WT cells. Caspase-8 and its cleavage products p43/41 were precipitated with the K63-TUBE, but not the K48-TUBE, while the p18 cleavage product was not detectable at all. Slightly more K63-linked p43/41 caspase-8 was detectable in  $\Delta$ A20 cells.

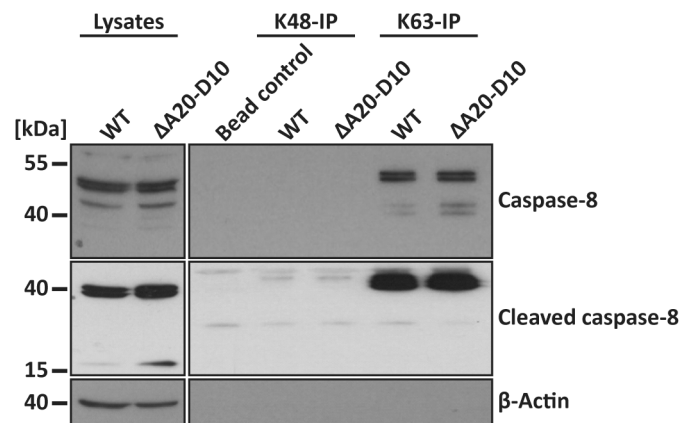


**Figure 32:** WT and  $\Delta$ A20-D10 cells were treated with CD95L for one hour. After lysis, K48- and K63-linked proteins were immunoprecipitated via TUBEs. Analysis of ubiquitinated proteins was done by western blotting.  $\beta$ -Actin was used as loading control.

In summary, A20 is negatively regulating apoptosis. However, the precise mechanism how A20 is influencing CD95L-mediated apoptosis, remains unclear. It was shown that A20 does not interfere with caspase-8 activation, but is involved in proteasomal degradation of active caspase-8.

## 5 Discussion

### 5.1 The role of c-FLIP in renal cell carcinoma

Regulation of death receptor mediated apoptosis by c-FLIP is well characterised. Interestingly, despite c-FLIP's anti-apoptotic function, pro-apoptotic and pro-survival signals, like NF- $\kappa$ B activation, mediated by c-FLIP have also been described<sup>159,167,363–365</sup>. Controversially, c-FLIP additionally acts as a NF- $\kappa$ B suppressor downstream of CD95<sup>366</sup> and the T cell receptor<sup>367</sup>. Cancer research focuses on TRAIL-induced apoptosis as a promising therapy to combat different types of cancer, since it induces apoptosis in tumour cells while not affecting healthy tissue<sup>86,368</sup>. However, this approach is limited by several resistance mechanisms, which are gained by mutations in pro- and anti-apoptotic genes<sup>218,369,370</sup>. Hereby, c-FLIP is a prominent target in tumour therapy, since it is linked to many drug-resistant tumour types by inhibiting TRAIL-induced apoptosis, also in renal cell carcinoma<sup>371,372</sup>. However, stimulation with TRAIL can also lead to c-FLIP-independent NF- $\kappa$ B activation, inducing an opposing effect<sup>373,374</sup>. Because of this, it is worthwhile to look for other death-inducing pathways, such as the CD95 pathway, for cancer treatment. While the impact of c-FLIP on protecting cancer cells from CD95-induced apoptosis is characterised in a broad variety of cancers<sup>201,203,207,340</sup>, there were no studies in renal cell carcinoma up to now.

Genomic analysis of the 3' splicing site of exon 6 in the *CFLAR* gene, which encodes for c-FLIP, revealed heterogeneous expression of c-FLIP<sub>S</sub> and c-FLIP<sub>R</sub> in different renal cell carcinoma cell lines. Increased frequency of c-FLIP<sub>R</sub> is linked to several tumours<sup>152</sup>, but a tendency to c-FLIP<sub>R</sub> expression could not be found within the characterised RCC cell lines. It has been reported that c-FLIP<sub>L</sub> has pro- and anti-apoptotic functions after CD95L-stimulation, depending on the ratio of c-FLIP<sub>L</sub> to c-FLIP<sub>S</sub> and c-FLIP<sub>R</sub> expression levels<sup>160</sup>. Interestingly, although clearCa-2 and clearCa-3 only expressed very low amounts of c-FLIP<sub>R</sub> or c-FLIP<sub>S</sub> and c-FLIP<sub>R</sub> respectively, these two cell lines were resistant to CD95L-induced apoptosis to a similar extent as clearCa-4 and clearCa-6, which expressed comparable levels of c-FLIP<sub>L</sub> and c-FLIP<sub>S</sub> or c-FLIP<sub>S</sub> and c-FLIP<sub>R</sub>, respectively. This argues that the ratio of c-FLIP<sub>L</sub> to c-FLIP<sub>S</sub> and c-FLIP<sub>R</sub> expression is not the only factor which determines the pro- and anti-apoptotic behaviour of c-FLIP<sub>L</sub>. However, more RCC cell lines should be tested to verify these findings.

---

Treatment of RCC with CHX negatively affected the expression levels of all c-FLIP isoforms, Bcl-x only to a certain extent and XIAP not at all, demonstrating that c-FLIP is a short-lived protein <sup>375</sup>. Under normal conditions, all RCC cell lines were resistant against CD95L-induced apoptosis, irrespective of the used CD95L-concentration. Co-stimulation with CHX and CD95L induced high death rates, assuming that c-FLIP is an essential factor of apoptosis-resistance in RCC. Since clearCa-2 and clearCa-3 express only very low levels of short c-FLIP isoforms in steady state conditions, resistance against CD95L-induced apoptosis is probably mediated primarily by c-FLIP<sub>L</sub> <sup>376</sup>.

Lentiviral transduction with shRNA constructs, targeting either c-FLIP<sub>L</sub> or c-FLIP<sub>S</sub>, did not alter the phenotype and viability of the renal cell carcinoma cell lines. Interestingly, knockdown of c-FLIP<sub>L</sub> only prompted increased c-FLIP<sub>S</sub>-expression in clearCa-4, leading to the assumption that c-FLIP<sub>S</sub> or c-FLIP<sub>R</sub> are upregulated to compensate the lack of c-FLIP<sub>L</sub> and sustain apoptosis-resistance. Strikingly, simultaneous knockdown of all expressed c-FLIP isoforms c-FLIP<sub>L</sub>, c-FLIP<sub>S</sub> and c-FLIP<sub>R</sub>, initiated spontaneous cell death within a few days in all cell lines. The cells showed all phenotypic and biochemical hallmarks of apoptosis, such as membrane blebs, caspase activation and PARP-cleavage <sup>9,35</sup>. This demonstrates that c-FLIP is an essential survival-factor for all renal cell carcinoma cell lines which were analysed within this study. Additionally, c-FLIP<sub>L</sub>, c-FLIP<sub>S</sub> and c-FLIP<sub>R</sub> are potent by oneself to maintain cell survival, since single knockdowns did not lead to spontaneous apoptosis. It was shown for breast cancer cells that downregulation of c-FLIP leads to spontaneous TRAIL-R2-mediated activation of caspase-8 <sup>377</sup>. Contradictory results were reported in Hodgkin's lymphoma. While Dutton et al. describe that knockdown of c-FLIP leads to spontaneous CD95L-induced apoptosis <sup>203</sup>, this phenotype was not discovered in a study by Mathas et al. <sup>210</sup>. However, the c-FLIP knockdown in the study of Mathas et al. was less efficient, and cycloheximide already led to an increased apoptosis rate in one cell line. This leads to the assumption that low levels of c-FLIP are competent to maintain resistance against spontaneous cell death in Hodgkin's lymphoma, while complete loss of c-FLIP also leads to apoptosis. These studies underline the importance of c-FLIP in controlling spontaneous apoptosis. The observations match the results of this study and reveal a mechanism which is not specific for RCC only. Studies of c-FLIP's role in mediating apoptosis-resistance in RCCs are also diverse. While some showed that downregulation of c-FLIP is sufficient to sensitise renal cell

---

carcinoma to TRAIL-induced apoptosis<sup>372,378</sup>, others reported that apoptosis sensitivity is also dependent on TRAIL-receptor expression<sup>379</sup> or NF- $\kappa$ B activation<sup>380</sup>. These diverse findings might be explainable by differences in tumour stage and altering mutations within different pro- and anti-apoptotic genes. For a further validation and an optimised treatment of RCC, a genetic characterisation of apoptosis-relevant genes is necessary for each patient. Conflicting results make it difficult to identify possible mechanisms how diseases can be treated.

Although the precise mechanism of c-FLIP in maintaining cell survival in RCCs is not revealed, it might be a potential target to treat renal cell carcinoma, even in late stages. However, this might not be true for all types of RCC, since other studies reported that inhibition of c-FLIP alone only sensitises cells for apoptosis induction, without inducing spontaneous cell death in ACHN, Caki cells and others<sup>371,381</sup>. Still, c-FLIP is a prominent target for sensitising tumours against ligand-induced cell death<sup>223</sup>. Available drugs, which are known to interfere with c-FLIP, might be suitable for spontaneous apoptosis induction in renal cell carcinoma<sup>223,340</sup>.

Since the c-FLIP<sub>L</sub> cleavage product p43-FLIP was identified in steady state conditions, it is possible that this factor supports proliferation and cell survival through NF- $\kappa$ B activation<sup>165,166</sup>. However, p43-FLIP could not be detected throughout all experiments. It might be possible that the generation of p43-FLIP is dependent of unknown signals from outside or inside the cell, which could not be identified within this study. Although a pre-activated status with phosphorylation of p65 and I $\kappa$ B $\alpha$  was detected, this finding was independent of c-FLIP<sub>L</sub> expression, assuming a different mechanism of steady state NF- $\kappa$ B activation. Moderate activation of the NF- $\kappa$ B pathway is e.g. important for embryonic development<sup>382</sup>, but excessive NF- $\kappa$ B activation may lead to inflammation and subsequently to tumour formation due to inhibited cell death and enhanced proliferation<sup>383</sup>. According to this, increased activation of NF- $\kappa$ B can be found in various cancer types<sup>384-386</sup>. Oya et al. demonstrated that constitutive NF- $\kappa$ B activation plays an important role in TRAIL-resistant RCCs<sup>380</sup>. Additionally, apoptosis- and drug-resistance is often mediated by excessive NF- $\kappa$ B activation<sup>386-388</sup>, which induces the expression of anti-apoptotic proteins such as c-FLIP<sup>363,389-391</sup>.

CD95L is reported to induce apoptosis when it is membrane bound<sup>392</sup>. Upon cleavage by metalloproteases it is converted to a soluble ligand and alters its activity, also

---

through NF- $\kappa$ B activation<sup>183,392</sup>. The recombinant CD95L used in this thesis mimics the membrane bound form of CD95L and is capable to induce apoptosis<sup>164,201</sup>. Since stimulation of RCC cell lines with CD95L did not induce apoptosis, but contrarily activated the NF- $\kappa$ B pathway, a survival mechanism for late stage RCCs is suggested. Besides the known induction by TNF $\alpha$  and TRAIL, CD95L was also linked to NF- $\kappa$ B activation<sup>169,393</sup>. This leads to the assumption that cancerous cells protect themselves against death receptor-mediated apoptosis by constant NF- $\kappa$ B activation<sup>394</sup>. Indeed, stimulation with CD95L triggers the phosphorylation of p65 and I $\kappa$ B $\alpha$  to a greater extent, without inducing apoptosis, confirming the pro-survival function of the CD95 pathway<sup>181</sup>. It was already described that CD95 stimulation leads to NF- $\kappa$ B activation and increased tumour growth<sup>395,396</sup>. This mechanism allows tumours to evade immunosurveillance, by converting a death into a proliferation signal<sup>183</sup>. Lymphocytes, which infiltrate tumour tissue, might support tumour progression by activating the NF- $\kappa$ B pathway instead of inducing apoptosis. While T cells clear abnormal cells by CD95-mediated apoptosis, tumour cells can develop resistance mechanisms against CD95L-induced cell death and also benefit from CD95 stimulation<sup>397,398</sup>.

Although CD95 expression is generally decreased in early progression of renal cell carcinomas compared to healthy kidney tissue, qualitative high expression levels are linked to later tumour stages, involving formation of metastases<sup>219,220,399</sup>. Late staged renal cell carcinomas also benefit from elevated CD95 expression<sup>222</sup>. Thus, CD95 can be used as a prognostic marker with a poor prognosis in high CD95 expressing tumours<sup>400</sup>. Additionally, high CD95L expression by tumours is a survival factor. This feature helps tumour cells to escape the control mechanisms of the immune system by killing tumour-directed lymphocytes<sup>401,402</sup>. In previous studies the CD95 mRNA expression, encoded on the *FAS* gene, was analysed<sup>222,347</sup>. For some of the generated tumour cell lines, also the surface expression was verified. The RCC cell lines which were characterised within this thesis expressed high levels of CD95 and CD95L on their surface, consistent with a late-stage RCC and a poor prognosis. Besides its function to kill tumour directed lymphocytes, high expression of CD95L might also act as a paracrine activator of the CD95 pathway within the tumour tissue<sup>190,395</sup>. By this action, RCC can benefit from pro-survival factors, such as NF- $\kappa$ B activation, mediated by CD95 signalling. CD95L, commonly acting as an inducer of apoptosis, contrarily exhibits an anti-apoptotic function with pro-survival features in clearCa-4. The de-

---

tected aggregation of CD95 upon cell-cell-contact events in steady-state conditions, supports the assumption of a paracrine activation of this pathway. However, detection of the DISC failed in steady-state conditions. Also, no translocation of RIP to the CD95-DISC was observed (data not shown). Nonetheless, the aggregation of CD95 might be sufficient to trigger the NF- $\kappa$ B pathway via phosphorylation of p65 and I $\kappa$ B $\alpha$ , without inducing caspase-8 activation in the presence of c-FLIP<sup>169,403</sup>. It is likely that a pre-activated status of the CD95 pathway leads to spontaneous apoptosis after loss of protective c-FLIP in RCC cell lines, but this concept could not be verified.

Loss of CD95 or CD95L drives tumour cells into a recently described new form of death: death induced by CD95 or CD95 ligand elimination (DICE)<sup>404</sup>. Most strikingly, DICE is induced by different death pathways, which are activated simultaneously. This suggests that the CD95 pathway mediates a crucial survival signal within some tumours. In RCCs, blocking of CD95L by functional antibodies induced spontaneous cell death, which could be blocked by the pan-caspase inhibitor QVD. The phenotypic hallmarks were identical to those observed after knockdown of c-FLIP<sub>L/S</sub>, including membrane blebs, caspase activation and DNA fragmentation. While DICE is characterised by simultaneous induction of multiple cell death pathways, which can only be blocked by an inhibitor cocktail<sup>404</sup>, apoptosis in RCCs could be blocked by caspase inhibition only. Therefore, loss of CD95 signalling leads to a spontaneous cell death form, which is different from DICE. The mechanism how caspase activation is triggered in this incident is unclear, but it is assumed that CD95 is a type of dependence receptor for at least clearCa-4<sup>405</sup>. Opposed to these findings, blocking of the CD95 pathway alone was not sufficient to kill renal cell carcinoma cell lines which were generated by the same work group as the ones, which were used in this thesis<sup>347</sup>. However, it has to be mentioned that the experimental setup was different. In this thesis, the solely addition of anti-CD95 to the medium was also not affecting cell viability, while seeding the cells on pre-bound antibody dramatically induced spontaneous apoptosis. This can be explained by the microscopic data, where cell-cell contact events led to high CD95 aggregation. Once this receptor complex is formed, the blocking antibody cannot exert its function anymore, because it fails to disrupt the interaction between CD95 and CD95L. Additionally, the attempt to knockdown CD95 by introducing shRNA, induced a transient reduction of CD95 expression, only (data not shown). These results help to understand a possible new form of therapy, by disrupting the CD95-mediated pro-



---

survival signal in RCCs, instead of inducing apoptosis. Indeed, systemic administration of CD95 activating agents in mice is lethal<sup>219,396,406,407</sup>, since CD95 is ubiquitously expressed by many cell types<sup>408</sup>. Approaches to inhibit the CD95 signal might be a new possibility to treat cancer cells, where DICE or similar death mechanisms like spontaneous apoptosis, which was shown in this thesis, were identified. This makes CD95 and CD95L attractive for tumour treatment again, since it is not dependent on activating this pathway and thereby avoiding side effects on bystander cells.

## 5.2 The role of A20 in apoptosis regulation

The ubiquitin-editing enzyme A20 was shown to interact with many proteins in different signalling pathways. For instance, it was identified as an inhibitor of the NF- $\kappa$ B pathway<sup>311</sup>. Moreover, an interaction between A20 and caspase-8 was shown during TRAIL-induced apoptosis, limiting caspase-8 activity<sup>349</sup>. Recently, it was described that it also plays an important role in inhibiting CD95-, TRAIL- and TNF-receptor-mediated apoptosis<sup>327,339,342</sup>. However, while the role of A20 in attenuating NF- $\kappa$ B activation and apoptosis induction by TRAIL and TNF $\alpha$  is commonly accepted, it is still controversial how A20 might be involved in regulation of CD95L-induced apoptosis. While no effect of A20 on CD95L-induced apoptosis was found in Jurkat cells, B cells became resistant upon loss of A20<sup>342,409</sup>. Therefore, the exact mechanism of A20 in CD95L-induced apoptosis is not characterised yet, but it is assumed that it also limits caspase-8 activation, similar to TRAIL-induced apoptosis<sup>339</sup>.

It was reported that A20 translocates to the TRAIL-induced DISC and inhibits caspase-8 activation. Besides A20, RIP1 is needed to mediate inhibition of caspase-8 activity<sup>327</sup>. In Jurkat cells, stimulation with CD95L did not result in consistent A20 recruitment to the DISC, upon stimulation to activate NF- $\kappa$ B<sup>25,170,410</sup>. This implies an additional mechanism how A20 might be involved in apoptosis regulation. It is possible that, besides translocation to the DISC, A20 may act in the cytosol as an inhibitor of apoptosis.

To target A20 in Jurkat E6-1 cells, the newly established method CRISPR/Cas9 was employed. It allows to specifically target genomic sequences to induce double strand breaks and thereby mutations in chosen target genes<sup>359,360</sup>. Researchers use this tool to easily modify genomes in bacteria, mice and human cells<sup>411–413</sup>. To generate an

---

A20 knockout cell line, the online tool CRISPR Design was used to identify specific target sequences (gRNA) with limited off-target effects within the *TNFAIP3* gene<sup>351</sup>. The three best sequences with a high score and low off-target probabilities were chosen. Although CRISPR Design calculated high scores for all three used gRNAs, only one sequence efficiently targeted the gene *TNFAIP3* for Cas9 cleavage and thereby inducing mutations. Single clone analysis of cells, targeted with the competent gRNA, revealed an A20 knockout efficiency of  $\sim 50\%$  (8/17 clones). To improve the algorithmic selection of suitable target sequences is challenging, but ongoing<sup>414</sup>. Genetic engineering already increased the enzymatic specificity of Cas9 to target sequences<sup>415,416</sup>. In general, the CRISPR/Cas9 system is suitable to modify genomes efficiently and fast with a broad spectrum of possible applications. A big advantage of this new technique is that an efficient genomic intervention results in complete loss of protein expression, whereas shRNA and siRNA approaches often only reduce the expression, leading to a knockdown. TALENs, which also introduce genomic modifications, have to be genetically engineered and are not suitable for high throughput screenings<sup>417-419</sup>. Taken together, targeting genes by CRISPR/Cas9 *in vitro* and *in vivo* knockout studies can be carried out more efficiently and faster.

Knockout of A20 did not influence cell death in steady-state conditions, concluding that A20 is not vital for Jurkat cells. Additionally, single clones with a knockout for A20, were further analysed for protein expression, relevant for executing CD95L-induced apoptosis. In general, expression of proteins was identical in WT and  $\Delta$ A20 cells, showing that A20 has no impact on proteins of the extrinsic apoptosis pathway in steady-state conditions.

Since translocation of A20 to the CD95-DISC was not consistent, further experiments focused on cell death in general. Jurkat cells are susceptible to CD95L-induced apoptosis without the need to inhibit anti-apoptotic proteins, like c-FLIP<sup>368</sup>. This allows to analyse the impact of proteins on CD95-mediated apoptosis without downregulation of other proteins than the ones of interest. Knockout of A20 increased the susceptibility of Jurkat cells to CD95L-induced apoptosis upon stimulation with CD95L, indicating that A20 mediates apoptosis inhibiting properties. Since this effect was pronounced only upon stimulation with low doses, A20 only can exert its anti-apoptotic function when the receptor-stimulation is weak. To further validate the role of A20 in mediating apoptosis resistance, cell lines showing resistance against CD95L-induced apoptosis

---

should be tested. Additionally, the impact of A20 on apoptosis induction should be addressed in different cell types.

Analysis of caspase-8 activation revealed similar reduction of pro-caspase-8, while levels of activated caspase-8 were increased in  $\Delta$ A20 cells. This leads to the assumption that A20 does not interfere with the processing of pro-caspase-8, but with its cleavage products. Also, cleavage of c-FLIP<sub>L</sub> to p43-FLIP was not altered in  $\Delta$ A20 cells, supporting the theory that activation of caspase-8 is similar in both cell lines. Strong stimulation with CD95L lead to higher caspase-8 activation. Since cell death was similar in WT and  $\Delta$ A20 cells upon high CD95L doses, A20 may not be capable to dampen the accelerated active caspase-8 in WT cells. Since caspase activation was found to be equal, but active caspase-8 to be different, there might be another mechanism how A20 regulates caspase-8 at a later stage of apoptosis induction. As cleaved caspase-8 disassociates from the DISC to activate downstream substrates, A20 might work also in the cytosol, which might explain why translocation to the CD95-DISC is not consistent. While it was shown that A20 already inhibits activation of caspase-8 at the level of the DISC after stimulation with TNF $\alpha$ , only reduced caspase-8 activity was evaluated, without displaying an impaired caspase activation in CD95L-induced apoptosis<sup>339</sup>. Therefore, differences in the mode of action of A20 on caspase-8 or active caspase-8 are possible. Induction of the TNF-receptor complex II and the CD95-DISC differ in the recruitment of proteins, such as TRADD<sup>420</sup>. Due to different DISC compositions, it is possible that A20 is recruited more efficiently to the TNF $\alpha$ -induced DISC to block caspase-8 activation, while this inhibition is not functional in the CD95L-induced DISC.

In this context, the ubiquitin-editing enzyme activity of A20 might play an important role to target active caspase-8 for its proteasomal degradation. Caspase-8 is targeted and K63-polyubiquitinated by Cullin3 in the p10 region and K48-polyubiquitinated in the p18 region by TRAF2<sup>349,421</sup>. Ubiquitination of caspase-8 to target it for proteasomal degradation appears after the initial cleavage step on the p18 subunit<sup>176</sup>. Additionally, an interaction of A20 with caspase-8 was reported upon TRAIL stimulation, editing the polyubiquitination in the p10 region from K63- to K48-polyubiquitination<sup>349</sup>. Inhibition of the proteasome adjusted levels of active caspase-8 in WT to levels in  $\Delta$ A20 cells after CD95L stimulation, assuming that K48-linked polyubiquitination of active caspase-8 is important for its degradation. K63-linked caspase-8 was precipitated in CD95L-stimulated samples in WT and  $\Delta$ A20 cells without detecting any differences in

---

the status of ubiquitination. Though a direct interaction between caspase-8 and A20 could not be demonstrated, a binding of A20 to caspase-8 cannot be completely excluded. For mediating the anti-apoptotic effect, A20 might also indirectly affect active caspase-8 in CD95L-induced apoptosis. Therefore, A20 would need to target a protein for proteasomal degradation, which has a stabilising function on caspase-8. One of those proteins might be p62 which was shown to promote aggregation of caspase-8<sup>349</sup>. But also RIP1 is another candidate, since it is targeted by A20 in TRAIL-induced apoptosis to inhibit caspase-8 activation<sup>327</sup>. To address this hypothesis, binding of A20, caspase-8 and active caspase-8 to these proteins has to be tested. Also, an improved method to detect differences in ubiquitination patterns might help to reveal the target proteins of A20 for limiting CD95L-induced apoptosis.

The findings of He et al., demonstrating that A20 does not influence CD95L-induced apoptosis in Jurkat cells, contradict the results of this thesis<sup>342</sup>. However, a different Jurkat cell line was used in that study, where IKK $\gamma$ , essential for the activation of the NF- $\kappa$ B pathway, was chemically knocked out. Chemical mutagenesis is an undirected method to induce genomic mutations and might also affect other genomic regions, responsible for apoptosis-mediation<sup>422,423</sup>. The solely re-expression of A20 does not restore the activation of the NF- $\kappa$ B pathway and, thus, might not be sufficient to restore the phenotypic hallmarks of WT Jurkat cells, since anti-apoptotic proteins, such as Bcl-2 and Bcl-xL, are upregulated by NF- $\kappa$ B activation<sup>424,425</sup>. Differences in TNF $\alpha$ - and CD95L-induced apoptosis execution were also not excluded. In addition to the findings in this thesis, increased susceptibility to CD95L-induced apoptosis was found in primary CD4<sup>+</sup> T cells from A20<sup>flx/flx</sup> CD4-Cre mice (data not published).

Taken together, A20 might be a promising target to overcome receptor-mediated apoptosis resistant tumours. Upregulation of A20 was linked with resistance to drug-induced apoptosis in various cancer cells<sup>327,328,337</sup>. However, targeting A20 to sensitise cells for apoptosis induction might not work straightforward, since loss of A20 may also lead to an accelerated NF- $\kappa$ B activation and thereby to an inflammatory environment<sup>322</sup>. Loss of A20 in conjunction with increased NF- $\kappa$ B activation and higher proliferation rates was described for B cell<sup>426</sup> and T cell<sup>427</sup> lymphomas. Additionally, A20's function is cell type specific and can function as a tumour suppressing, but also tumour promoting protein<sup>332,333</sup>. Hence, targeting A20 for apoptosis induction, without triggering unwanted side effects might be difficult.

---

### 5.3 Concluding remarks

Apoptosis is a strictly regulated pathway in multicellular organisms. It is a complex network of pro- and anti-apoptotic proteins to maintain cell homeostasis. Impaired apoptosis can lead to various diseases, like cancer and autoimmune diseases. Upregulation of anti-apoptotic proteins is often linked with tumour resistance and progression. Especially, c-FLIP is an important anti-apoptotic protein, since it blocks caspase activation at the level of the DISC, but can also induce NF- $\kappa$ B activation. This makes c-FLIP a prominent target for tumour therapy. Interestingly, the renal cell carcinoma cell lines which were characterised within this thesis, required c-FLIP to survive. This phenotype was found very rarely until now. Typically, c-FLIP mediates resistance to ligand-induced apoptosis in a broad variety of tumours, but is not vital for their survival. Additionally, CD95 signalling is necessary for viability of RCC cells. NF- $\kappa$ B was shown to be pre-activated and induced upon CD95 stimulation, showing the importance of this pathway. Taken together, c-FLIP might have a dual function in renal cell carcinoma. Besides blocking apoptosis, it might also be involved in mediating proliferative effects. This makes c-FLIP an attractive target for treating renal cell carcinoma efficiently.

Ubiquitination of proteins is a major way to control their stability and interplay with other proteins. Ubiquitination of pro- and anti-apoptotic proteins also alters the outcome of apoptosis induction. The effect of the ubiquitin-editing enzyme A20 on regulation of apoptosis is controversial and seems to be cell type specific. The findings of this thesis support the assumption that A20 reduces CD95L-induced apoptosis by inhibiting caspase-8 activity. However, whether this effect is mediated directly or indirectly could not be identified. To validate these findings, a better understanding of how A20 is acting in the complex apoptotic machinery is needed.

In general, manipulating the apoptotic pathway is a promising tool to treat tumours. Still, a lot of research has to be carried out to fully understand this pathway and how it can be altered for an efficient treatment. This knowledge might help to discover specific drugs which reduce side effects on bystander cells. Since tumours develop diverse mechanisms to gain resistance against apoptotic stimuli, it is difficult to find a general approach for tumour therapy. For the best outcome, a thorough genetic and phenotypic characterisation of each patient's tumour is recommended.

## 6 Abbreviations

7AAD	7-amino-actinomycin D
A1	Bcl-2-related gene A1
AICD	Activation-induced cell death
AIDS	Acquired immune deficiency syndrome
AIF	Apoptosis inducing factor
ALPS	Autoimmune lymphoproliferative syndrome
APAF-1	Apoptotic protease activating factor 1
AIP	Activation-induced cell death
ASC	Adaptor protein apoptosis-associated speck-like protein containing CARD
ADP	Adenosine diphosphate
APP	Amyloid precursor protein
ATG	Autophagy-related gene
ATP	Adenosine triphosphate
Bak	Bcl-2 antagonist killer 1
Bax	Bcl-2-associated x protein
BCA	Bicinchoninic acid
Bcl-2	B cell lymphoma-2
Bcl-xL	B cell lymphoma x, large form
BH	Bcl-2 homology
Bid	BH3-interacting domain
Bok	Bcl-2-related ovarian killer
C	Cysteine
C-terminal	Carboxy-terminal
c-FLIP	Cellular FLICE-inhibitory protein
c-FLIP <sub>L</sub>	c-FLIP long isoform
c-FLIP <sub>R</sub>	c-FLIP Raji isoform
c-FLIP <sub>S</sub>	c-FLIP short isoform
Cas	CRISPR-associated endonuclease
Caspase	CysteinyI-aspartate specific protease

---

CAD	Caspase-activated DNase
CARD	Caspase recruitment domain
CD	Cluster of differentiation
CHX	Cycloheximide
cIAP	Cellular inhibitors of apoptosis
clearCa	clear carcinoma cell line
CRISPR	Clustered regularly interspaced short palindromic repeats
CX3CL1	C-X3-C Motif Chemokine Ligand 1
CytC	Cytochrome c
D	Aspartate
DAMP	Damage-associated molecular pattern
DAPI	4',6-Diamidin-2-phenylindol
DcR	Decoy receptor
DD	Death domain
DED	Death effector domain
DIABLO	Direct IAP binding protein with low pI
DISC	Death inducing signaling complex
DMEM	Dulbecco's modified Eagle's medium
DNA	Deoxyribonucleic acid
DR	Death receptor
DUB	Deubiquitinating enzyme
E	Glutamate
E1	Ubiquitin-activating enzyme
E2	Ubiquitin-conjugating enzyme
E3	Ubiquitin ligase
<i>E. coli</i>	<i>Escherichia coli</i>
EDTA	Ethylenediaminetetraacetic acid
EndoG	Endonuclease G
EGF	Epidermal growth Factor receptor
FADD	Fas-associated via death domain protein
FCS	Fetal calf serum

---

---

FITC	Fluorescein isothiocyanate
FLICE	FADD-like Interleukin-1 $\beta$ converting enzyme
FLIP	FLICE-inhibitory protein
gRNA	guide RNA
GM-CSF	Granulocyte-macrophage colony-stimulating factor
H	Histidine
HECT	Homologous to E6-AP carboxyl terminus
HEK293T	Human embryonic kidney 293 cells with SV40 large T-Antigen
HMGB1	High-Mobility-Group-Protein B1
HRP	Horseradish peroxidase
I	Isoleucine
iCAD	Inhibitor of caspase-activated DNase
Ig	Immunoglobulin
I $\kappa$ B	Inhibitor of NF $\kappa$ B protein
IKK	I $\kappa$ B kinase
IL	Interleukin
Iono	Ionomycin
IP	Immunoprecipitation
K	Lysine
L	Leucine
LB	Luria-Bertani
LPC	Lysophosphatidylcholine
LPS	Lipopolysaccharide
LUBAC	Linear ubiquitin chain assembly complex
Mcl-1	Myeloid cell leukemia-1
MCP-1	Monocyte Chemoattractant Protein-1
MHC	Major histocompatibility complex
MJD	Machado-Josephin domain proteases
MLKL	Mixed-lineage kinase domain-like
MOMP	Mitochondrial outer membrane permeabilization
mtDNA	Mitochondrial DNA

---



---

n.s.	not significant
Nec-1	Necrostatin-1
NEMO	NF $\kappa$ -B essential modulator
NF- $\kappa$ B	Nuclear factor 'kappa-light-chain-enhancer' of activated B-cells
NK	Natural killer cells
NLRP3	NACHT domain-, leucine-rich repeat-, and PYD-containing protein 3
NOD	Nucleotide-binding oligomerization domain
OTU	Ovarian tumour protease
P	Phospho
P/I	PMA/Ionomycin
PAK2	p21-activated kinase 2
PARP	Poly (ADP-ribose) polymerase
PBS	Phosphate-buffered saline
PCR	Polymerase chain reaction
PE	R-Phycoerythrin
PerCP-Cy	Peridinin chlorophyll protein-Cyanin
pHVL	Von Hippel-Landau protein
PMA	Phorbol 12-myristate-13-acetate
PVDF	Polyvinylidene fluoride
qRT-PCR	Quantitative real-time PCR
QVD	(3S)-5-(2,6-Difluorophenoxy)-3-[[[(2S)-3-methyl-1-oxo-2-[(2-quinolinylcarbonyl)amino]butyl]amino]-4-oxo-pentanoic acid hydrate
RCC	Renal cell carcinoma
RING	Really interesting new gene
RBR	RING between RING
RIP1	Receptor-interacting serine/threonine-protein kinase 1
RNA	Ribonucleic acid
RNF	Ring finger protein
RPMI	Roswell Park Memorial Institute
ROCK-1	rho-associated coiled-coil kinase-1

---

---

ROS	Reactive oxygen species
RSB	Reducing sample buffer
S1P	sphingosine 1-phosphate
SAP130	Sin3A-associated protein
shRNA	Short hairpin RNA
siRNA	small interfering RNA
Smac	Second mitochondria-derived activator of caspases
SNP	Single nucleotide polymorphism
TAE	Tris base-acetic acid-EDTA buffer
TAK1	Transforming growth factor $\beta$ -activated kinase 1
TAX1BP1	TAX1 binding protein 1
TBS	Tris-buffered saline
TCR	T cell receptor
TGF $\beta$	Transforming growth factor beta
TLR	Toll-like receptor
TNF	Tumor necrosis factor
TNF-R	TNF receptor
TNFAIP3	TNF $\alpha$ -induced protein 3
TRADD	TNF-R type 1-associated death domain protein
TRAF	TNF-receptor associated factor
TRAIL	Tumor necrosis factor related apoptosis inducing ligand
TRAIL-R	TRAIL receptor
TUBE	Tandem ubiquitin binding entity
Ub	Ubiquitin
UBD	Ubiquitin binding domain
UBL	Ubiquitin-like protein
UCH	Ubiquitin C-terminal hydrolases
USP	Ubiquitin-specific proteases
V	Valin
v-FLIP	Viral FLIP
WT	Wildtype

---

X	Any amino acid
XIAP	X-linked inhibitor of apoptosis protein
ZnF	Zinc finger

## References

- 1 Lockshin, R. A. and Williams, C. M. Programmed Cell Death - I. Cytology of Degeneration in the Intersegmental Muscles of the Pernyi Silkmoth. *J. Insect Physiol.*, 11:123–33, 1965.
- 2 Steller, H. Mechanisms and genes of cellular suicide. *Science*, 267(5203):1445–9, 1995.
- 3 Galluzzi, L. *et al.* Essential versus accessory aspects of cell death: recommendations of the NCCD 2015. *Cell Death Differ.*, (2014):1–16, 2014.
- 4 Fuchs, Y. and Steller, H. Live to die another way: modes of programmed cell death and the signals emanating from dying cells. *Nat. Rev. Mol. Cell Biol.*, 16(6):329–44, 2015.
- 5 Tait, S. W. G. *et al.* Die another way – non-apoptotic mechanisms of cell death. *J. Cell Sci.*, 127(10):2135–44, 2014.
- 6 Kuranaga, E. Beyond apoptosis: caspase regulatory mechanisms and functions in vivo. *Genes Cells*, 17(2):83–97, 2012.
- 7 Kepp, O. *et al.* Cell death assays for drug discovery. *Nat. Rev. Drug Discov.*, 10(3):221–37, 2011.
- 8 Krysko, D. V. *et al.* Apoptosis and necrosis: Detection, discrimination and phagocytosis. *Methods*, 44(3):205–21, 2008.
- 9 Galluzzi, L. *et al.* Guidelines for the use and interpretation of assays for monitoring cell death in higher eukaryotes. *Cell Death Differ.*, 16(8):1093–107, 2009.
- 10 Mariño, G. *et al.* Self-consumption: the interplay of autophagy and apoptosis. *Nat. Rev. Mol. Cell Biol.*, 15(2):81–94, 2014.
- 11 Kroemer, G. and Levine, B. Autophagic cell death: the story of a misnomer Guido. *Nat Rev Mol Cell Biol.*, 9(12):1004–10, 2008.
- 12 Majno, G. and Joris, I. Apoptosis, oncosis, and necrosis. An overview of cell death. *Am. J. Pathol.*, 146(1):3–15, 1995.
- 13 Vanden Berghe, T. *et al.* Regulated necrosis: the expanding network of non-apoptotic cell death pathways. *Nat. Rev. Mol. Cell Biol.*, 15(2):135–47, 2014.
- 14 Han, J. *et al.* Programmed necrosis: backup to and competitor with apoptosis in the immune system. *Nat. Immunol.*, 12(12):1143–9, 2011.
- 15 Sun, L. *et al.* Mixed lineage kinase domain-like protein mediates necrosis signaling downstream of RIP3 kinase. *Cell*, 148(1-2):213–27, 2012.

- 
- 16 Wu, X.-N. *et al.* Distinct roles of RIP1-RIP3 hetero- and RIP3-RIP3 homo-interaction in mediating necroptosis. *Cell Death Differ.*, 21(11):1709–20, 2014.
  - 17 Schulze-Osthoff, K. *et al.* Cytotoxic activity of tumor necrosis factor is mediated by early damage of mitochondrial functions. Evidence for the involvement of mitochondrial radical generation. *J. Biol. Chem.*, 267(8):5317–23, 1992.
  - 18 Degtarev, A. *et al.* Chemical inhibitor of nonapoptotic cell death with therapeutic potential for ischemic brain injury. *Nat. Chem. Biol.*, 1(2):112–9, 2005.
  - 19 Chen, X. *et al.* Translocation of mixed lineage kinase domain-like protein to plasma membrane leads to necrotic cell death. *Cell Res.*, 24(1):105–21, 2014.
  - 20 Vandenabeele, P. *et al.* Molecular mechanisms of necroptosis: an ordered cellular explosion. *Nat. Rev. Mol. Cell Biol.*, 11(10):700–714, 2010.
  - 21 Scaffidi, P. *et al.* Release of chromatin protein HMGB1 by necrotic cells triggers inflammation. *Nature*, 418(6894):191–5, 2002.
  - 22 Martin, S. J. *et al.* A Perspective on Mammalian Caspases as Positive and Negative Regulators of Inflammation. *Mol. Cell*, 46(4):387–97, 2012.
  - 23 Raucci, A. *et al.* HMGB1: A signal of necrosis. *Autoimmunity*, 40(4):285–9, 2007.
  - 24 Green, D. R. *et al.* Immunogenic and tolerogenic cell death. *Nat. Rev. Immunol.*, 9(5):353–63, 2009.
  - 25 Ewald, F. K. *The apoptosis-regulator c-FLIP Functional role in urothelial carcinoma and autoimmunity and Identification of novel CD95 DISC-interacting proteins.* PhD thesis, Otto-von-Guericke-Universität Magdeburg, 2013.
  - 26 Kerr, J. F. *et al.* Apoptosis: a basic biological phenomenon with wide-ranging implications in tissue kinetics. *Br. J. Cancer*, 26(4):239–57, 1972.
  - 27 Cotter, T. G. *et al.* Microfilament-disrupting agents prevent the formation of apoptotic bodies in tumor cells undergoing apoptosis. *Cancer Res.*, 52(4):997–1005, 1992.
  - 28 Ravichandran, K. S. and Lorenz, U. Engulfment of apoptotic cells: signals for a good meal. *Nat. Rev. Immunol.*, 7(12):964–74, 2007.
  - 29 Cullen, S. P. *et al.* Fas/CD95-induced chemokines can serve as "find-me" signals for apoptotic cells. *Mol. Cell*, 49(6):1034–48, 2013.
  - 30 Rongvaux, A. *et al.* Apoptotic Caspases Prevent the Induction of Type I Interferons by Mitochondrial DNA. *Cell*, 159(7):1563–77, 2014.
  - 31 Ronchetti, a. *et al.* Immunogenicity of apoptotic cells in vivo: role of antigen load, antigen-presenting cells, and cytokines. *J.Immunol.*, 163:130–6, 1999.
-

- 
- 32 Nicholson, D. W. and Thornberry, N. A. Caspases: Killer proteases. *Trends Biochem. Sci.*, 22(8):299–306, 1997.
- 33 Kaczmarek, A. *et al.* Necroptosis: The Release of Damage-Associated Molecular Patterns and Its Physiological Relevance. *Immunity*, 38(2):209–23, 2013.
- 34 Matsumura, H. *et al.* Necrotic Death Pathway in Fas Receptor Signaling. *J Cell Biol.*, 151(6):1247–56, 2000.
- 35 Galluzzi, L. *et al.* Molecular definitions of cell death subroutines: recommendations of the Nomenclature Committee on Cell Death 2012. *Cell Death Differ.*, 19(1):107–20, 2012.
- 36 Lauber, K. *et al.* Apoptotic cells induce migration of phagocytes via caspase-3-mediated release of a lipid attraction signal. *Cell*, 113(6):717–30, 2003.
- 37 Hornung, V. *et al.* AIM2 recognizes cytosolic dsDNA and forms a caspase-1-activating inflammasome with ASC. *Nature*, 458(7237):514–8, 2009.
- 38 Martinon, F. *et al.* The Inflammasomes: Guardians of the Body. *Annu. Rev. Immunol.*, 27(1):229–65, 2009.
- 39 Fantuzzi, G. and Dinarello, C. A. Interleukin-18 and interleukin-1 beta: two cytokine substrates for ICE (caspase-1). *J. Clin. Immunol.*, 19(1):1–11, 1999.
- 40 Cookson, B. T. and Brennan, M. a. Pro-inflammatory programmed cell death. *Trends Microbiol*, 9(3):113–4, 2001.
- 41 Shi, J. *et al.* Cleavage of GSDMD by inflammatory caspases determines pyroptotic cell death. *Nature*, 526(7575):660–5, 2015.
- 42 Kayagaki, N. *et al.* Caspase-11 cleaves gasdermin D for non-canonical inflammasome signalling. *Nature*, 526(7575):666–71, 2015.
- 43 Aravind, L. *et al.* Apoptotic molecular machinery: vastly increased complexity in vertebrates revealed by genome comparisons. *Science*, 291(5507):1279–84, 2001.
- 44 Joza, N. *et al.* Essential role of the mitochondrial apoptosis-inducing factor in programmed cell death. *Nature*, 410(6828):549–54, 2001.
- 45 Danial, N. N. and Korsmeyer, S. J. Cell Death: Critical Control Points. *Cell*, 116(2):205–19, 2004.
- 46 Henson, P. M. and Hume, D. A. Apoptotic cell removal in development and tissue homeostasis. *Trends Immunol.*, 27(5):244–50, 2006.
- 47 Raff, M. C. Social controls on cell survival and cell death. *Nature*, 356(6368):397–400, 1992.
-

- 
- 48 Raff, M. C. *et al.* Programmed cell death and the control of cell survival: lessons from the nervous system. *Science*, 262(5134):695–700, 1993.
- 49 Opferman, J. T. Apoptosis in the development of the immune system. *Cell Death Differ.*, 15(2):234–42, 2008.
- 50 Salmena, L. *et al.* Essential role for caspase 8 in T-cell homeostasis and T-cell-mediated immunity. *Genes Dev.*, 17(7):883–95, 2003.
- 51 Krammer, P. H. *et al.* Life and death in peripheral T cells. *Nat. Rev. Immunol.*, 7(7):532–42, 2007.
- 52 Lai, Y.-M. *et al.* Induction of cell cycle arrest and apoptosis by BCG infection in cultured human bronchial airway epithelial cells. *AJP Lung Cell. Mol. Physiol.*, 293(2):L393–L401, 2007.
- 53 Li, J. and Yuan, J. Caspases in apoptosis and beyond. *Oncogene*, 27(48):6194–206, 2008.
- 54 Rendl, M. *et al.* Caspase-14 Expression by Epidermal Keratinocytes is Regulated by Retinoids in a Differentiation-associated Manner. *J. Invest. Dermatol.*, 119(5):1150–5, 2002.
- 55 Shi, Y. Mechanisms of caspase activation and inhibition during apoptosis. *Mol. Cell*, 9(3):459–70, 2002.
- 56 Fuentes-Prior, P. and Salvesen, G. S. The protein structures that shape caspase activity, specificity, activation and inhibition. *Biochem. J.*, 384(Pt 2):201–32, 2004.
- 57 Kersse, K. *et al.* The death-fold superfamily of homotypic interaction motifs. *Trends Biochem. Sci.*, 36(10):541–52, 2011.
- 58 Riedl, S. J. and Shi, Y. Molecular mechanisms of caspase regulation during apoptosis. *Nat. Rev. Mol. Cell Biol.*, 5(11):897–907, 2004.
- 59 Degterev, A. *et al.* A decade of caspases. *Oncogene*, 22(53):8543–67, 2003.
- 60 Cohen, G. M. Caspases: the executioners of apoptosis. *Biochem J*, 326:1–16, 1997.
- 61 Chang, D. W. *et al.* Interdimer processing mechanism of procaspase-8 activation. *EMBO J.*, 22(16):4132–42, 2003.
- 62 Kallenberger, S. M. *et al.* Intra- and Interdimeric Caspase-8 Self-Cleavage Controls Strength and Timing of CD95-Induced Apoptosis. *Sci. Signal.*, 7(316):ra23, 2014.
- 63 Poreba, M. *et al.* Caspase substrates and inhibitors. *Cold Spring Harb. Perspect. Biol.*, 5(8):1–20, 2013.
-

- 
- 64 Thornberry, N. A. *et al.* A Combinatorial Approach Defines Specificities of Members of the Caspase Family and Granzyme B. *J. Biol. Chem.*, 272(29):17907–11, 1997.
- 65 Falschlehner, C. *et al.* TRAIL signalling: decisions between life and death. *Int. J. Biochem. cell Biol.*, 39(7-8):1462–75, 2007.
- 66 Wajant, H. The Fas Signaling Pathway: More Than a Paradigm. *Science*, 296(5573):1635–6, 2002.
- 67 Bouillet, P. and O'Reilly, L. A. CD95, BIM and T cell homeostasis. *Nat. Rev. Immunol.*, 9(7):514–9, 2009.
- 68 Wilson, N. S. *et al.* Death receptor signal transducers: nodes of coordination in immune signaling networks. *Nat. Immunol.*, 10(4):348–55, 2009.
- 69 Ashkenazi, a. and Dixit, V. M. Death receptors: signaling and modulation. *Science*, 281(5381):1305–8, 1998.
- 70 Lavrik, I. N. and Krammer, P. H. Regulation of CD95/Fas signaling at the DISC. *Cell Death Differ.*, 19(1):36–41, 2012.
- 71 Penna, A. *et al.* The CD95 signaling pathway: To not die and fly. *Commun. Integr. Biol.*, 5(2):190–2, 2012.
- 72 Pan, G. *et al.* The receptor for the cytotoxic ligand TRAIL. *Science*, 276(5309):111–3, 1997.
- 73 Walczak, H. TRAIL-R2: a novel apoptosis-mediating receptor for TRAIL. *EMBO J.*, 16(17):5386–97, 1997.
- 74 Rauert, H. *et al.* TNFR1 and TNFR2 regulate the extrinsic apoptotic pathway in myeloma cells by multiple mechanisms. *Cell Death Dis.*, 2:e194, 2011.
- 75 Marsters, S. A. *et al.* Apo-3, a new member of the tumor necrosis factor receptor family, contains a death domain and activates apoptosis and NF- $\kappa$ B. *Curr. Biol.*, 6(12):1669–76, 1996.
- 76 Igney, F. H. and Krammer, P. H. Death and Anti-Death: Tumour Resistance To Apoptosis. *Nat. Rev. Cancer*, 2(4):277–88, 2002.
- 77 Ashkenazi, A. Targeting death and decoy receptors of the tumour-necrosis factor superfamily. *Nat. Rev. Cancer*, 2(June):420–30, 2002.
- 78 Itoh, N. and Nagata, S. A Novel Protein Domain Required for Apoptosis. Mutational analysis of human Fas antigen. *J. Biol. Chem.*, 268(15):10932–7, 1993.
- 79 Tartaglia, L. A. *et al.* A novel domain within the 55 kd TNF receptor signals cell death. *Cell*, 74(5):845–53, 1993.
-



- 
- 80 Kischkel, F. C. *et al.* Cytotoxicity-dependent APO-1 (Fas/CD95)-associated proteins form a death-inducing signaling complex (DISC) with the receptor. *EMBO J.*, 14(22):5579–88, 1995.
- 81 Pan, G. *et al.* An antagonist decoy receptor and a death domain-containing receptor for TRAIL. *Science*, 277(5327):815–8, 1997.
- 82 Körner, H. and Sedgwick, J. D. Tumour necrosis factor and lymphotoxin: Molecular aspects and role in tissue-specific autoimmunity. *Immunol. Cell Biol.*, 74(5):465–72, 1996.
- 83 Marsters, S. a. *et al.* Identification of a ligand for the death-domain-containing receptor Apo3. *Curr. Biol.*, 8(9):525–8, 1998.
- 84 Nikolaev, A. *et al.* APP binds DR6 to trigger axon pruning and neuron death via distinct caspases. *Nature*, 457(7232):981–9, 2009.
- 85 O’Brien, R. and Wong, P. Amyloid precursor protein processing and alzheimer’s disease. *Annu. Rev. Neurosci.*, 1987:185–204, 2011.
- 86 Wang, S. and El-Deiry, W. S. TRAIL and apoptosis induction by TNF-family death receptors. *Oncogene*, 22(53):8628–33, 2003.
- 87 Holler, N. *et al.* Two adjacent trimeric Fas ligands are required for Fas signaling and formation of a death-inducing signaling complex. *Mol. Cell. Biol.*, 23(4):1428–40, 2003.
- 88 Hymowitz, S. G. *et al.* Triggering cell death: the crystal structure of Apo2L/TRAIL in a complex with death receptor 5. *Mol. Cell*, 4(4):563–71, 1999.
- 89 Jin, Z. and El-Deiry, W. S. Distinct signaling pathways in TRAIL- versus tumor necrosis factor-induced apoptosis. *Mol. Cell. Biol.*, 26(21):8136–48, 2006.
- 90 Algeciras-Schimmich, A. *et al.* Molecular ordering of the initial signaling events of CD95. *Mol. Cell. Biol.*, 22(1):207–20, 2002.
- 91 Dickens, L. S. *et al.* A Death Effector Domain Chain DISC Model Reveals a Crucial Role for Caspase-8 Chain Assembly in Mediating Apoptotic Cell Death. *Mol. Cell*, 95(2):1–15, 2012.
- 92 Medema, J. P. *et al.* FLICE is activated by association with the CD95 death-inducing signaling complex (DISC). *EMBO J.*, 16(10):2794–804, 1997.
- 93 Schleich, K. *et al.* Stoichiometry of the CD95 Death-Inducing Signaling Complex: Experimental and Modeling Evidence for a Death Effector Domain Chain Model. *Mol. Cell*, 47(2):1–14, 2012.
-

- 
- 94 Peter, M. E. and Krammer, P. H. The CD95(APO-1/Fas) DISC and beyond. *Cell Death Differ.*, 10(1):26–35, 2003.
- 95 Tsao, D. H. H. *et al.* Solution structure of N-TRADD and characterization of the interaction of N-TRADD and C-TRAF2, a key step in the TNFR1 signaling pathway. *Mol. Cell*, 5(6):1051–7, 2000.
- 96 Micheau, O. and Tschopp, J. Induction of TNF receptor I-mediated apoptosis via two sequential signaling complexes. *Cell*, 114(2):181–90, 2003.
- 97 Green, D. R. and Reed, J. C. Mitochondria and apoptosis. *Science*, 281(5381):1309–12, 1998.
- 98 Xiang, J. *et al.* BAX-induced cell death may not require interleukin 1 $\beta$ -converting enzyme-like proteases. *Proc. Natl. Acad. Sci. U. S. A.*, 93(25):14559–63, 1996.
- 99 Tsujimoto, Y. Role of Bcl-2 family proteins in apoptosis: apoptosomes or mitochondria? *Genes to cells devoted to Mol. Cell. Mech.*, 3(11):697–707, 1998.
- 100 Youle, R. J. and Strasser, A. The BCL-2 protein family: opposing activities that mediate cell death. *Nat. Rev. Mol. Cell Biol.*, 9(1):47–59, 2008.
- 101 Tait, S. W. and Green, D. R. Mitochondria and cell death: outer membrane permeabilization and beyond. *Nat Rev Mol Cell Biol*, 11(9):621–32, 2010.
- 102 Lindsten, T. *et al.* The combined functions of proapoptotic Bcl-2 family members Bak and Bax are essential for normal development of multiple tissues. *Mol. Cell*, 6(6):1389–99, 2000.
- 103 Li, L. Y. *et al.* Endonuclease G is an apoptotic DNase when released from mitochondria. *Nature*, 412(6842):95–9, 2001.
- 104 Susin, S. A. *et al.* Molecular characterization of mitochondrial apoptosis-inducing factor. *Nature*, 397(6718):441–6, 1999.
- 105 Schafer, Z. T. and Kornbluth, S. The apoptosome: physiological, developmental, and pathological modes of regulation. *Dev. Cell*, 10(5):549–61, 2006.
- 106 Cain, K. *et al.* The Apaf-1 apoptosome: a large caspase-activating complex. *Biochimie*, 84(2-3):203–14, 2002.
- 107 Galbán, S. and Duckett, C. S. XIAP as a ubiquitin ligase in cellular signaling. *Cell Death Differ.*, 17(1):54–60, 2010.
- 108 Rehm, M. *et al.* Systems analysis of effector caspase activation and its control by X-linked inhibitor of apoptosis protein. *EMBO J.*, 25(18):4338–49, 2006.
- 109 Algeciras-Schimmich, A. and Peter, M. E. Actin dependent CD95 internalization is specific for Type I cells. *FEBS Lett.*, 546(2-3):185–8, 2003.
-

- 
- 110 Jost, P. J. *et al.* XIAP discriminates between type I and type II FAS-induced apoptosis. *Nature*, 460(7258):1035–9, 2009.
- 111 Lavrik, I. N. Systems biology of death receptor networks: live and let die. *Cell Death Dis.*, 5(5):e1259, 2014.
- 112 Grosse, L. *et al.* Bax assembles into large ring-like structures remodeling the mitochondrial outer membrane in apoptosis. *EMBO J.*, 35(4):402–13, 2016.
- 113 Brumatti, G. *et al.* Conversion of CD95 (Fas) Type II into Type I signaling by sub-lethal doses of cycloheximide. *Exp. Cell Res.*, 314(3):554–63, 2008.
- 114 Ravichandran, K. S. Beginnings of a Good Apoptotic Meal: The Find-Me and Eat-Me Signaling Pathways. *Immunity*, 35(4):445–55, 2011.
- 115 Widlak, P. The DFF40/CAD endonuclease and its role in apoptosis. *Acta Biochim. Pol.*, 47(4):1037–44, 2000.
- 116 Taylor, R. C. *et al.* Apoptosis: controlled demolition at the cellular level. *Nat. Rev. Mol. Cell Biol.*, 9(3):231–41, 2008.
- 117 Oropesa Ávila, M. *et al.* Emerging roles of apoptotic microtubules during the execution phase of apoptosis. *Cytoskeleton*, 72(9):435–46, 2015.
- 118 Sebbagh, M. *et al.* Caspase-3-mediated cleavage of ROCK I induces MLC phosphorylation and apoptotic membrane blebbing. *Nat. Cell Biol.*, 3(4):346–52, 2001.
- 119 Coleman, M. L. *et al.* Membrane blebbing during apoptosis results from caspase-mediated activation of ROCK I. *Nat. Cell Biol.*, 3(4):339–45, 2001.
- 120 Brancolini, C. *et al.* Dismantling cell-cell contacts during apoptosis is coupled to a caspase-dependent proteolytic cleavage of  $\beta$ -catenin. *J. Cell Biol.*, 139(3):759–771, 1997.
- 121 Rudel, T. Membrane and Morphological Changes in Apoptotic Cells Regulated by Caspase-Mediated Activation of PAK2. *Science*, 276(5318):1571–4, 1997.
- 122 Segawa, K. *et al.* Caspase-mediated cleavage of phospholipid flippase for apoptotic phosphatidylserine exposure. *Science*, 344(6188):1164–8, 2014.
- 123 Oberhammer, F. *et al.* Apoptotic death in epithelial cells: cleavage of DNA to 300 and/or 50 kb fragments prior to or in the absence of internucleosomal fragmentation. *EMBO J.*, 12(9):3679–84, 1993.
- 124 Germain, M. *et al.* Cleavage of automodified poly (ADP-ribose) polymerase during apoptosis. *J. Biol. Chem.*, 274(40):28379–84, 1999.
-

- 
- 125 Bokoch, G. M. Caspase-mediated activation of PAK2 during apoptosis: proteolytic kinase activation as a general mechanism of apoptotic signal transduction? *Cell Death Differ.*, 5(8):637–45, 1998.
- 126 Enari, M. *et al.* A caspase-activated DNase that degrades DNA during apoptosis, and its inhibitor ICAD. *Nature*, 391(6662):43–50, 1998.
- 127 Rao, L. *et al.* Lamin proteolysis facilitates nuclear events during apoptosis. *J. Cell Biol.*, 135(6):1441–55, 1996.
- 128 Khadiha, S. *et al.* Glucotoxic and diabetic conditions induce caspase 6-mediated degradation of nuclear lamin A in human islets, rodent islets and INS-1 832/13 cells. *Apoptosis*, 19(12):1691–1701, 2014.
- 129 Rosen, A. and Casciola-Rosen, L. Autoantigens as substrates for apoptotic proteases: implications for the pathogenesis of systemic autoimmune disease. *Cell Death Differ.*, 6(1):6–12, 1999.
- 130 Gude, D. R. *et al.* Apoptosis induces expression of sphingosine kinase 1 to release sphingosine-1-phosphate as a "come-and-get-me" signal. *FASEB J.*, 22(8):2629–38, 2008.
- 131 Peter, C. *et al.* Release of lysophospholipid 'find-me' signals during apoptosis requires the ATP-binding cassette transporter A1. *Autoimmunity*, 45(8):568–73, 2012.
- 132 Truman, L. *et al.* CX3CL1/fractalkine is released from apoptotic lymphocytes to stimulate macrophage chemotaxis. *Blood*, 112(13):5026–36, 2008.
- 133 Elliott, M. R. *et al.* Nucleotides released by apoptotic cells act as a find-me signal for phagocytic clearance. *Nature*, 461(7261):282–6, 2009.
- 134 Fadok, V. A. *et al.* Loss of phospholipid asymmetry and surface exposure of phosphatidylserine is required for phagocytosis of apoptotic cells by macrophages and fibroblasts. *J. Biol. Chem.*, 276(2):1071–7, 2001.
- 135 Gregory, C. D. and Pound, J. D. Cell death in the neighbourhood: direct microenvironmental effects of apoptosis in normal and neoplastic tissues. *J. Pathol.*, 223(2):177–94, 2011.
- 136 Bournazou, I. *et al.* Apoptotic human cells inhibit migration of granulocytes via release of lactoferrin. *J. Clin. Invest.*, 119(1):20–32, 2009.
- 137 Rivas, J. M. and Ullrich, S. E. Systemic suppression of delayed-type hypersensitivity by supernatants from UV-irradiated keratinocytes. An essential role for keratinocyte-derived IL-10. *J. Immunol.*, 149(12):3865–71, 1992.
-

- 
- 138 Gao, Y. *et al.* Antiinflammatory effects of CD95 ligand (FasL)-induced apoptosis. *J. Exp. Med.*, 188(5):887–96, 1998.
- 139 Chen, W. *et al.* TGF- $\beta$  Released by Apoptotic T Cells Contributes to an Immunosuppressive Milieu. *Immunity*, 14(6):715–25, 2001.
- 140 Thome, M. *et al.* Viral FLICE-inhibitory proteins (FLIPs) prevent apoptosis induced by death receptors., 1997.
- 141 Goltsev, Y. V. *et al.* CASH, a novel caspase homologue with death effector domains. *J. Biol. Chem.*, 272(32):19641–4, 1997.
- 142 Han, D. K. *et al.* MRIT, a novel death-effector domain-containing protein, interacts with caspases and BclXL and initiates cell death. *Proc. Natl. Acad. Sci. U. S. A.*, 94(21):11333–8, 1997.
- 143 Hu, S. *et al.* I-FLICE, a novel inhibitor of tumor necrosis factor receptor-1- and CD-95-induced apoptosis. *J. Biol. Chem.*, 272(28):17255–7, 1997.
- 144 Inohara, N. *et al.* CLARP, a death effector domain-containing protein interacts with caspase-8 and regulates apoptosis. *Proc. Natl. Acad. Sci. U. S. A.*, 94(20):10717–22, 1997.
- 145 Rasper, D. M. *et al.* Cell death attenuation by 'Usurpin', a mammalian DED-caspase homologue that precludes caspase-8 recruitment and activation by the CD-95 (Fas, APO-1) receptor complex. *Cell Death Differ.*, 5(4):271–88, 1998.
- 146 Shu, H. B. *et al.* Casper is a FADD- and caspase-related inducer of apoptosis. *Immunity*, 6(6):751–63, 1997.
- 147 Srinivasula, S. M. *et al.* FLAME-1, a Novel FADD-like Anti-apoptotic Molecule That Regulates Fas/TNFR1-induced Apoptosis. *J. Biol. Chem.*, 272(30):18542–5, 1997.
- 148 Djerbi, M. *et al.* Characterization of the human FLICE-inhibitory protein locus and comparison of the anti-apoptotic activity of four different flip isoforms. *Scand. J. Immunol.*, 54(1-2):180–9, 2001.
- 149 Golks, A. *et al.* c-FLIPR, a new regulator of death receptor-induced apoptosis. *J. Biol. Chem.*, 280(15):14507–13, 2005.
- 150 Scaffidi, C. *et al.* The role of c-FLIP in modulation of CD95-induced apoptosis. *J. Biol. Chem.*, 274(3):1541–8, 1999.
- 151 Budd, R. C. *et al.* cFLIP regulation of lymphocyte activation and development. *Nat. Rev. Immunol.*, 6(3):196–204, 2006.
-

- 
- 152 Ueffing, N. *et al.* A single nucleotide polymorphism determines protein isoform production of the human c-FLIP protein. *Blood*, 114(3):572–9, 2009.
- 153 Hughes, M. A. *et al.* Co-operative and Hierarchical Binding of c-FLIP and Caspase-8: A Unified Model Defines How c-FLIP Isoforms Differentially Control Cell Fate. *Mol. Cell*, 61(6):834–49, 2016.
- 154 Kavuri, S. M. *et al.* Cellular FLICE-inhibitory protein (cFLIP) isoforms block CD95- and TRAIL death receptor-induced gene induction irrespective of processing of caspase-8 or cFLIP in the death-inducing signaling complex. *J. Biol. Chem.*, 286(19):16631–46, 2011.
- 155 Krueger, a. *et al.* Cellular FLICE-inhibitory protein splice variants inhibit different steps of caspase-8 activation at the CD95 death-inducing signaling complex. *J. Biol. Chem.*, 276(23):20633–40, 2001.
- 156 Ueffing, N. *et al.* Mutational analyses of c-FLIPR, the only murine short FLIP isoform, reveal requirements for DISC recruitment. *Cell Death Differ.*, 15(4):773–82, 2008.
- 157 Lee, J.-S. *et al.* FLIP-mediated autophagy regulation in cell death control. *Nat. Cell Biol.*, 11(11):1355–62, 2009.
- 158 Piao, X. *et al.* c-FLIP Maintains Tissue Homeostasis by Preventing Apoptosis and Programmed Necrosis. *Sci. Signal.*, 5(255):ra93, 2012.
- 159 Chang, D. W. *et al.* C-FLIPL is a dual function regulator for caspase-8 activation and CD95-mediated apoptosis. *EMBO J.*, 21(14):3704–14, 2002.
- 160 Fricker, N. *et al.* Model-based dissection of CD95 signaling dynamics reveals both a pro- and antiapoptotic role of c-FLIPL. *J. Cell Biol.*, 190(3):377–89, 2010.
- 161 Tschopp, J. *et al.* Inhibition of fas death signals by FLIPs. *Curr. Opin. Immunol.*, 10(5):552–8, 1998.
- 162 Schmitz, I. *et al.* An IL-2-dependent switch between CD95 signaling pathways sensitizes primary human T cells toward CD95-mediated activation-induced cell death. *J. Immunol.*, 171(6):2930–6, 2003.
- 163 He, M.-X. and He, Y.-W. A role for c-FLIPL in the regulation of apoptosis, autophagy, and necroptosis in T lymphocytes. *Cell Death Differ.*, 20(2):188–97, 2013.
- 164 Ueffing, N. *et al.* Up-regulation of c-FLIP short by NFAT contributes to apoptosis resistance of short-term activated T cells. *Blood*, 112(3):690–8, 2008.
-

- 
- 165 Koenig, A. *et al.* The c-FLIPL Cleavage Product p43FLIP Promotes Activation of ERK, NF- $\kappa$ B, Caspase-8 and T Cell Survival. *J. Biol. Chem.*, 289(2):1183–91, 2014.
- 166 Kataoka, T. and Tschopp, J. N-terminal fragment of c-FLIP(L) processed by caspase 8 specifically interacts with TRAF2 and induces activation of the NF- $\kappa$ B signaling pathway. *Mol. Cell. Biol.*, 24(7):2627–36, 2004.
- 167 Kataoka, T. *et al.* The caspase-8 inhibitor FLIP promotes activation of NF- $\kappa$ B and Erk signaling pathways. *Curr. Biol.*, 10(11):640–8, 2000.
- 168 Dohrman, A. *et al.* Cellular FLIP (Long Form) Regulates CD8+ T Cell Activation through Caspase-8-Dependent NF- $\kappa$ B Activation. *J. Immunol.*, 174(9):5270–8, 2005.
- 169 Neumann, L. *et al.* Dynamics within the CD95 death-inducing signaling complex decide life and death of cells. *Mol. Syst. Biol.*, 6(352):352, 2010.
- 170 Matsuda, I. *et al.* The C-terminal Domain of c-FLIPL Inhibits the Interaction of the Caspase 8 Prodomain with RIP1 Death Domain and Regulates Caspase 8-dependent NF- $\kappa$ B activation. *J. Biol. Chem.*, 289(7):3876–87, 2014.
- 171 Fuchs, Y. and Steller, H. Programmed cell death in animal development and disease. *Cell*, 147(4):742–58, 2014.
- 172 Laurent-Crawford, A. G. *et al.* The cytopathic effect of HIV is associated with apoptosis. *Virology*, 185(2):829–39, 1991.
- 173 Martinou, J. C. *et al.* Overexpression of BCL-2 in transgenic mice protects neurons from naturally occurring cell death and experimental ischemia. *Neuron*, 13(4):1017–30, 1994.
- 174 Rao, V. K. and Oliveira, J. B. How I treat autoimmune lymphoproliferative syndrome. *Blood*, 118(22):5741–51, 2011.
- 175 Lowe, S. W. and Lin, a. W. Apoptosis in cancer. *Carcinogenesis*, 21(3):485–95, 2000.
- 176 Fiandalo, M. V. *et al.* Proteasomal regulation of caspase-8 in cancer cell apoptosis. *Apoptosis*, 18(6):766–76, 2013.
- 177 Evan, G. I. *et al.* Proliferation, cell cycle and apoptosis in cancer. *Nature*, 411(May):342–48, 2001.
- 178 Tsujimoto, Y. *et al.* Involvement of the bcl-2 gene in human follicular lymphoma. *Science*, 228(4706):1440–3, 1985.
-

- 
- 179 Reed, J. C. *et al.* Oncogenic potential of bcl-2 demonstrated by gene transfer. *Nature*, 336(6196):259–61, 1988.
- 180 Vaux, D. L. *et al.* Bcl-2 gene promotes haemopoietic cell survival and cooperates with c-myc to immortalize pre-B cells., 1988.
- 181 Alderson, M. R. *et al.* Fas transduces activation signals in normal human T lymphocytes. *J. Exp. Med.*, 178(6):2231–5, 1993.
- 182 Desbarats, J. *et al.* Fas engagement induces neurite growth through ERK activation and p35 upregulation. *Nat. Cell Biol.*, 5(2):118–25, 2003.
- 183 Barnhart, B. C. *et al.* CD95 ligand induces motility and invasiveness of apoptosis-resistant tumor cells. *EMBO J.*, 23(15):3175–85, 2004.
- 184 Lee, J.-K. *et al.* Lack of FasL-mediated killing leads to in vivo tumor promotion in mouse Lewis lung cancer. *Apoptosis*, 8(2):151–60, 2003.
- 185 Zhang, Y. *et al.* Fas Signal Promotes Lung Cancer Growth by Recruiting Myeloid-Derived Suppressor Cells via Cancer Cell-Derived PGE2. *J. Immunol.*, 182(6):3801–8, 2009.
- 186 Park, S.-M. *et al.* CD95 is cytoprotective for intestinal epithelial cells in colitis. *Inflamm. Bowel Dis.*, 16(6):1063–70, 2010.
- 187 Yuan, K. *et al.* Calmodulin Mediates Fas-induced FADD-independent Survival Signaling in Pancreatic Cancer Cells via Activation of Src-Extracellular Signal-regulated Kinase (ERK). *J. Biol. Chem.*, 286(28):24776–84, 2011.
- 188 Trauzold, A. CD95 and TRAF2 promote invasiveness of pancreatic cancer cells. *FASEB J.*, 19(6):620–2, 2005.
- 189 Nijkamp, M. W. *et al.* CD95 is a key mediator of invasion and accelerated outgrowth of mouse colorectal liver metastases following radiofrequency ablation. *J. Hepatol.*, 53(6):1069–77, 2010.
- 190 Steller, E. J. A. *et al.* The death receptor CD95 activates the cofilin pathway to stimulate tumour cell invasion. *EMBO Rep.*, 12(9):931–7, 2011.
- 191 Teodorczyk, M. *et al.* CD95 promotes metastatic spread via Sck in pancreatic ductal adenocarcinoma. *Cell Death Differ.*, 22(7):1192–202, 2015.
- 192 Baldwin, R. L. *et al.* Primary Ovarian Cancer Cultures are Resistant to Fas-Mediated Apoptosis. *Gynecol. Oncol.*, 74(2):265–71, 1999.
- 193 Konno, R. *et al.* Serum soluble fas level as a prognostic factor in patients with gynecological malignancies. *Clin. Cancer Res.*, 6(9):3576–80, 2000.
-



- 
- 194 Osorio, L. M. *et al.* Increased serum levels of soluble Fas in progressive B-CLL. *Eur. J. Haematol.*, 66(5):342–6, 2001.
- 195 Mizutani, Y. *et al.* Prognostic Significance of a Combination of Soluble Fas and Soluble Fas Ligand in the Serum of Patients with Ta Bladder Cancer. *Cancer Biother. Radiopharm.*, 17(5):563–7, 2002.
- 196 Fisher, G. H. *et al.* Dominant Interfering Fas Gene-Mutations Impair Apoptosis in a Human Autoimmune Lymphoproliferative Syndrome. *Cell*, 81(6):935–46, 1995.
- 197 van den Berg, A. *et al.* Germline FAS gene mutation in a case of ALPS and NLP Hodgkin lymphoma. *Blood*, 99(4):1492–4, 2002.
- 198 Infante, A. J. *et al.* The clinical spectrum in a large kindred with autoimmune lymphoproliferative syndrome caused by a Fas mutation that impairs lymphocyte apoptosis. *J. Pediatr.*, 133(5):629–33, 1998.
- 199 Zang, F. *et al.* Relationship of c-FLIP(L) protein expression with molecular subtyping and clinical prognosis in invasive breast cancer. *Zhonghua Bing Li Xue Za Zhi*, 43(7):442–6, 2014.
- 200 Bedolla, R. G. *et al.* Predictive Value of Sp1/Sp3/FLIP Signature for Prostate Cancer Recurrence. *PLoS One*, 7(9):e44917, 2012.
- 201 Ewald, F. *et al.* The role of c-FLIP splice variants in urothelial tumours. *Cell Death Dis.*, 2(12):e245, 2011.
- 202 Gao, X. *et al.* hnRNPK inhibits GSK3 $\beta$  Ser9 phosphorylation, thereby stabilizing c-FLIP and contributes to TRAIL resistance in H1299 lung adenocarcinoma cells. *Sci. Rep.*, 6:22999, 2016.
- 203 Dutton, A. *et al.* Expression of the cellular FLICE-inhibitory protein (c-FLIP) protects Hodgkin’s lymphoma cells from autonomous Fas-mediated death. *Proc Natl Acad Sci U S A*, 101(17):6611–6, 2004.
- 204 Tian, F. *et al.* Expression of c-FLIP in malignant melanoma, and its relationship with the clinicopathological features of the disease. *Clin. Exp. Dermatol.*, 37(3):259–65, 2012.
- 205 Du, X. *et al.* Expression and biological significance of c-FLIP in human hepatocellular carcinomas. *J. Exp. Clin. Cancer Res.*, 28(1):24, 2009.
- 206 Kinoshita, H. *et al.* Cisplatin (CDDP) sensitizes human osteosarcoma cell to Fas/CD95-mediated apoptosis by down-regulating FLIP-L expression. *Int. J. cancer*, 88(6):986–91, 2000.
-

- 
- 207 Geserick, P. *et al.* Suppression of cFLIP is sufficient to sensitize human melanoma cells to TRAIL- and CD95L-mediated apoptosis. *Oncogene*, 27(22):3211–20, 2008.
- 208 Riley, J. S. *et al.* Prognostic and therapeutic relevance of FLIP and procaspase-8 overexpression in non-small cell lung cancer. *Cell Death Dis.*, 4:e951, 2013.
- 209 Rippo, M. R. *et al.* FLIP overexpression inhibits death receptor-induced apoptosis in malignant mesothelial cells. *Oncogene*, 23(47):7753–60, 2004.
- 210 Mathas, S. *et al.* c-FLIP Mediates Resistance of Hodgkin/Reed-Sternberg Cells to Death Receptor-induced Apoptosis. *J. Exp. Med.*, 199(8):1041–52, 2004.
- 211 Ljungberg, B. *et al.* EAU guidelines on renal cell carcinoma: 2014 update. *Eur. Urol.*, 67(5):913–24, 2015.
- 212 Rini, B. I. *et al.* Renal cell carcinoma. *Curr. Opin. Oncol.*, 20(3):300–6, 2008.
- 213 Iliopoulos, O. *et al.* Tumour suppression by the human von Hippel-Lindau gene product. *Nat. Med.*, 1(8):822–6, 1995.
- 214 Schermer, B. *et al.* The von Hippel-Lindau tumor suppressor protein controls ciliogenesis by orienting microtubule growth. *J. Cell Biol.*, 175(4):547–54, 2006.
- 215 van Dijk, B. A. C. *et al.* Cigarette smoking, von Hippel-Lindau gene mutations and sporadic renal cell carcinoma. *Br. J. Cancer*, 95(3):374–7, 2006.
- 216 Kaelin, W. G. The von Hippel-Lindau Tumor Suppressor Protein and Clear Cell Renal Carcinoma. *Clin. Cancer Res.*, 13(2):680s–4s, 2007.
- 217 Gerharz, C. D. *et al.* Resistance to CD95 (APO-1/Fas)-mediated apoptosis in human renal cell carcinomas: an important factor for evasion from negative growth control. *Lab. Invest.*, 79(12):1521–34, 1999.
- 218 Ramp, U. *et al.* Apoptosis induction in renal cell carcinoma by TRAIL and  $\gamma$ -radiation is impaired by deficient caspase-9 cleavage. *Br. J. Cancer*, 88(11):1800–7, 2003.
- 219 Sejima, T. and Miyagawa, I. Significance of Fas expression alteration during tumor progression of renal cell carcinoma. *Int. J. Urol.*, 13(3):257–64, 2006.
- 220 Sejima, T. *et al.* Fas expression in renal cell carcinoma accurately predicts patient survival after radical nephrectomy. *Urol. Int.*, 88(3):263–70, 2012.
- 221 Kim, J. W. *et al.* Activation of death-inducing signaling complex (DISC) by pro-apoptotic C-terminal fragment of RIP. *Oncogene*, 19(39):4491–9, 2000.
- 222 Macher-Goeppinger, S. *et al.* Expression and prognostic relevance of the death receptor CD95 (Fas/APO1) in renal cell carcinomas. *Cancer Lett.*, 301(2):203–11, 2011.
-

- 
- 223 Safa, A. R. *et al.* Cellular FLICE-like inhibitory protein (C-FLIP): a novel target for cancer therapy. *Curr. Cancer Drug Targets*, 8(1):37–46, 2008.
- 224 Kimura, Y. and Tanaka, K. Regulatory mechanisms involved in the control of ubiquitin homeostasis. *J. Biochem.*, 147(6):793–8, 2010.
- 225 Muratani, M. and Tansey, W. P. How the ubiquitin-proteasome system controls transcription. *Nat. Rev. Mol. Cell Biol.*, 4(3):192–201, 2003.
- 226 Miller, J. and Gordon, C. The regulation of proteasome degradation by multi-ubiquitin chain binding proteins. *FEBS Lett.*, 579(15):3224–30, 2005.
- 227 Wickliffe, K. E. *et al.* K11-linked ubiquitin chains as novel regulators of cell division. *Trends Cell Biol.*, 21(11):656–63, 2011.
- 228 Huang, T. T. and D’Andrea, A. D. Regulation of DNA repair by ubiquitylation. *Nat Rev Mol Cell Biol*, 7(5):323–34, 2006.
- 229 Di Fiore, P. P. *et al.* When ubiquitin meets ubiquitin receptors: a signalling connection. *Nat. Rev. Mol. Cell Biol.*, 4(6):491–97, 2003.
- 230 Haglund, K. and Dikic, I. Ubiquitylation and cell signaling. *EMBO J.*, 24(19):3353–9, 2005.
- 231 Goldstein, G. *et al.* Isolation of a polypeptide that has lymphocyte-differentiating properties and is probably represented universally in living cells. *Proc. Natl. Acad. Sci. U. S. A.*, 72(1):11–5, 1975.
- 232 Webb, G. C. *et al.* Localization of the human UBA52 ubiquitin fusion gene to chromosome band 19p13.1-p12. *Genomics*, 19(3):567–9, 1994.
- 233 Webb, G. C. *et al.* Localization of the Human UbB Polyubiquitin Gene to Chromosome Band 17p 1 . I-I 7pI 2. *Am J Hum Genet*, pages 308–15, 1990.
- 234 Board, P. G. *et al.* Localization of the human UBC polyubiquitin gene to chromosome band 12q24.3. *Genomics*, 12(4):639–42, 1992.
- 235 Kenmochi, N. *et al.* A map of 75 human ribosomal protein genes. *Genome Res.*, 8(5):509–23, 1998.
- 236 Ozkaynak, E. *et al.* The yeast ubiquitin genes: a family of natural gene fusions. *EMBO J.*, 6(5):1429–39, 1987.
- 237 Wiborg, O. *et al.* The human ubiquitin multigene family: some genes contain multiple directly repeated ubiquitin coding sequences. *EMBO J.*, 4(3):755–9, 1985.
- 238 Lund, P. K. *et al.* Nucleotide sequence analysis of a cDNA encoding human ubiquitin reveals that ubiquitin is synthesized as a precursor. *J. Biol. Chem.*, 260(12):7609–13, 1985.
-

- 
- 239 Ryu, K.-Y. *et al.* The mouse polyubiquitin gene UbC is essential for fetal liver development, cell-cycle progression and stress tolerance. *EMBO J.*, 26(11):2693–706, 2007.
- 240 Busch, H. and Goldknopf, I. L. Ubiquitin - protein conjugates. *Mol. Cell. Biochem.*, 40(3):173–87, 1981.
- 241 Pickart, C. M. Mechanisms Underlying Ubiquitination. *Annu. Rev. Biochem.*, 70(1):503–33, 2001.
- 242 Avram Hershko and Aaron Ciechanover. THE UBIQUITIN SYSTEM. *Annu. Rev. Biochem.*, 67:425–79, 1998.
- 243 Ye, Yihong, M. R. Building ubiquitin chains: E2 enzymes at work. *Nat Rev Mol Cell Biol*, 10(11):755–64, 2009.
- 244 Li, W. *et al.* Genome-Wide and Functional Annotation of Human E3 Ubiquitin Ligases Identifies MULAN, a Mitochondrial E3 that Regulates the Organelle’s Dynamics and Signaling. *PLoS One*, 3(1):e1487, 2008.
- 245 Hershko, A. *et al.* Components of Ubiquitin-Protein Ligase System. *J. Biol. Chem.*, 258(13):8206–14, 1983.
- 246 Haas, A. L. and Rose, I. A. The mechanism of ubiquitin activating enzyme. A kinetic and equilibrium analysis. *J. Biol. Chem.*, 257(17):10329–37, 1982.
- 247 Pickart, C. M. and Eddins, M. J. Ubiquitin: structures, functions, mechanisms. *Biochim. Biophys. Acta*, 1695(1-3):55–72, 2004.
- 248 Spratt, D. E. *et al.* RBR E3 ubiquitin ligases: new structures, new insights, new questions. *Biochem. J.*, 458(3):421–37, 2014.
- 249 Wenzel, D. M. and Klevit, R. E. Following Ariadne’s thread: a new perspective on RBR ubiquitin ligases. *BMC Biol.*, 10(24), 2012.
- 250 Varland, S. *et al.* N-terminal modifications of cellular proteins: The enzymes involved, their substrate specificities and biological effects. *Proteomics*, 15(14):2385–401, 2015.
- 251 Haglund, K. *et al.* Distinct monoubiquitin signals in receptor endocytosis. *Trends Biochem. Sci.*, 28(11):598–604, 2003.
- 252 Dikic, I. Mechanisms controlling EGF receptor endocytosis and degradation. *Biochem. Soc. Trans.*, 31(6):1178–81, 2003.
- 253 Hicke, L. and Dunn, R. Regulation of Membrane Protein Transport by Ubiquitin and Ubiquitin-Binding Proteins. *Annu. Rev. Cell Dev. Biol.*, 19(1):141–72, 2003.
-

- 
- 254 Haglund, K. *et al.* Multiple monoubiquitination of RTKs is sufficient for their endocytosis and degradation. *Nat. Cell Biol.*, 5(5):461–6, 2003.
- 255 Suryadinata, R. *et al.* Mechanisms of generating polyubiquitin chains of different topology. *Cells*, 3(3):674–89, 2014.
- 256 Duncan, L. M. *et al.* Lysine-63-linked ubiquitination is required for endolysosomal degradation of class I molecules. *EMBO J.*, 25(8):1635–45, 2006.
- 257 Shin, J. S. *et al.* Surface expression of MHC class II in dendritic cells is controlled by regulated ubiquitination. *Nature*, 444(7115):115–8, 2006.
- 258 Kravtsova-Ivantsiv, Y. and Ciechanover, A. Non-canonical ubiquitin-based signals for proteasomal degradation. *J. Cell Sci.*, 125(3):539–48, 2012.
- 259 Shang, F. *et al.* Lys6-modified Ubiquitin Inhibits Ubiquitin-dependent Protein Degradation. *J. Biol. Chem.*, 280(21):20365–74, 2005.
- 260 Gatti, M. *et al.* RNF168 promotes noncanonical K27ubiquitination to signal DNA damage. *Cell Rep.*, 10(2):226–38, 2015.
- 261 Kristariyanto, Y. A. *et al.* K29-Selective Ubiquitin Binding Domain Reveals Structural Basis of Specificity and Heterotypic Nature of K29 Polyubiquitin. *Mol. Cell*, 58(1):83–94, 2015.
- 262 Al-Hakim, A. K. *et al.* Control of AMPK-related kinases by USP9X and atypical Lys(29)/Lys(33)-linked polyubiquitin chains. *Biochem. J.*, 411(2):249–60, 2008.
- 263 Kim, W. *et al.* Systematic and quantitative assessment of the ubiquitin modified proteome. *Mol. Cell*, 44(2):325–40, 2011.
- 264 Xu, P. *et al.* Quantitative Proteomics Reveals the Function of Unconventional Ubiquitin Chains in Proteasomal Degradation. *Cell*, 137(1):133–45, 2009.
- 265 Chau, V. *et al.* A multiubiquitin chain is confined to specific lysine in a targeted short-lived protein. *Science*, 243(4898):1576–83, 1989.
- 266 Thrower, J. S. *et al.* Recognition of the polyubiquitin proteolytic signal. *EMBO J.*, 19(1):94–102, 2000.
- 267 Spence, J. *et al.* A ubiquitin mutant with specific defects in DNA repair and multiubiquitination. *Mol. Cell. Biol.*, 15(3):1265–73, 1995.
- 268 Tokunaga, F. Linear ubiquitination-mediated NF- $\kappa$ B regulation and its related disorders. *J. Biochem.*, 154(4):313–23, 2013.
- 269 Meyer, H. J. and Rape, M. Enhanced protein degradation by branched ubiquitin chains. *Cell*, 157(4):910–21, 2014.
-

- 
- 270 Emmerich, C. H. *et al.* Activation of the canonical IKK complex by K63/M1-linked hybrid ubiquitin chains. *Proc. Natl. Acad. Sci. U. S. A.*, 110(38):15247–52, 2013.
- 271 David, Y. *et al.* E3 ligases determine ubiquitination site and conjugate type by enforcing specificity on E2 enzymes. *J. Biol. Chem.*, 286(51):44104–15, 2011.
- 272 Sadowski, M. and Sarcevic, B. Mechanisms of mono- and poly-ubiquitination: Ubiquitination specificity depends on compatibility between the E2 catalytic core and amino acid residues proximal to the lysine. *Cell Div.*, 5(19), 2010.
- 273 Hochstrasser, M. Lingering mysteries of ubiquitin-chain assembly. *Cell*, 124(1):27–34, 2006.
- 274 Boname, J. M. *et al.* Efficient internalization of MHC I requires lysine-11 and lysine-63 mixed linkage polyubiquitin chains. *Traffic*, 11(2):210–20, 2010.
- 275 Nakasone, M. A. *et al.* Mixed-Linkage Ubiquitin Chains Send Mixed Messages. *Structure*, 21(5):727–40, 2013.
- 276 Hurley, J. H. *et al.* Ubiquitin-binding domains. *Biochem. J.*, 399(3):361–72, 2006.
- 277 Grice, G. L. *et al.* The proteasome distinguishes between heterotypic and homotypic lysine-11-Linked polyubiquitin chains. *Cell Rep.*, 12(4):545–53, 2015.
- 278 Nathan, J. a. *et al.* Why do cellular proteins linked to K63-polyubiquitin chains not associate with proteasomes? *EMBO J.*, 32(4):552–65, 2013.
- 279 Welchman, R. L. *et al.* Ubiquitin and ubiquitin-like proteins as multifunctional signals. *Nat. Rev. Mol. Cell Biol.*, 6(8):599–609, 2005.
- 280 Pearce, M. J. *et al.* Ubiquitin-Like Protein Involved in the Proteasome Pathway of *Mycobacterium tuberculosis*. *Darwin*, 322(5904):1104–7, 2008.
- 281 Bienkowska, J. R. *et al.* A search method for homologs of small proteins. Ubiquitin-like proteins in prokaryotic cells? *Protein Eng.*, 16(12):897–904, 2003.
- 282 Mizushima, N. *et al.* A protein conjugation system essential for autophagy. *Nature*, 395(6700):395–8, 1998.
- 283 Romanov, J. *et al.* Mechanism and functions of membrane binding by the Atg5–Atg12/Atg16 complex during autophagosome formation. *EMBO J.*, 31(22):4304–17, 2012.
- 284 Turcu, F. E. *et al.* Regulation and Cellular Roles of Ubiquitin-specific Deubiquitinating Enzymes. *Annu Rev Biochem*, 78:363–97, 2009.
- 285 Komander, D. *et al.* Breaking the chains: structure and function of the deubiquitinases. *Nat. Rev. Mol. Cell Biol.*, 10(8):550–63, 2009.
-

- 
- 286 Wilkinson, K. D. Regulation of ubiquitin-dependent processes by deubiquitinating enzymes. *FASEB J.*, 11(14):1245–56, 1997.
- 287 Wilkinson, K. D. *et al.* Metabolism of the polyubiquitin degradation signal: structure, mechanism, and role of isopeptidase T. *Biochemistry*, 34(44):14535–46, 1995.
- 288 Dikic, I. *et al.* Ubiquitin-binding domains - from structures to functions. *Nat. Rev. Mol. Cell Biol.*, 10(10):659–71, 2009.
- 289 Song, L. and Rape, M. Reverse the curse - the role of deubiquitination in cell cycle control. *Curr Opin Cell Biol*, 20(2):156–63, 2008.
- 290 de la Fouchardière, A. *et al.* Germline BAP1 mutations predispose also to multiple basal cell carcinomas. *Clin. Genet.*, 88(3):273–7, 2015.
- 291 van Loosdregt, J. *et al.* Stabilization of the Transcription Factor Foxp3 by the Deubiquitinase USP7 Increases Treg-Cell-Suppressive Capacity. *Immunity*, 39(2):259–71, 2013.
- 292 Nijman, S. M. B. *et al.* A genomic and functional inventory of deubiquitinating enzymes. *Cell*, 123(5):773–86, 2005.
- 293 Rothe, M. *et al.* TRAF2-mediated activation of NF- $\kappa$ B by TNF receptor 2 and CD40. *Science*, 269(5229):1424–7, 1995.
- 294 Ting, A. T. *et al.* RIP mediates tumor necrosis factor receptor 1 activation of NF- $\kappa$ B but not Fas/APO-1-initiated apoptosis. *EMBO J.*, 15(22):6189–96, 1996.
- 295 Lee, T. H. *et al.* The kinase activity of Rip1 is not required for tumor necrosis factor- $\alpha$ -induced I $\kappa$ B kinase or p38 MAP kinase activation or for the ubiquitination of Rip1 by Traf2. *J. Biol. Chem.*, 279(32):33185–91, 2004.
- 296 Bertrand, M. J. M. *et al.* cIAP1 and cIAP2 Facilitate Cancer Cell Survival by Functioning as E3 Ligases that Promote RIP1 Ubiquitination. *Mol. Cell*, 30(6):689–700, 2008.
- 297 Dynek, J. N. *et al.* c-IAP1 and UbcH5 promote K11-linked polyubiquitination of RIP1 in TNF signalling. *EMBO J.*, 29(24):4198–209, 2010.
- 298 Tokunaga, F. *et al.* SHARPIN is a component of the NF- $\kappa$ B-activating linear ubiquitin chain assembly complex. *Nature*, 471(7340):633–6, 2011.
- 299 Kanayama, A. *et al.* TAB2 and TAB3 activate the NF- $\kappa$ B pathway through binding to polyubiquitin chains. *Mol. Cell*, 15(4):535–48, 2004.
- 300 Iwai, K. and Tokunaga, F. Linear polyubiquitination: a new regulator of NF- $\kappa$ B activation. *EMBO Rep.*, 10(7):706–13, 2009.
-

- 
- 301 Tokunaga, F. *et al.* Involvement of linear polyubiquitylation of NEMO in NF- $\kappa$ B activation. *Nat. Cell Biol.*, 11(2):123–32, 2009.
- 302 Xia, Z.-P. *et al.* Direct activation of protein kinases by unanchored polyubiquitin chains. *Nature*, 461(7260):114–9, 2009.
- 303 Suzuki, H. *et al.* I $\kappa$ B $\alpha$  ubiquitination is catalyzed by an SCF-like complex containing Skp1, cullin-1, and two F-box/WD40-repeat proteins,  $\beta$ TrCP1 and  $\beta$ TrCP2. *Biochem. Biophys. Res. Commun.*, 256(1):127–32, 1999.
- 304 Hayden, M. S. and Ghosh, S. Signaling to NF- $\kappa$ B. *Genes Dev.*, 18:2195–224, 2004.
- 305 Brummelkamp, T. R. *et al.* Loss of the cylindromatosis tumour suppressor inhibits apoptosis by activating NF- $\kappa$ B. *Nature*, 424(6950):797–801, 2003.
- 306 Opipari, A. W. *et al.* The A20 cDNA Induced by Tumor Necrosis Factor  $\alpha$  Encodes a Novel Type of Zinc Finger Protein. *J. Biol. Chem.*, 265(25):14705–8, 1990.
- 307 Cooper, J. T. *et al.* A20 blocks endothelial cell activation through a NF- $\kappa$ B-dependent mechanism. *J. Biol. Chem.*, 271(30):18068–73, 1996.
- 308 Honma, K. *et al.* TNFAIP3 / A20 functions as a novel tumor suppressor gene in several subtypes of non-Hodgkin lymphomas. *Blood*, 114(12):2467–75, 2009.
- 309 Vereecke, L. *et al.* The ubiquitin-editing enzyme A20 (TNFAIP3) is a central regulator of immunopathology. *Trends Immunol.*, 30(8):383–91, 2009.
- 310 Ma, A. and Malynn, B. A. A20: linking a complex regulator of ubiquitylation to immunity and human disease. *Nat. Rev. Immunol.*, 12(11):774–85, 2012.
- 311 Wertz, I. E. *et al.* De-ubiquitination and ubiquitin ligase domains of A20 down-regulate NF- $\kappa$ B signalling. *Nature*, 430(7000):694–9, 2004.
- 312 Bosanac, I. *et al.* Ubiquitin binding to A20 ZnF4 is required for modulation of NF- $\kappa$ B signaling. *Mol. Cell*, 40(4):548–57, 2010.
- 313 Skaug, B. *et al.* Direct, noncatalytic mechanism of IKK inhibition by A20. *Mol. Cell*, 44(4):559–71, 2011.
- 314 Verhelst, K. *et al.* A20 inhibits LUBAC-mediated NF- $\kappa$ B activation by binding linear polyubiquitin chains via its zinc finger 7. *EMBO J.*, 31(19):3845–55, 2012.
- 315 Heyninck, K. *et al.* The zinc finger protein A20 inhibits TNF-induced NF- $\kappa$ B-dependent gene expression by interfering with an RIP- or TRAF2-mediated trans-activation signal and directly binds to a novel NF- $\kappa$ B-inhibiting protein ABIN. *J. Cell Biol.*, 145(7):1471–82, 1999.
- 316 Heyninck, K. and Beyaert, R. A20 inhibits NF- $\kappa$ B activation by dual ubiquitin-editing functions. *Trends Biochem. Sci.*, 30(1):1–4, 2005.
-



- 
- 317 Yuan, S. *et al.* Emergence of the A20/ABIN-mediated inhibition of NF- $\kappa$ B signaling via modifying the ubiquitinated proteins in a basal chordate. *Proc. Natl. Acad. Sci. U. S. A.*, 111(18):6720–5, 2014.
- 318 Mauro, C. *et al.* ABIN-1 binds to NEMO/IKK $\gamma$  and co-operates with A20 in inhibiting NF- $\kappa$ B. *J. Biol. Chem.*, 281(27):18482–8, 2006.
- 319 Shembade, N. *et al.* Essential role for TAX1BP1 in the termination of TNF- $\alpha$ -, IL-1- and LPS-mediated NF- $\kappa$ B and JNK signaling. *EMBO J.*, 26(17):3910–22, 2007.
- 320 Shembade, N. *et al.* The E3 ligase Itch negatively regulates inflammatory signaling pathways by controlling the function of the ubiquitin-editing enzyme A20. *Nat. Immunol.*, 9(3):254–62, 2008.
- 321 Shembade, N. *et al.* The ubiquitin-editing enzyme A20 requires RNF11 to down-regulate NF- $\kappa$ B signalling. *EMBO J.*, 28(5):513–22, 2009.
- 322 Shembade, N. *et al.* Inhibition of NF- $\kappa$ B signaling by A20 through disruption of ubiquitin enzyme complexes. *Science*, 327(5969):1135–9, 2010.
- 323 Boone, D. L. *et al.* The ubiquitin-modifying enzyme A20 is required for termination of Toll-like receptor responses. *Nat Immunol*, 5(10):1052–60, 2004.
- 324 Hitotsumatsu, O. *et al.* The Ubiquitin-Editing Enzyme A20 Restricts Nucleotide-Binding Oligomerization Domain Containing 2-Triggered Signals. *Immunity*, 28(3):381–90, 2008.
- 325 Düwel, M. *et al.* A20 Negatively Regulates T Cell Receptor Signaling to NF- $\kappa$ B by Cleaving Malt1 Ubiquitin Chains. *J. Immunol.*, 182(12):7718–28, 2009.
- 326 Jäättelä, M. *et al.* A20 zinc finger protein inhibits TNF and IL-1 signaling. *J. Immunol.*, 156(3):1166–73, 1996.
- 327 Bellail, A. C. *et al.* A20 Ubiquitin Ligase-Mediated Polyubiquitination of RIP1 Inhibits Caspase-8 Cleavage and TRAIL-Induced Apoptosis in Glioblastoma. *Cancer Discov.*, 2(2):140–55, 2012.
- 328 Dong, B. *et al.* Targeting A20 enhances TRAIL-induced apoptosis in hepatocellular carcinoma cells. *Biochem. Biophys. Res. Commun.*, 418(2):433–8, 2012.
- 329 Malewicz, M. *et al.* NF $\kappa$ B Controls the Balance between Fas and Tumor Necrosis Factor Cell Death Pathways during T Cell Receptor-induced Apoptosis Via the Expression of Its Target Gene A20. *J. Biol. Chem.*, 278(35):32825–33, 2003.
-

- 
- 330 Onizawa, M. *et al.* The ubiquitin-modifying enzyme A20 restricts ubiquitination of the kinase RIPK3 and protects cells from necroptosis. *Nat. Immunol.*, 16(6):618–27, 2015.
- 331 Storz, P. *et al.* Functional dichotomy of A20 in apoptotic and necrotic cell death. *Biochem. J.*, 387(1):47–55, 2005.
- 332 Ferran, C. *The Multiple Therapeutic Targets of A20*. Landes Bioscience, 2014.
- 333 Abbasi, A. *et al.* The role of the ubiquitin-editing enzyme A20 in diseases of the central nervous system and other pathological processes. *Front. Mol. Neurosci.*, 8(21), 2015.
- 334 Hymowitz, S. G. and Wertz, I. E. A20: from ubiquitin editing to tumour suppression. *Nat. Rev. Cancer*, 10(5):332–41, 2010.
- 335 Hammer, G. E. *et al.* Expression of A20 by dendritic cells preserves immune homeostasis and prevents colitis and spondyloarthritis. *Nat. Immunol.*, 12(12):1184–93, 2012.
- 336 Kato, M. *et al.* Frequent inactivation of A20 in B-cell lymphomas. *Nature*, 459(7247):712–6, 2009.
- 337 Vendrell, J. A. *et al.* A20/TNFAIP3, a new estrogen-regulated gene that confers tamoxifen resistance in breast cancer cells. *Oncogene*, 26(32):4656–67, 2007.
- 338 Codd, J. D. *et al.* A20 RNA expression is associated with undifferentiated nasopharyngeal carcinoma and poorly differentiated head and neck squamous cell carcinoma. *J. Pathol.*, 187(5):549–55, 1999.
- 339 Daniel, S. *et al.* A20 protects endothelial cells from TNF-, Fas-, and NK-mediated cell death by inhibiting caspase 8 activation. *Blood*, 104(8):2376–84, 2004.
- 340 Verbrugge, I. *et al.* Radiation and anticancer drugs can facilitate mitochondrial bypass by CD95/Fas via c-FLIP downregulation. *Cell Death Differ.*, 17(3):551–61, 2010.
- 341 De Valck, D. *et al.* The zinc finger protein A20 interacts with a novel anti-apoptotic protein which is cleaved by specific caspases. *Oncogene*, 18(29):4182–90, 1999.
- 342 He, K.-L. and Ting, A. T. A20 Inhibits Tumor Necrosis Factor (TNF) Alpha-Induced Apoptosis by Disrupting Recruitment of TRADD and RIP to the TNF Receptor 1 Complex in Jurkat T Cells. *Mol. Cell. Biol.*, 22(17):6034–45, 2002.
- 343 Hollingsworth, J. M. *et al.* Rising incidence of small renal masses: A need to reassess treatment effect. *J. Natl. Cancer Inst.*, 98(18):1331–34, 2006.
-

- 
- 344 Fuhrman, S. a. *et al.* Prognostic significance of morphologic parameters in renal cell carcinoma. *Am. J. Surg. Pathol.*, 6(7):655–63, 1982.
- 345 Gerharz, C. D. *et al.* Ultrastructural appearance and cytoskeletal architecture of the clear, chromophilic, and chromophobe types of human renal cell carcinoma in vitro. *Am. J. Pathol.*, 142(3):851–9, 1993.
- 346 Gerharz, C. D. *et al.* Cytomorphological, cytogenetic, and molecular biological characterization of four new human renal carcinoma cell lines of the clear cell type. *Virchows Arch.*, 424(4):403–9, 1994.
- 347 Ramp, U. *et al.* Deficient activation of CD95 (APO-1/Fas)-mediated apoptosis: a potential factor of multidrug resistance in human renal cell carcinoma. *Br. J. Cancer*, 82(11):1851–9, 2000.
- 348 Lee, E.-W. *et al.* Ubiquitination and degradation of the FADD adaptor protein regulate death receptor-mediated apoptosis and necroptosis. *Nat. Commun.*, 3(978), 2012.
- 349 Jin, Z. *et al.* Cullin3-based polyubiquitination and p62-dependent aggregation of caspase-8 mediate extrinsic apoptosis signaling. *Cell*, 137(4):721–35, 2009.
- 350 Lu, M. and Krauss, R. S. N-cadherin ligation, but not Sonic hedgehog binding, initiates Cdo-dependent p38alpha/beta MAPK signaling in skeletal myoblasts. *Proc. Natl. Acad. Sci. U. S. A.*, 107(9):4212–7, 2010.
- 351 Hsu, P. D. *et al.* DNA targeting specificity of RNA-guided Cas9 nucleases. *Nat. Biotechnol.*, 31(9):827–32, 2013.
- 352 Mulders, P. *et al.* Renal cell carcinoma: recent progress and future directions. *Cancer Res.*, 57(22):5189–95, 1997.
- 353 Heikaus, S. *et al.* Caspase-8 and its inhibitors in RCCs in vivo: The prominent role of ARC. *Apoptosis*, 13(7):938–49, 2008.
- 354 Fulda, S. *et al.* Metabolic Inhibitors Sensitize for CD95 (APO-1/Fas)-induced Apoptosis by Down-Regulating Fas-associated Death Domain-like Interleukin 1-Converting Enzyme Inhibitory Protein Expression 1. *Cancer Res.*, 95(32):3947–56, 2000.
- 355 Caserta, T. M. *et al.* Q-VD-OPh, a broad spectrum caspase inhibitor with potent antiapoptotic properties. *Apoptosis*, 8(4):345–52, 2003.
- 356 Ponton, A. *et al.* The CD95 (APO-1/Fas) receptor activates NF- $\kappa$ B independently of its cytotoxic function. *J. Biol. Chem.*, 271(15):8991–5, 1996.
-

- 
- 357 Legembre, P. *et al.* Induction of apoptosis and activation of NF- $\kappa$ B by CD95 require different signalling thresholds. *EMBO Rep.*, 5(11):1084–9, 2004.
- 358 Lademann, U. *et al.* A20 zinc finger protein inhibits TNF-induced apoptosis and stress response early in the signaling cascades and independently of binding to TRAF2 or 14-3-3 proteins. *Cell Death Differ.*, 8(3):265–72, 2001.
- 359 Jinek, M. *et al.* A programmable dual-RNA-guided DNA endonuclease in adaptive bacterial immunity. *Science*, 337(6096):816–21, 2012.
- 360 Cong, L. *et al.* Multiplex genome engineering using CRISPR/Cas systems. *Science*, 339(6121):819–23, 2013.
- 361 Chen, D. *et al.* Bortezomib as the first proteasome inhibitor anticancer drug: current status and future perspectives. *Curr. Cancer Drug Targets*, 11(3):239–53, 2011.
- 362 Crowder, R. N. *et al.* Caspase-8 regulation of TRAIL-mediated cell death 1. *Exp. Oncol.*, 2012:160–4, 2012.
- 363 Chaudhary, P. M. *et al.* Activation of the NF- $\kappa$ B pathway by caspase 8 and its homologs. *Oncogene*, 19(39):4451–60, 2000.
- 364 Misra, R. S. *et al.* Caspase-8 and c-FLIPL Associate in Lipid Rafts with NF- $\kappa$ B Adaptors during T Cell Activation. *J. Biol. Chem.*, 282(27):19365–74, 2007.
- 365 Golks, A. *et al.* The c-FLIP–NH 2 terminus (p22-FLIP) induces NF- $\kappa$ B activation. *J. Exp. Med.*, 203(5):1295–305, 2006.
- 366 Kreuz, S. *et al.* NF $\kappa$ B activation by Fas is mediated through FADD, caspase-8, and RIP and is inhibited by FLIP. *JCB*, 166(3):369–80, 2003.
- 367 Hinshaw-Makepeace, J. *et al.* c-FLIPS reduces activation of caspase and NF- $\kappa$ B pathways and decreases T cell survival. *Eur. J. Immunol.*, 38(1):54–63, 2008.
- 368 Mariani, S. M. *et al.* Interleukin 1 $\beta$ -converting Enzyme Related Proteases/Caspases Are Involved in TRAIL-induced Apoptosis of Myeloma and Leukemia Cells. *J. Cell Biol.*, 137(1):221–9, 1997.
- 369 Matte, I. *et al.* MUC16 mucin (CA125) attenuates TRAIL-induced apoptosis by decreasing TRAIL receptor R2 expression and increasing c-FLIP expression. *BMC Cancer*, 14(234):1–14, 2014.
- 370 Pasquini, L. *et al.* Sensitivity and resistance of human cancer cells to TRAIL: mechanisms and therapeutical perspectives. *Cancer Ther.*, 4:47–72, 2006.
-

- 
- 371 Park, E. J. *et al.* Dicoumarol sensitizes renal cell carcinoma Caki cells to TRAIL-induced apoptosis through down-regulation of Bcl-2, Mcl-1 and c-FLIP in a NQO1-independent manner. *Exp. Cell Res.*, 323(1):144–54, 2014.
- 372 Brooks, A. D. and Sayers, T. J. Reduction of the antiapoptotic protein cFLIP enhances the susceptibility of human renal cancer cells to TRAIL apoptosis. *Cancer Immunol. Immunother.*, 54(5):499–505, 2005.
- 373 Keane, M. M. *et al.* Inhibition of NF- $\kappa$ B activity enhances TRAIL mediated apoptosis in breast cancer cell lines. *Breast Cancer Res. Treat.*, 64(2):211–9, 2000.
- 374 Kim, Y.-S. *et al.* TRAIL-mediated apoptosis requires NF- $\kappa$ B inhibition and the mitochondrial permeability transition in human hepatoma cells. *Hepatology*, 36(6):1498–508, 2002.
- 375 Fulda, S. Targeting c-FLICE-like inhibitory protein (CFLAR) in cancer. *Expert Opin Ther Targets*, 17(2):195–201, 2013.
- 376 Sharp, D. A. *et al.* Selective knockdown of the long variant of cellular FLICE inhibitory protein augments death receptor-mediated caspase-8 activation and apoptosis. *J. Biol. Chem.*, 280(19):19401–9, 2005.
- 377 Day, T. W. *et al.* c-FLIP Knockdown Induces Ligand-independent DR5-, FADD-, Caspase-8-, and Caspase-9-dependent Apoptosis in Breast Cancer Cells. *Biochem Pharmacol*, 76(12):1694–704, 2008.
- 378 Henrich, C. J. *et al.* Withanolide E sensitizes renal carcinoma cells to TRAIL-induced apoptosis by increasing cFLIP degradation. *Cell Death Dis.*, 6(e1666):1–10, 2015.
- 379 Griffith, T. S. *et al.* Induction and regulation of tumor necrosis factor-related apoptosis-inducing ligand/Apo-2 ligand-mediated apoptosis in renal cell carcinoma. *Cancer Res.*, 62(11):3093–9, 2002.
- 380 Oya, M. *et al.* Constitutive activation of nuclear factor- $\kappa$ B prevents TRAIL-induced apoptosis in renal cancer cells. *Oncogene*, 20(29):3888–96, 2001.
- 381 Kim, E.-a. *et al.* Inhibition of c-FLIPL expression by miRNA-708 increases the sensitivity of renal cancer cells to anti-cancer drugs. *Oncotarget*, 7(22):31832–46, 2016.
- 382 Beg, A. A. *et al.* Embryonic lethality and liver degeneration in mice lacking the RelA component of NF- $\kappa$ B. *Nature*, 376(6536):167–70, 1995.
- 383 Meylan, E. *et al.* Requirement for NF- $\kappa$ B signalling in a mouse model of lung adenocarcinoma. *Nature*, 462(7269):104–7, 2009.
-

- 
- 384 Huang, S. *et al.* Blockade of NF- $\kappa$ B activity in human prostate cancer cells is associated with suppression of angiogenesis, invasion, and metastasis. *Oncogene*, 20(31):4188–97, 2001.
- 385 Karin, M. NF- $\kappa$ B as a Critical Link Between Inflammation and Cancer. *Cold Spring Harb. Perspect. Biol.*, 1(5):1–14, 2009.
- 386 Hoesel, B. and Schmid, J. A. The complexity of NF- $\kappa$ B signaling in inflammation and cancer. *Mol. Cancer*, 12(86):1–15, 2013.
- 387 Beg, A. A. and Baltimore, D. An essential role for NF- $\kappa$ B in preventing TNF- $\alpha$ -induced cell death. *Science*, 274(5288):782–4, 1996.
- 388 Jeremias, I. *et al.* Inhibition of Nuclear Factor  $\kappa$ B Activation Attenuates Apoptosis Resistance in Lymphoid Cells. *Blood*, 91:4624–31, 1998.
- 389 Luo, J.-l. *et al.* IKK/NF- $\kappa$ B signaling: balancing life and death - a new approach to cancer therapy. *J. Clin. Invest.*, 115(10):2625–32, 2005.
- 390 Micheau, O. *et al.* NF- $\kappa$ B Signals Induce the Expression of c-FLIP. *Mol. Cell Biol.*, 21(16):5299–305, 2001.
- 391 Bagnoli, M. *et al.* Cellular FLICE-inhibitory protein (c-FLIP) signalling: A key regulator of receptor-mediated apoptosis in physiologic context and in cancer. *Int. J. Biochem. Cell Biol.*, 42(2):210–3, 2010.
- 392 Schneider, P. *et al.* Conversion of Membrane-bound Fas(CD95) Ligand to Its Soluble Form Is Associated with Downregulation of Its Proapoptotic Activity and Loss of Liver Toxicity. *J. Exp. Med.*, 187(8):1205–13, 1998.
- 393 Bivona, T. G. *et al.* FAS and NF- $\kappa$ B signalling modulate dependence of lung cancers on mutant EGFR. *Nature*, 471(7339):523–6, 2011.
- 394 Okamoto, K. *et al.* Human T-cell leukemia virus type-I oncoprotein Tax inhibits Fas-mediated apoptosis by inducing cellular FLIP through activation of NF- $\kappa$ B. *Genes to Cells*, 11(2):177–91, 2006.
- 395 Chen, L. *et al.* CD95 promotes tumour growth. *Nature*, 465(7297):492–6, 2010.
- 396 Debatin, K. and Krammer, P. H. Death receptors in chemotherapy and cancer. *Oncogene*, 23(16):2950–66, 2004.
- 397 Peter, M. E. *et al.* Does CD95 have tumor promoting activities? *Biochim. Biophys. Acta - Rev. Cancer*, 1755(1):25–36, 2005.
- 398 Peter, M. E. *et al.* The role of CD95 and CD95 ligand in cancer. *Cell Death Differ.*, 22(4):549–59, 2015.
-

- 
- 399 Horie, S. *et al.* Expression of Fas in Renal Cell Carcinoma. *Jpn J Clin Oncol*, 27(6):384–8, 1997.
- 400 Kim, Y. S. *et al.* Fas (APO-1/CD95) ligand and Fas expression in renal cell carcinomas - correlation with the prognostic factors. *Arch. Pathol. Lab. Med.*, 124(5):687–93, 2000.
- 401 Hahne, M. *et al.* Melanoma Cell Expression of Fas(Apo-1/CD95) Ligand: Implications for Tumor Immune Escape. *Science*, 274(5291):1363–6, 1996.
- 402 O’Connell, J. The Fas counterattack: Fas-mediated T cell killing by colon cancer cells expressing Fas ligand. *J. Exp. Med.*, 184(3):1075–82, 1996.
- 403 Schmidt, J. H. *et al.* Quantification of CD95-induced apoptosis and NF- $\kappa$ B activation at the single cell level. *J. Immunol. Methods*, 423:12–7, 2015.
- 404 Hadji, A. *et al.* Death induced by CD95 or CD95 ligand elimination. *Cell Rep.*, 7(1):208–22, 2014.
- 405 Goldschneider, D. and Mehlen, P. Dependence receptors: a new paradigm in cell signaling and cancer therapy. *Oncogene*, 29(13):1865–82, 2010.
- 406 Ogasawara, J. *et al.* Lethal effect of the anti-Fas antibody in mice. *Nature*, 364(6440):806–9, 1993.
- 407 Walczak, H. *et al.* Tumoricidal activity of tumor necrosis factor-related apoptosis-inducing ligand in vivo. *Nat. Med.*, 5(2):157–63, 1999.
- 408 Nagata, S. Apoptosis by Death Factor. *Cell*, 88(3):355–65, 1997.
- 409 Tavares, R. M. *et al.* The ubiquitin modifying enzyme A20 restricts B cell survival and prevents autoimmunity. *Immunity*, 33(2):181–91, 2010.
- 410 Stanger, B. Z. *et al.* RIP: A novel protein containing a death domain that interacts with Fas/APO-1 (CD95) in yeast and causes cell death. *Cell*, 81(4):513–23, 1995.
- 411 Jiang, W. *et al.* CRISPR-assisted editing of bacterial genomes. *Nat. Biotechnol.*, 31(3):233–9, 2013.
- 412 Heckl, D. *et al.* Generation of mouse models of myeloid malignancy with combinatorial genetic lesions using CRISPR-Cas9 genome editing. *Nat. Biotechnol.*, 32(9):941–6, 2014.
- 413 Mali, P. *et al.* RNA-guided human genome engineering via Cas9. *Science*, 339(6121):823–6, 2013.
- 414 Shen, B. *et al.* Efficient genome modification by CRISPR-Cas9 nickase with minimal off-target effects. *Nat. Methods*, 11(4):399–402, 2014.
-

- 
- 415 Slaymaker, I. M. *et al.* Rationally engineered Cas9 nucleases with improved specificity. *Science*, 351(6268):84–8, 2016.
- 416 Kleinstiver, B. P. *et al.* High-fidelity CRISPR–Cas9 nucleases with no detectable genome-wide off-target effects. *Nature*, 529(7587):490–5, 2016.
- 417 Gaj, T. *et al.* ZFN, TALEN, and CRISPR/Cas-based methods for genome engineering. *Trends Biotechnol.*, 31(7):397–405, 2013.
- 418 Heintze, J. *et al.* A CRISPR CASE for high-throughput silencing. *Front. Genet.*, 4(193), 2013.
- 419 Barrangou, R. *et al.* Advances in CRISPR-Cas9 genome engineering: lessons learned from RNA interference. *Nucleic Acids Res.*, 43(7):3407–19, 2015.
- 420 Hsu, H. *et al.* The TNF receptor 1-associated protein TRADD signals cell death and NF- $\kappa$ B activation. *Cell*, 81(4):495–504, 1995.
- 421 Gonzalvez, F. *et al.* TRAF2 Sets a threshold for extrinsic apoptosis by tagging caspase-8 with a ubiquitin shutoff timer. *Mol. Cell*, 48(6):888–99, 2012.
- 422 Sahasrabudhe, S. R. *et al.* Specificity of base substitutions induced by the acridine mutagen ICR-191: mispairing by guanine N7 adducts as a mutagenic mechanism. *Genetics*, 129(4):981–9, 1991.
- 423 Barbour, L. *et al.* Yeast Protocols. In Xiao, W., editor, *Methods Mol Biol*, volume 313, chapter Mutagenesi, pages 121–7. Humana Press, New Jersey, 2006.
- 424 Catz, S. D. and Johnson, J. L. Transcriptional regulation of bcl-2 by nuclear factor  $\kappa$ B and its significance in prostate cancer. *Oncogene*, 20(50):7342–51, 2001.
- 425 Chen, C. *et al.* The Rel/NF- $\kappa$ B Family Directly Activates Expression of the Apoptosis Inhibitor Bcl-xL. *Mol. Cell. Biol.*, 20(8):2687–95, 2000.
- 426 Schmitz, R. *et al.* TNFAIP3 (A20) is a tumor suppressor gene in Hodgkin lymphoma and primary mediastinal B cell lymphoma. *J. Exp. Med.*, 206(5):981–9, 2009.
- 427 Braun, F. C. M. *et al.* Tumor suppressor TNFAIP3 (A20) is frequently deleted in Sézary syndrome. *Leukemia*, 25(9):1494–501, 2011.



# Acknowledgements

First of all, I want to thank my supervisor Prof Dr. Ingo Schmitz for giving me the great opportunity to accomplish my PhD thesis in his work group. He always was open for helpful support, fruitful discussions and new ideas and theories.

I want to thank my colleagues Anne-Marie, Carlos, Claudia, Christian, Daniela, Konstantinos, Lisa, Neda, Sabrina, Svenja and Yan-Yan, as well as my former colleagues Alisha, Frida, Marc, Michaela, Ralf, Tanja and Yvonne for having a great time in a very helpful working atmosphere.

I especially want to thank Frida for having been my mentor within the first time of my PhD. I additionally want to thank her and Carlos for proofreading this work.

I want to thank my Thesis Committee members Prof. Dr. Inna Lavrik and Dr. Andrea Scrima for giving me very helpful input during the last years to successfully accomplish this thesis.

Furthermore, I want to thank the HZI Graduate School for strengthen my scientific and social skills during my time as a PhD student.

I am very grateful that my parents and my brother for the support they provided me through my entire life.

My biggest thanks go out to Maike for her encouragement and love.

# Curriculum vitae

## Persönliche Daten

Name	Tobias Lübke
Geburtstag	09.06.1984
Geburtsort	Hannover
Familienstand	ledig
Nationalität	deutsch

## Bildungsweg

1990-1994	Grundschule Am Sandberge, Hannover
1994-1996	Orientierungsstufe im Schulzentrum Bemerode, Hannover
1996-2004	Gymnasium Schillerschule Hannover
2004-2008	Studium der Biotechnologie (B. Sc.), Hochschule Anhalt, Köthen Titel der Bachelorarbeit: „Produktion von biotinylierten Antikörper- fragmenten für den Einsatz in der Diagnostik“
2009-2011	Studium der Biotechnologie (M. Sc.), Technische Universität Braun- schweig Titel der Masterarbeit: „Isolierung und Charakterisierung von rekombinanten Antikörperfragmenten gegen therapeutisch relevante Targets“

## Wissenschaftliche Tätigkeit

07/2012-06/2016	Dissertation an der Otto-von-Guericke Universität (Magdeburg) und am Helmholtz-Zentrum für Infektionsforschung (Braunschweig) in der AG von Prof. Dr. Ingo Schmitz
-----------------	--

## Berufstätigkeit

01-09/2009	Wissenschaftlicher Mitarbeiter bei der IVD GmbH, Hannover
11/2011-06/2012	Wissenschaftlicher Mitarbeiter bei der IVD GmbH, Hannover

## Publikationen

Knievel J., Schulz W. A., Greife A., Hader C., Lübke T., Schmitz I., Albers P., Niegisch G. Multiple mechanisms mediate resistance to sorafenib in urothelial cancer. *Int J Mol Sci*, 15(11):20500-17, 2014.

# Declaration of originality

Tobias Lübke

Heinrich-Heine-Straße 25

38102 Braunschweig

Hiermit erkläre ich, dass ich die von mir eingereichte Dissertation mit dem Thema

## **Influence of c-FLIP and A20 on apoptosis regulation**

selbstständig verfasst, nicht schon als Dissertation verwendet habe und die benutzten Hilfsmittel und Quellen vollständig angegeben habe.

Weiterhin erkläre ich, dass ich weder diese noch eine andere Arbeit zur Erlangung des akademischen Grades doctor rerum naturalium (Dr. rer. nat.) an anderen Einrichtungen eingereicht habe.

Magdeburg, 31.08.2016

---

Tobias Lübke